

DISSERTATION ZUR ERLANGUNG DES DOKTORGRADES
DER FAKULTÄT FÜR CHEMIE UND PHARMAZIE
DER LUDWIG-MAXIMILIANS-UNIVERSITÄT MÜNCHEN

**Sensory Monitoring of the Initiation of Primary
Explosives by Means of Impact and
Photonic Irradiation**



Matthias Muhr

aus

Bonn, Deutschland

2024

Erklärung

Diese Dissertation wurde im Sinne von §7 der Promotionsordnung vom 28. November 2011 von Prof. Dr. Thomas M. Klapötke betreut.

Eidesstattliche Versicherung

Diese Dissertation wurde eigenständig und ohne unerlaubte Hilfe erarbeitet.

Bonn, den 08.10.2024

Matthias Muhr

Dissertation eingereicht am: 10.10.2024

Erstgutachter: Prof. Dr. Thomas M. Klapötke

Zweitgutachter: Prof. Dr. Peter-Michael Kaul

Mündliche Prüfung am: 17.02.2025

jack of all trades, master of none

Contents

I	Introduction	1
1	Explosives	3
1.1	Explosion	3
1.1.1	Deflagration	4
1.1.2	Detonation	4
1.2	Types of Explosives	4
1.2.1	Primary Explosives	4
1.2.2	Secondary Explosives	5
1.2.3	Other Explosives	5
1.2.4	Triacetone Triperoxide (TATP)	5
1.2.5	Hexamethylene Triperoxide Diamine (HMTD)	6
1.3	Initiation Mechanisms	7
1.4	Testing Methods	8
1.4.1	Impact Sensitivity	8
1.4.2	Optical Initiation	9
1.5	Multivariate Statistics	10
1.6	Motivation	11
	References	12
II	Summary and Conclusion	17
2	Sensory Monitoring of Primary Explosives Using Drop Hammer Impact Sensitivity Tests	19
3	Ignition of Explosives Based on Primary Peroxide With an ns Pulsed Laser	21

4	Rapid Identification of Explosives	23
III	Results and Discussion: Drop Hammer Experiments	25
5	Sensory Monitoring of drop hammer Experiments with Multivariate Statistics	27
5.1	Introduction	28
5.2	Experimental Section	30
5.2.1	drop hammer	30
5.2.2	Sensor Array	31
5.2.3	Samples and Sample Preparation	32
5.2.4	Measurement Parameters	33
5.2.5	Pre-Processing and Statistics	33
5.3	Results and Discussion	35
5.3.1	Sensor Data	35
5.3.2	Reproducibility of Lead Styphnate Measurements	38
5.3.3	Feature Extraction and Discrimination	40
5.4	Conclusion	44
	References	47
6	Sensor-Monitored Impact Sensitivity Investigations on HMTD of Different Ageing Stages With Accompanying PTR-TOF Measurements of the Substances	51
6.1	Introduction	52
6.2	Experimental	54
6.2.1	Synthesis	54
6.2.2	Analytical Methods	54
6.2.3	Sensor Array	57
6.2.4	Measurement Parameters	57
6.2.5	Pre-processing and Statistics	59
6.3	Results and Discussion	60
6.3.1	Analytical Methods	60
6.3.2	Validation Measurements	63
6.3.3	Influence of the ball size	67

6.4 Conclusion	77
References	79

IV Results and Discussion: Laser Initiation 83

7 Sensory Monitoring and Analytical Study of Laser Initiated Graphite-Coated TATP Using PTR-ToF-MS and Microphone 85	85
7.1 Introduction	86
7.2 Experimental Section	88
7.2.1 Synthesis of TATP	88
7.2.2 Sample Preparation	89
7.2.3 Analytical Methods	90
7.3 Results and Discussion	92
7.4 Conclusion and Outlook	101
7.5 Declarations	102
References	102
8 Investigation of laser initiation of graphite-coated TATP and HMTD with regard to the influence of coating thickness accompanied by sensor-safe surveillance using a microphone 107	107
8.1 Introduction	108
8.2 Experimental	109
8.2.1 Synthesis of TATP	109
8.2.2 Synthesis of HMTD	110
8.2.3 Sample Preparation	110
8.2.4 Analytical methods	112
8.2.5 Experiments	112
8.2.6 Preprocessing	113
8.3 Results and Discussion	114
8.3.1 Raman Measurements	114
8.3.2 Microphone Measurements	114
8.4 Conclusion and Outlook	122
8.5 Data Availability Statement	125
References	125

V Appendix	129
List of Abbreviations	131
List of Publications	133
8.6 Publications	133
8.7 Conference Presentations	134
8.8 Conference Poster Presentations	134
Acknowledgement	135

Part I

Introduction

Explosives

Explosives are a class of materials that comprise a wide range of energetic compounds and mixtures. These substances are characterised by their ability to undergo rapid, self-propagating chemical reactions without the need for external reactants such as atmospheric oxygen. They are typically in a metastable state and can be initiated in various ways, including mechanical stress from impact or friction, thermal effects from heat sources or photonic irradiation, and detonation shocks from devices such as detonators. The variety of explosive materials ranges from primary explosives, which are highly sensitive and used to initiate detonative reactions, to secondary explosives, which are valued for their high explosive energy and relative low insensitivity. Additionally, the category of explosives also includes propellants and pyrotechnics, used for propulsion and visual effects [1, 2, 3]. The sensitivity of an explosive is a measure of how much energy must be applied to a substance in a certain form (mechanical, thermal, electrical, photonic) before it undergoes a self-propagating reaction and decomposes. The reaction products of explosives are mainly gases that can expand rapidly, exert pressure and generate explosive effects. The speed at which the reaction takes place can range from rapid burning to deflagration to detonation [1, 2, 4].

1.1 Explosion

Explosions are characterised by the spontaneous release of energy. These events involve a rapid chemical reaction that simultaneously generates substantial quantities of gas and heat. The fast expansion of gases results in a powerful force that can cause significant physical disruption. When an explosive is converted, a distinction is made between deflagration and detonation. These classifications are based on the specific speed of sound in the material at which the reaction front propagates and the nature of the energy the

reaction propagates. Each type has distinct characteristics and implications for the effects and damage caused by the explosion [1, 2].

1.1.1 Deflagration

A Deflagration is a decomposition reaction that takes place at subsonic speed, i.e. below the specific speed of sound of the material. It can be described as a rapid combustion process within the material in which the reaction is self-sustained by the heat generated and the resulting gases flow in the opposite direction to the advancing reaction front. The reaction front propagates through thermal transfer. Depending on the type of initiation or the specific burning conditions, deflagration can sometimes turn into detonation, which is known as a deflagration-detonation transition (DDT) [1, 2].

1.1.2 Detonation

During a detonation, the decomposition reaction takes place at speeds far in excess of the speed of sound, usually between 1500 and 9000 m/s. This rapid reaction generates a shock wave characterized by a sudden and extreme increase in pressure and temperature. The reaction front propagates via the shock wave. Detonations are much more violent than deflagrations [1, 2].

1.2 Types of Explosives

In the following, the classes of primary and secondary substances are relevant for the following work and are briefly explained.

1.2.1 Primary Explosives

Explosives can be divided into two main categories: primary and secondary explosives. Primary explosives, also known as initiating explosives, are extremely sensitive to external stimuli such as mechanical shock, heating or sparks. Used in detonators, they are designed to initiate secondary explosives. These compounds, like lead azide ($\text{Pb}(\text{N}_3)_2$), silver azide (AgN_3) and tetrazene ($\text{C}_2\text{H}_8\text{N}_{10}$), are characterised by high brisance and sensitivities. [1, 2, 3, 5].

1.2.2 Secondary Explosives

Secondary explosives, such as trinitrotoluene (TNT) and cyclotrimethylenetrinitramine (RDX), are less sensitive and require a substantial energy input for detonation. They are generally utilised where a high degree of control over the explosive reaction is necessary, as in military or industrial settings. These explosives need the detonation impulse of a primary explosive to initiate their own detonation. Compared to the primary substances, the secondary substances have a significantly higher power and explosion energy [1, 2, 3].

1.2.3 Other Explosives

Certain explosives, including those like HMTD or TATP, which are unsuitable for industrial or military applications because of their high reactivity and unpredictable behavior [6, 7, 8, 9, 10, 11].

1.2.4 Triacetone Triperoxide (TATP)

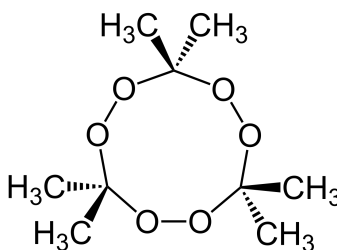


Figure 1.1: Structure formula of TATP

Triacetone triperoxide (TATP), whose structural form can be seen in Figure 1.1, is a highly sensitive and explosive organic peroxide known for its ease of synthesis and the availability of its starting materials. TATP is synthesised by the acid-catalysed reaction of acetone and hydrogen peroxide and is therefore accessible to people with little knowledge of chemistry. Common catalysts for this reaction include hydrochloric acid, sulphuric acid or nitric acid, which are also relatively easy to obtain. The simple production process and availability of precursor chemicals have contributed to TATP's use in illicit activities. Due to its high explosive power and the difficulty of detecting it with conventional security controls, the compound has been implicated in several terrorist attacks. However, TATP

is extremely dangerous to handle. It is very sensitive to shock, friction and temperature fluctuations, which can lead to accidental detonation. The instability of TATP presents significant challenges in synthesis and storage, posing risks even for trained professionals. The decomposition of TATP has been extensively studied, revealing that it can rapidly decompose into volatile and potentially hazardous by-products, further complicating its safe handling and forensic analysis. Forensic analysis of TATP is challenging due to its instability and risk of spontaneous decomposition. However, the risks associated with TATP make it a compound of great importance in terms of both safety and security [12, 13, 14].

1.2.5 Hexamethylene Triperoxide Diamine (HMTD)

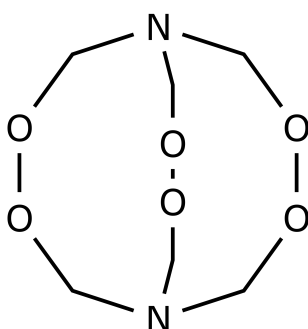


Figure 1.2: Structure formula of HMTD

Hexamethylene triperoxide diamine (HMTD), whose structural form can be seen in Figure 1.2, is also a highly sensitive and powerful organic peroxide explosive, notable for its straightforward synthesis and the ready availability of its precursor chemicals. HMTD is produced through an acid-catalyzed reaction between hexamine and hydrogen peroxide, with citric or hydrochloric acid typically serving as the catalyst. These readily accessible components make HMTD a frequent choice among individuals with limited chemical expertise and resources. The ease of its synthesis, combined with the broad availability of the necessary materials, has unfortunately led to HMTD's involvement in certain high-profile incidents, such as the attempted millennium bombing at Los Angeles airport in 1999 and the 2005 London public transport bombings [7, 6, 8, 9, 10]. Although HMTD exhibits considerable destructive power, it is generally avoided by military forces due to its extreme sensitivity to mechanical shock, friction, and heat. Handling HMTD is par-

ticularly hazardous due to this instability, as even minor mechanical impact, friction, or thermal exposure can result in accidental detonation. The instability of HMTD not only complicates its synthesis and storage but also challenges its safe handling. Studies indicate that HMTD decomposes over time into volatile by-products, a key consideration for forensic identification. Forensic analysis of HMTD is challenging, given its spontaneous decomposition and high sensitivity. Consequently, its inherent instability poses significant safety and security concerns [15, 16, 6].

1.3 Initiation Mechanisms

The initiation of explosives can be triggered by various stimuli, including heat, shock, electrostatic discharge, or photonic irradiation. These triggers can lead to different reactions, such as deflagration or detonation, depending on substance-specific properties and the intensity of the initiating force. Every explosive substance has a certain ignition temperature at which it ignites if the heat generated by its exothermic reaction exceeds the heat released into the environment and the reaction is self-propagating. Secondary explosives generally have an ignition temperature of more than 400 °C [4]. The ignition of explosives is essentially a thermal process. When ignition is triggered by a shock wave, the resulting adiabatic compression generates considerable heat. Mechanical effects such as friction, electrostatic discharge (ESD) or photonic irradiation also convert their respective energy into heat. This conversion creates hotspots, i.e. small areas (0.1 to 10 μm) that can heat up to 900 °C due to the adiabatic compression of gas bubbles in the explosive. These hotspots are transient, existing for only brief periods (in the range of 10^{-3} to 10^{-5} s). These gas bubbles, present in both liquid and solid forms of explosives, are critical to the ignition process. However, not every hotspot leads to ignition or detonation; it depends on whether the heat generated is sufficient to sustain the reaction before it dissipates. In general, the temperature in a hotspot must reach at least 430 °C to trigger a secondary explosive. With primary explosives, ignition by impact is usually caused by the formation of hotspots through intercrystalline friction. In secondary explosives, initiation by impact is usually caused by hotspots formed by gas bubbles between the crystals and lasts for an even shorter time (approx. 10^{-6} s). Understanding these mechanisms is crucial for the safe handling and effective use of explosives, as it helps in designing materials that are both stable and capable of controlled reactions. This foundational knowledge

aids in further research and development in the field of energetic materials, ensuring both safety and efficiency in their application [1, 2, 3, 17].

1.4 Testing Methods

1.4.1 Impact Sensitivity

The drop hammer test is a basic method for determining the impact sensitivity of explosives. In this test, a weight is dropped from a certain height onto a sample to measure the energy required to trigger a reaction such as ignition or detonation. The simplicity and efficiency of the drop hammer test make it a popular method for the preliminary assessment of explosives. One of the main advantages of the drop hammer test is its simplicity and speed. The procedure is straightforward and requires only a drop weight, a height-adjustable fixture and the sample material. This simple set-up and execution allows for rapid testing and quick results, which is an advantage in both research and industry. The drop hammer test is also versatile as it can be applied to a variety of explosive forms including single crystals, powder coatings, pressed pellets, polymer bonded explosives (PBX) and propellants. This adaptability makes it a valuable tool for evaluating different types of energetic materials [1, 18, 17, 19].

However, the drop hammer test also has limitations. One major limitation is that it cannot provide detailed information about the nature and severity of the reaction. While it can indicate whether a reaction is occurring, it cannot distinguish between different types of decomposition such as detonation and deflagration. This lack of specificity can be a disadvantage when a more detailed analysis of explosion behaviour is required [20, 21, 22, 23]. Another disadvantage is variability in results due to differences in test methods and operator handling. Results can be influenced by sample preparation, precise alignment of the device and subjective interpretation of the result, leading to inconsistencies. In addition, the drop hammer test is limited by sample-to-sample variability and potential operator subjectivity, which can affect the reproducibility and reliability of results. In addition, the BAM drop hammer, a specific type of drop hammer used for the characterisation of explosives, can provide limited results in terms of impact sensitivity due to the sample preparation method, where the sample can be ignited by adiabatic compression [1, 17].

Studies have shown that by equipping drop hammers with a wide variety of sensors,

significantly more information can be extracted than a classic yes/no answer. For example, drop hammers have been equipped with microphones to measure sound emissions or with optical measurement methods such as spectrometers or high-speed cameras have been used. The results of these measurements have improved our understanding of the initiation of explosives - for example, hotspots could be detected and visualised [22, 24, 25].

1.4.2 Optical Initiation

Laser initiation of explosives utilises the interaction between laser light and energetic materials to achieve ignition and detonation. This method offers significant advantages over conventional initiation techniques, including insensitivity to electromagnetic interference, the possibility of precise control and the ability to detonate less sensitive explosives. Laser initiation is usually achieved by one of three mechanisms: direct interaction with the explosive, rapid heating of a thin film in contact with the explosive, or ablation of a thin metal foil to create a high-speed flying plate that strikes the explosive [26, 27].

In the first mechanism, the laser beam interacts directly with the explosive, causing it to absorb the laser energy and heat up. This absorption can lead to the formation of hot spots in the material, which then ignite and trigger a self-propagating reaction. The effectiveness of this method depends on factors such as the wavelength of the laser, the pulse duration and the physical properties of the explosive, including its density and specific surface area. The second mechanism involves the rapid heating of a thin metal film that comes into contact with the explosive. The laser energy causes the metal film to heat up and transfer this heat to the explosive, triggering a reaction. This method can be useful for controlled detonation, but may not be reliable for all types of explosives. The third and most effective mechanism, especially for insensitive explosives such as Hexanitrostilbene (HNS), is the use of laser-guided flying discs. In this method, a thin metal foil is ablated with the laser to create a high-speed flyer plate that strikes the explosive, causing a shock wave that triggers detonation. Due to its reliability and effectiveness in detonating insensitive explosives, this method is currently the most viable for practical applications [27].

When testing laser initiation systems, the aim is to evaluate the sensitivity of different explosives to laser energy, determine the optimal laser parameters and assess the reliability of detonation under different conditions. The experiments generally use pulsed high-power lasers such as Nd:YAG, CO₂ and excimer lasers to transfer the required energy

to the explosive. The most important parameters include the wavelength of the laser, the pulse duration, the size of the beam spot and the presence of confinement materials. Studies have shown that factors such as the density and purity of the explosive and the presence of dopants can significantly influence the ignition threshold. For example, the addition of carbon black or other dopants can increase the sensitivity of explosives such as pentaerythritol tetranitrate (PETN) and RDX to laser ignition. However, pure HNS explosives are still difficult to ignite directly with lasers and usually require the use of flying discs [26, 28, 29, 30, 31, 4, 27].

1.5 Multivariate Statistics

Multivariate statistics involves analysing multidimensional data to analyse relationships within the data. This statistical approach is particularly valuable in complex areas such as explosives detection, where it improves the accuracy and reliability of the identification of hazardous substances by analysing data from different sources. In explosives detection, multivariate statistics is used in two main applications: sensor array-based detection and spectroscopy-based detection.

Sensor array-based detection utilises sensor arrays that generate complex data patterns when exposed to different substances. By applying multivariate methods such as Principal Component Analysis (PCA) or Partial Least Squares Discriminant Analysis (PLS-DA), researchers can differentiate between explosives and non-explosives based on the sensor responses. For example, sensor arrays can detect explosive residues by analysing the sensor outputs, with multivariate statistics enabling the classification and identification of the substances present [32, 14]. In spectroscopy-based detection, multivariate statistics are combined with spectroscopic methods such as Fourier transform infrared spectroscopy (FTIR) and laser-induced breakdown spectroscopy (LIBS). These techniques provide spectral data that reflect the molecular composition of the samples. Multivariate statistical methods are applied to the spectral data to distinguish between different types of explosives. For example, FTIR spectra of different explosives are analysed using PCA and other clustering methods to identify the most discriminating spectral regions, enabling the differentiation of explosives.

Principal component analysis (PCA) is a method of reducing the dimensionality of a data set while retaining most of the variance. It involves converting the original variables

into a new set of uncorrelated variables, called principal components, which are ordered by the amount of variance they capture in the data. This facilitates the visualisation and analysis of complex data sets by focusing on the most important components. Linear discriminant analysis (LDA), on the other hand, is used for classification. It aims to find a linear combination of features that best separates two or more classes of objects or events. LDA maximises the ratio between the between-class variance and the within-class variance in a given dataset, ensuring maximum separability [33]. These approaches enable a more accurate distinction between explosive and non-explosive materials and thus contribute significantly to advances in security and forensic applications.

1.6 Motivation

The critical study of explosives initiation mechanisms is important for ensuring the safe handling and use of energetic materials in various sectors, including military, mining and security. While conventional methods such as the drop hammer test are suitable for determining the impact sensitivity of explosives, they offer limited insight into the complexity of explosive reactions and the exact nature of initiation at a granular level. To fill this gap and gain a deeper understanding of the response of explosives to different types of loads, the following publications have equipped test rigs with various sensors, which can be crucial for improving safety protocols and reducing accidental detonations. By combining sensors and pre-processing based on multivariate statistics, better reproducibility of the results of sensitivity tests can be achieved. This makes it possible to make estimates of the reaction behavior based on the evaluated sensor data and to identify explosives based on their physical reaction characteristics. Another focus of the work listed here is the processing of explosives using pulsed lasers. The use of coatings is intended to investigate the possibility of controlled ablation of explosives, especially TATP. The main focus was on causing an ablation without causing the respective substance to ignite. Substance-independent laser parameters are to be determined with which it is possible to process the substances without igniting them.

References

- [1] T.M. Klapötke and C.M. Rienäcker. “Drophammer test investigations on some inorganic and organic azides”. In: *Propellants, Explosives, Pyrotechnics* 26.1 (2001), pp. 43–47. DOI: 10.1002/prop.200100073.
- [2] Josef Köhler, Rudolf Meyer, and Axel Homburg. *Explosivstoffe*. 10th revised and expanded edition. Weinheim: Wiley-VCH, 2008.
- [3] Robert Matyáš and Jiří Pachman. “Explosive Properties of Primary Explosives”. In: *Primary Explosives*. Springer, 2012, pp. 11–36. DOI: 10.1007/978-94-007-2482-1_2. URL: https://link.springer.com/chapter/10.1007/978-94-007-2482-1_2.
- [4] Ernst-Christian Koch. *Sprengstoffe, Treibmittel, Pyrotechnika*. 2nd. Berlin: De Gruyter, 2019. ISBN: 978-3-11-055784-8.
- [5] Paul W. Cooper and Stanley R. Kurowski. *Introduction to the Technology of Explosives*. New York: Wiley-VCH, 1996.
- [6] J.C. Oxley, J.L. Smith, W. Luo, and J. Brady. “Determining the vapor pressures of diacetone diperoxide (DADP) and hexamethylene triperoxide diamine (HMTD)”. In: *Propellants, Explosives, Pyrotechnics* 34.6 (2009), pp. 539–543. DOI: 10.1002/prop.200800073.
- [7] DER STANDARD. *Moscheenanschlag in hernalds: Selber sprengstoff wie in london verwendet*. Available at: <https://www.derstandard.at/story/2637639/moscheenanschlag-in-hernalds-selber-sprengstoff-wie-in-london-verwendet>. Accessed: 13-11-2023. 2007.
- [8] G.M. Segell. “Terrorism on london public transport”. In: *Defense & Security Analysis* 22.1 (2006), pp. 45–59. DOI: 10.1080/14751790600577132.
- [9] A.G. Simon and L.E. DeGreeff. “Variation in the headspace of bulk hexamethylene triperoxide diamine (HMTD): Part II. Analysis of non-detonable canine training aids”. In: *Forensic Chemistry* 13 (2019), p. 100155. DOI: 10.1016/j.forc.2019.100155.

- [10] Merkur. *Sprengstoff-Brief an Gauck abgefangen*. Available at: <https://www.merkur.de/politik/sprengstoffverdaechtiger-brief-bundespraesidialamt-zr-2861520.html>. Accessed: 13-11-2023. 2023.
- [11] C.A. Mayhew et al. “Applications of proton transfer reaction time-of-flight mass spectrometry for the sensitive and rapid real-time detection of solid high explosives”. In: *International Journal of Mass Spectrometry* 289.1 (2010), pp. 58–63. DOI: 10.1016/j.ijms.2009.09.006.
- [12] Jimmie C. Oxley, James L. Smith, and H. Chen. “Decomposition of a Multi-Peroxidic Compound: Triacetone Triperoxide (TATP)”. In: *Propellants, Explosives, Pyrotechnics* 27.4 (2002), pp. 209–216. DOI: 10.1002/prop.200290019.
- [13] Jiri Pachman and Robert Matyas. “Study of TATP: Stability of TATP solutions”. In: *Forensic Science International* 207.1-3 (2010), pp. 212–214. DOI: 10.1016/j.forsciint.2010.03.003.
- [14] M. Muhr, T.M. Klapötke, and G. Holl. “Sensory monitoring of drop hammer experiments with multivariate statistics”. In: *Propellants, Explosives, Pyrotechnics* 47.11 (2022). DOI: 10.1002/prop.202200025.
- [15] Jimmie C. Oxley, James L. Smith, and H. Chen. “Synthesis and Degradation of Hexamethylene Triperoxide Diamine (HMTD)”. In: *Propellants, Explosives, Pyrotechnics* 40.4 (2015), pp. 394–398. DOI: 10.1002/prop.201400213.
- [16] Lauryn E. DeGreeff, Michelle M. Cerreta, and Christopher J. Katilie. “Variation in the headspace of bulk hexamethylene triperoxide diamine (HMTD) with time, environment, and formulation”. In: *Forensic Chemistry* 4 (2017), pp. 41–50. DOI: 10.1016/j.forc.2017.03.001.
- [17] Thomas M. Klapötke. *High Energy Materials*. Berlin, New York: Walter de Gruyter, 2009. ISBN: 9783110207453.
- [18] M. S. Gruhne, M. Lommel, M. H. H. Wurzenberger, N. Szimhardt, T. M. Klapötke, and J. Stierstorfer. “OZM Ball Drop Impact Tester (BIT-132) vs. BAM Standard Method – a Comparative Investigation”. In: *Propellants Explos. Pyrotech.* 45 (2020), pp. 147–153. URL: <https://doi.org/10.1002/prop.201900286>.

- [19] N. Lease, M. D. Holmes, M. A. Englert-Erickson, L. M. Kay, E. G. Francois, and V. W. Manner. “Analysis of Ignition Sites for the Explosives 3,3’-Diamino-4,4’-azoxyfurazan (DAAF) and 1,3,5,7-Tetranitro-1,3,5,7-tetrazoctane (HMX) Using Crush Gun Impact Testing”. In: *ACS Mater. Au* 1 (2021), pp. 116–129. URL: <https://doi.org/10.1021/acsmaterialsau.1c00013>.
- [20] Zhiwei Men, Kenneth S. Suslick, and Dana D. Dlott. “Thermal Explosions of Polymer-Bonded Explosives with High Time and Space Resolution”. In: *J. Phys. Chem. C* 122.26 (2018), pp. 14289–14295. DOI: 10.1021/acs.jpcc.8b02422.
- [21] Z. Men, K. S. Suslick, and D. D. Dlott. “Thermal Explosions of Polymer-Bonded Explosives with High Time and Space Resolution”. In: *J. Phys. Chem. C* 122 (2018), pp. 14289–14295. URL: <https://doi.org/10.1021/acs.jpcc.8b02422>.
- [22] David M. Williamson, Sue Gymer, Nicholas E. Taylor, Stephen M. Walley, Andrew P. Jardine, Annette Glauser, et al. “Characterisation of the impact response of energetic materials: observation of a low-level reaction in 2,6-diamino-3,5-dinitropyrazine-1-oxide (LLM-105)”. In: *RSC Advances* 6.33 (2016), pp. 27896–27900. DOI: 10.1039/C6RA03096C.
- [23] R. M. Doherty and D. S. Watt. “Relationship Between RDX Properties and Sensitivity”. In: *Propellants Explos. Pyrotech.* 33 (2008), pp. 4–13. URL: <https://doi.org/10.1002/prop.200800201>.
- [24] C. S. Coffey and V. F. de Vost. “Impact Testing of Explosives and Propellants”. In: *Propellants Explos. Pyrotech.* 20 (1995), pp. 105–115. URL: <https://doi.org/10.1002/prop.19950200302>.
- [25] P. J. Rae and P. M. Dickson. “Some Observations About the Drop-weight Explosive Sensitivity Test”. In: *Journal of Dynamic Behavior of Materials* 7.3 (2021), pp. 414–424. DOI: 10.1007/s40870-020-00276-2.
- [26] N.K. Bourne. “On the laser ignition and initiation of explosives”. In: *Proceedings of the Royal Society of London. Series A: Mathematical, Physical and Engineering Sciences* 457.2010 (2001), pp. 1401–1426. DOI: 10.1098/rspa.2000.0721.

- [27] Leo de Yong, Tam Nguyen, and John Waschl. *Laser Ignition of Explosives, Pyrotechnics and Propellants: A Review*. Tech. rep. DSTO-TR-0068. Melbourne, Victoria, Australia: Defence Science and Technology Organisation, May 1995. URL: <https://apps.dtic.mil/sti/citations/ADA299465>.
- [28] M.D Bowden. “Laser initiation of energetic materials: a historical overview”. In: *Optical Technologies for Arming, Safing, Fuzing, and Firing III*. Ed. by J.W.J. Thomes and F.M. Dickey. SPIE Proceedings. SPIE. 2007, p. 666208. DOI: 10.1117/12.734225.
- [29] J.G. Du, H.H. Ma, and Z.W. Shen. “Laser initiation of non–primary explosive detonators”. In: *Propellants, Explosives, Pyrotechnics* 38.4 (2013), pp. 502–504. DOI: 10.1002/prop.201200132.
- [30] X. Fang and W.G. McLuckie. “Laser ignitibility of insensitive secondary explosive 1,1-diamino-2,2-dinitroethene (FOX-7)”. In: *Journal of Hazardous Materials* 285 (2015), pp. 375–382. DOI: 10.1016/j.jhazmat.2014.12.006.
- [31] Y. Wang et al. “Laser ignition of energetic complexes: impact of metal ion on laser initiation ability”. In: *New Journal of Chemistry* 45.28 (2021), pp. 12705–12710. DOI: 10.1039/d1nj02345d.
- [32] S. Maurer, R. Makarow, J. Warmer, and P. Kaul. “Fast testing for explosive properties of mg-scale samples by thermal activation and classification by physical and chemical properties”. In: *Sens. Actuators B: Chem.* 215 (2015), pp. 70–76. URL: <https://doi.org/10.1016/j.snb.2015.03.045>.
- [33] Serge Kokot, Michael Grigg, Helen Panayiotou, and Tran Dong Phuong. “Data Interpretation by some Common Chemometrics Methods”. In: *Electroanalysis* 10.16 (1998), pp. 1081–1088.

Part II

Summary and Conclusion

Sensory Monitoring of Primary Explosives Using Drop Hammer Impact Sensitivity Tests

Sensory Monitoring of Drop Hammer Experiments with Multivariate Statistics

In this study, the initiation and decomposition reactions of four primary explosives - tetrazene, silver azide, lead azide and lead styphnate - were investigated in detail using a drop hammer setup equipped with a comprehensive sensor array. The test set-up was based on the conventional OZM ball impact tester (BIT), but was extended with sensors such as a pyrometer, spectrometer, VIS diode, microphone and piezo vibration sensor. These modifications aimed to overcome the limitations of conventional drop hammer tests, such as their inability to provide detailed insights into the nature and dynamics of explosive reactions.

Through experimental procedures, the kinetic energy of the ball was carefully adjusted to ensure the safe decomposition of all samples. In total, 42 different features were identified and extracted from the sensor data for each explosive material. These features were then analysed using multivariate statistical methods, including principal component analysis (PCA) and linear discriminant analysis (LDA). The analysis revealed compound-specific trends and significant parameters that could be used to classify the explosives based on their sensor responses.

In addition, the study investigated the possibility of distinguishing between different reaction mechanisms to improve the understanding of how these materials degrade upon impact. The application of multivariate statistics not only provided a deeper in-

sight into the characteristic values of the explosives, but also highlighted the potential of these techniques to outperform traditional binary assessment methods in predicting and understanding the complex behaviour of energetic materials.

The results show the potential of integrating sensor arrays and multivariate analysis into drop hammer testing, significantly improving the reproducibility and reliability of impact sensitivity measurements. This approach not only contributes to safer handling of explosives, but also paves the way for a more sophisticated understanding of energetic materials, which is essential for both industrial applications and safety measures.

Investigating the Aging Effects on the Impact Sensitivity of Hexamethylene Triperoxide Diamine (HMTD) using Drophammer and PTR-ToF-MS

Building on previous research, this study investigates the effects of aging on hexamethylene triperoxide diamine (HMTD), in particular its mechanical sensitivity and reaction behaviour. The study uses a specially designed drop hammer based on OZM BIT complemented with a sensor array to perform impact sensitivity experiments on two batches of HMTD - one freshly synthesised and one aged for three months. The analytical methods used include PTR-ToF and Raman spectroscopy.

The tests found a difference in ignition energy between new and aged HMTD, with the newer sample igniting at lower energies and partial burns occurring more frequently at these lower energies. The presence of acetic acid was significantly higher in the aged HMTD sample, although Raman spectroscopy revealed no significant differences between the new and old batches.

Statistical analyses, such as PCA and LDA, reduced the dimensionality of the sensor data to create classifiers, which were then validated by cross-validation methods. The classifiers have shown that it is possible to distinguish between different aged HMTD batches by observing sensor behaviour during decomposition reactions.

This work is a continuation of efforts to understand the nuanced behaviour of energetic materials and their impact on safety, focusing on the sensing behaviour of the decomposition reaction to potentially distinguish between differently aged batches of HMTD.

Ignition of Explosives Based on Primary Peroxide With an ns Pulsed Laser

Investigation of Laser-Initiation of Graphite Spray-Coated TATP Accompanied by Sensor-Safe Surveillance and Analytical Monitoring Using Microphone and PTR-ToF-MS

This study explores advanced methodologies for the detection and controlled initiation of triacetone triperoxide (TATP), a primary explosive known for its high sensitivity and the ease of its unauthorized manufacture from readily available precursors. The focus is on mitigating risks associated with the explosive characteristics of TATP by employing laser-based initiation techniques that do not lead to full detonation or deflagration. By incorporating coatings with known absorption coefficients, specifically graphite in this instance, it was aimed to achieve a controlled energy transfer to the explosive material, allowing for localized reactions below critical thresholds and without a self-propagating reaction.

In our experiments, TATP samples were prepared with and without a graphite coating and subjected to varying levels of laser power, ranging from 25 mW to 100 mW. The effects of these conditions on the decomposition processes were monitored using a highly sensitive microphone and Proton Transfer Reaction Time-of-Flight Mass Spectrometry (PTR-ToF-MS). This setup enabled detailed analysis of the reaction gases and the physical phenomena occurring during the irradiation process. The results show that a graphite coating influences the interaction between the laser light and the TATP, promotes partial reactions and makes a complete conversion of the explosive mass less frequent. The coated samples showed a stronger dependence on the power of the laser and the processing

settings, leading to reproducible and controlled results. These results are crucial for the development of safe methods for handling, analyzing and neutralizing sensitive explosives like TATP, with applications in security and demilitarization.

Investigation of laser initiation of graphite-coated TATP and HMTD with regard to the influence of coating thickness accompanied by sensor-safe surveillance using a microphone

This study explores advanced methodologies for the detection and controlled initiation of triacetone triperoxide (TATP) and hexamethylene triperoxide diamine (HMTD), primary explosives known for their high sensitivity and ease of unauthorized manufacture from readily available precursors. The focus is on mitigating risks associated with these explosives by employing laser-based initiation techniques that do not lead to full detonation or deflagration. By incorporating coatings with known absorption coefficients, in this case graphite, the aim is to achieve a controlled energy transfer to the explosive material, allowing for localized reactions below critical thresholds. In our experiments, TATP and HMTD samples were prepared with and without a graphite coating and subjected to varying levels of laser power, ranging from 12.5 mW to 100 mW. The effects of these conditions on the decomposition processes were monitored using a microphone. This setup enabled the detailed analysis of the reaction gases and the physical phenomena occurring during the irradiation process. The findings demonstrate that applying a graphite coating significantly influences the interaction between the laser light and the explosives, promoting partial reactions and preventing complete conversion of the explosive mass. The coated samples showed a higher dependence on the laser's power and processing settings, leading to reproducible and controlled outcomes. These results are crucial for the development of safe methods for handling, analyzing, and neutralizing sensitive explosives like TATP and HMTD, with potential applications in security and safety contexts.

Rapid Identification of Explosives

Rapid Library-Free Identification of Energetic Materials

This study presents the development of a high-performance detector system designed to rapidly and accurately identify explosive material systems. The collaborative research project, carried out by the Institute for Safety and Security at Bonn-Rhein-Sieg University of Applied Sciences with SME partners ExploTech GmbH and Innovatec GmbH, aimed to address the pressing need for potent detectors that can distinguish hazardous substances on-site within a very short time frame.

The detector system was engineered with simplicity in mind, allowing for easy operation by individuals without expert knowledge. It boasts a robust design suitable for field use, emphasising the capability for mobile deployment. A significant innovation of this system is its library-free detection feature. Unlike many market-available detectors that can only identify known substances from a predefined library, this system can recognise new and unlisted substances and mixtures, thereby flagging them as explosives, by analysing their physical properties during combustion.

With an array of chemical and physical sensors, the device delivers rapid assessments within 10 seconds of the potential danger posed by unidentified substances. This system's development signifies a substantial advancement in the on-the-spot detection of explosives, offering a powerful tool for security personnel in mitigating the threat of terrorism.

Part III

Results and Discussion: Drop Hammer Experiments

Sensory Monitoring of drop hammer Experiments with Multivariate Statistics

by

Matthias Muhr, Thomas M. Klapötke, Gerhard Holl

DOI: 10.1002/prop.202200025

as published in

Propellants, Explosives, Pyrotechnics 2022, 47, 1-10

Abstract: A precise characterization of substance is essential for the safe handling of explosives. One parameter regularly characterized is the impact sensitivity. This is typically determined using a drop hammer. However, the results can vary depending on the test method and even the operator, and it is not possible to distinguish the type of decomposition such as detonation and deflagration. This study monitors the reaction progress by constructing a drop hammer to measure the decomposition reaction of four different primary explosives (tetrazene, silver azide, lead azide, lead styphnate) in order to determine the reproducibility of this method. Additionally, further possible evaluation methods are explored to improve on the current binary statistical analysis. To determine whether classification was possible based on extracted features, the responses of equipped sensor array, which measures and monitor the reactions, were studied and evaluated. Features were extracted from this data and were evaluated using multivariate methods such as principal component analysis (PCA) and linear discriminant analysis (LDA). The results indicate that although the measurements show substance-specific trends, they also show a large scatter for each substance. By reducing the dimensions of the extracted features, different sample clusters can be represented and the calculated loadings allow significant parameters to be determined for classification. The results also suggest that differentiation of different reaction mechanisms is feasible. Testing of the regressor function shows reliable results considering the comparatively small amount of data.

5.1 Introduction

Performance and safety are important aspects of modern explosives [1]. In order to ensure safe handling of explosives and to prevent accidents, it is important to determine characteristic values for the sensitivity of these materials. The drop hammer test is one of the simplest and fastest methods for determining the impact sensitivity of energetic materials, which is a measure of the kinetic energy that must be applied to cause a material to combust [2, 3]. In drop hammer tests, this value is determined by the kinetic energy of a drop weight dropping on a sample. A major disadvantage, however, is that such measurements cannot provide information about the type and violence of the reaction [4]. Other disadvantage include ample-to-sample variability and subjectivity of the operator [1, 5, 6, 7, 8]. In addition, different types of drop hammers are used in different laboratories, and therefore, the results can only be compared to a limited extent [1, 4, 9, 10]. The

initiation with drop hammers is poorly understood and not comparable to other initiation mechanisms [5, 7, 11].

The Bundesamt für Materialprüfung (BAM) drop hammer is often used for the characterization of explosives [12, 13]. Klapötke et al. have found that results with the BAM drop hammer provide only limited results regarding the impact sensitivity. The reason for this is the sample preparation between two bolts in a cylinder, in which the impact on the weight can ignite the sample by adiabatic compression [1]. An apparatus that compensates for this shortcoming is the OZM ball impact tester (BIT) [14]. With this device, the sample is smoothed on a metal surface without damaging it, and a steel ball serves as a drop weight [14, 15]. Approaches to using the drop hammer method have been explored in various publications, such as equipping drop hammers and other methods for initiating explosives with sensors [7, 9, 16, 17, 18]. An important example of these methods is the glass anvil drop hammer, which enables recording of reaction processes using a high-speed camera. The use of the glass anvil drop hammer allows hot spots to be detected and measured. Likewise, processes such as phase transitions can be observed immediately before the ignition of the substance [4, 19]. In addition, Klapötke et al. determined that individual substances emit different sound levels during combustion [2]. Reactions were examined spectroscopically and with pyrometers. These publications show that it is possible to detect different kinds of reactions in substances and for some substances even two successive reactions can be observed [6, 20]. However, it is difficult to determine reproducible parameters for substances, since the reactions vary both in course and violence [6].

Various statistical methods such as E50, no-fire-level, 1-out-of-10 etc. are used to evaluate drop hammer tests [2, 12]. These methods are sufficient for the evaluation of the pure binary test response. However, the data resulting from sensory monitoring cannot be accurately and completely analyzed with such methods. Nefati et al. have attempted to train neural networks with databases of impact sensitivities of explosives and predict their characteristics [21]. By applying multivariate statistics, it is possible to determine characteristic values and their correlation to the properties of explosives, which could improve on a purely binary evaluation [16, 22]. Going further with this idea, we evaluate the possibility of visualization of the multidimensional measurement results of drop hammer experiments to find clusters and correlations according to substance-specific features.

In this publication, a drop hammer similar to the OZM BIT was constructed. It was equipped with a sensor array consisting of a pyrometer, a spectrometer, a VIS diode, a

microphone, and a piezo vibration sensor. This drop hammer was then used to measure tetrazene, silver azide, lead azide, and lead styphnate, whereby the energy of the ball was adjusted so that all samples decomposed safely. The measured data was checked for the progression of the reaction and 42 features were extracted from each measurement. The extracted features were analysed using multivariate statistics. Clusters and substance-specific features were extracted.

The aim of the measurement was to find out how reproducible the sensor reaction of the material are. Additionally, it was investigated whether the substance can be distinguished based on the sensor response and extracted feature.

5.2 Experimental Section

5.2.1 drop hammer

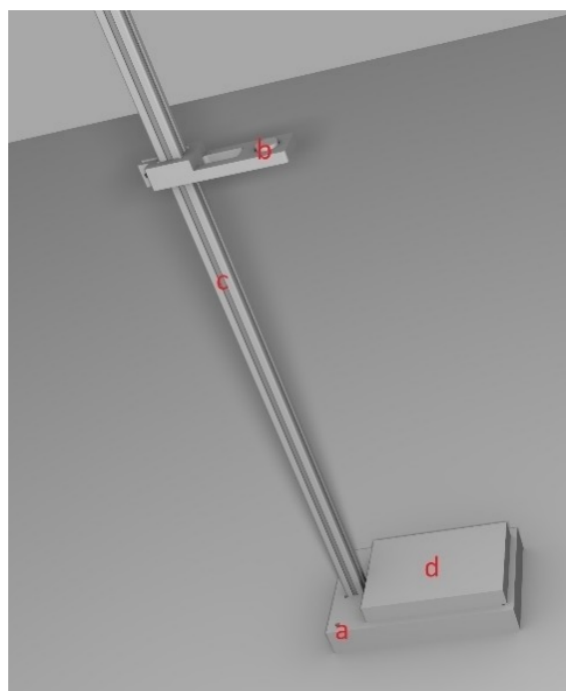


Figure 5.1: Model of the revised structure of the drop hammer - a: base plate, b: head plate with electromagnet, c: extrusion profile for height adjustment, d: ceramic plate for sample preparation

A drop hammer was constructed based on the Ball Impact Tester (BIT) from the com-

pany OZM, since measurements with this apparatus, compared to the BAM drop hammer, provide more realistic results [1]. A steel ball is dropped onto a sample from a defined height in order to initiate combustion. Figure 5.1 shows the basic setup of the test stand, consisting of a stainless-steel base plate, which can be screwed to the table for stability (a), a head part, on which an electromagnet is installed with which the ball can be held or dropped (b), an aluminum rod, on which the head can be fixed continuously (c), and a ceramic plate, on which the sample is placed (d). In the BIT, the sample is applied to a steel plate. However, this shows wear in the form of depression and corrosion after a few tests. Since these damages can tarnish or interfere with measurements, a significantly harder Al_2O_3 ceramic plate was used instead in this setup.

In the conventional BIT, the ball is released via a ramp with a flap, which causes the ball to rotate. This can cause friction, which initiates the sample in addition to impact [1]. The position at which the ball hits can also vary based on the height from which the ball is dropped. Thus, without camera monitoring, it is difficult to decide if a sample with a negative result was not hit, or if the initiation energy was not sufficient. To counteract this, an electromagnet was used in this setup, so that the ball always falls vertically. The height can be set between 5 cm and 95 cm by adjusting the position of the electromagnet on the rod. By using different steel balls (8.91 g – 23.86 g), energies of 4.4 mJ to 222 mJ can be achieved.

5.2.2 Sensor Array

For the sensory monitoring of the setup, a sensor array consisting of various sensors was attached to the drop hammer. Figure 5.2 shows a schematic diagram of the sensor chamber of the drop hammer. The sensor array consists of a pyrometer (Kleiber Series 840(a)), a spectrometer (Ocean Optics USB 2000) with a $50\ \mu\text{m}$ fibre and a collimating lens (Ocean Optics 74-VIS Collimating Lens(b)), a photodiode (Conrad Electronic TRU COMPONENTS 1000 nm 3004 M1 C (c)), a MEMS microphone (ELV MEMS1 (d)) and a piezo shock sensor (TE Connectivity Vibration Sensor (e)). The sensor chamber is encapsulated in a housing (f) with openings for the ball (f1) and for the pyrometer (f2). For data acquisition (apart from the spectrometer, since it has a Serial COM port), a DAQ card (National Instruments, PCI-6122) was used for differential and simultaneous readout. The sampling rate was 100 kS/s and all sensors on the DAQ card were read out single ended. The spectrometer recorded one spectrum per measurement with an integration time of 100 ms.

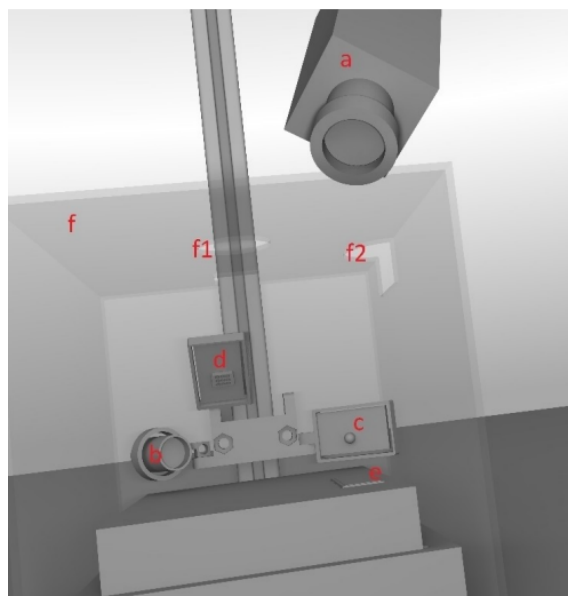


Figure 5.2: Sensor array of the drop hammer - a: pyrometer, b: spectrometer+collimator, c: VIS diode, d: MEMS microphone, e: piezo sensor, f: housing, f1: aperture for ball, f2: aperture for pyrometer

5.2.3 Samples and Sample Preparation

Four different explosives were tested during the measurements: tetrazene ($C_2H_6N_{10}$, water content: 30 %), silver azide (AgN_3 , water content: 15 %), lead azide ($Pb(N_3)_2$, water content: 30 %) and lead styphnate ($C_6HN_3O_8Pb$, water content: 30%). All explosives were provided by DyniTEC GmbH. Sugar was also measured to determine the influence of the ball impact on the microphone and the piezo crystal, and to differentiate it from the signal of the explosive. In addition, blank measurements were made. The sample preparation was standardised by first drying the sample in a desiccator for 12 hours, and subsequently placing it on the ceramic plate of the drop hammer according to the sample preparation used for the BIT [14]. As shown in Figure 5.3, the preparation involved a measuring spoon (a) being used to apply $10 \mu L$ of the sample (b). The sample was then smoothed to a thickness of 0.3 mm with a slider and a rail (c, d). The substances described above, and the corresponding sample preparation, were applied for all measurements.

5.2.4 Measurement Parameters

The drop hammer was set to a height of 50 cm. A 9.81 g ball was used, resulting in an energy of 48 mJ. This energy is higher than the impact sensitivity of the explosives used (tetrazene E16.6: 21 mJ, silver azide E16.6: 29 mJ, lead azide E16.6: 37 mJ, lead styphnate monohydrate: 2.5–5 J (all determined with BAM drop hammer) [14, 15]). The parameters were left unchanged across all measurements. The samples were neither tilted nor were individual particle sizes sieved out. 20 measurements per substance were performed. With each attempt, all sensors were logged for three seconds. The data recording starts one second before the magnet is deactivated and the ball falls.

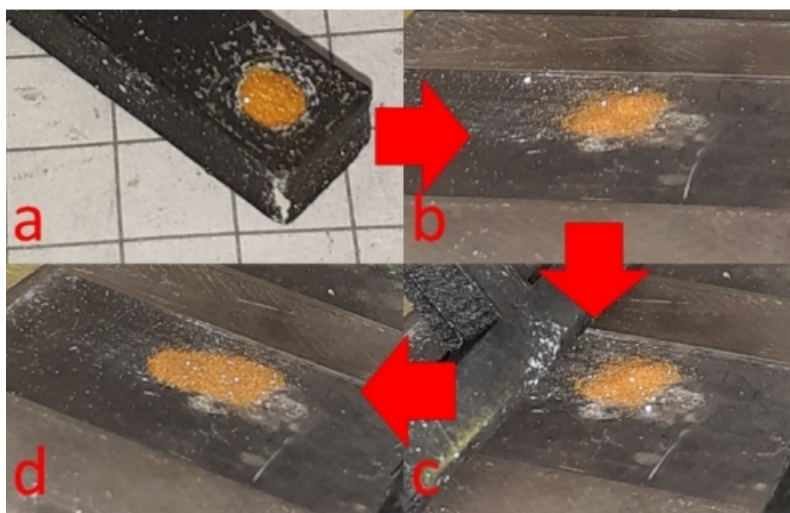


Figure 5.3: Sample preparation for the drop hammer test, a: measure the amount of substance, b: apply on the plate, c: smoothed with slider, d: prepared sample with 0.3 mm thickness

5.2.5 Pre-Processing and Statistics

The sensor responses of the measurements were pre-processed and evaluated using a Python script [23]. The time axis of the sensors (excluding the spectrometer) was normalised to the first exceeding of a threshold value of the piezo signal. For all plots of the raw data, a section of 10 ms before and 100 ms after this peak was extracted from the signals recorded by all sensors. The piezo sensor was chosen because a specific change in the sensor signal can be expected even with blank substances. By adjusting the temporal offsets of the sensor, signals can be estimated and compared. A blank spectrum was

performed immediately before the main measurement and subtracted as a background measurement from the spectrum. To extract and display substance specific characteristics from the measurements, 42 features were extracted from each measurement. The integral of the entire emission spectrum and the wavelength with the maximum intensity were extracted from the spectrometer data. Ten features were extracted from each of the other sensors: the maximum of the signal, the signal integrated over time, the time of the maximum, the time at which the signal exceeds the threshold for the first time, the time at which the signal exceeds the threshold for the last time, the slope from the start of the peak to the maximum, the width of the peak, the width of the peak at half the height of the maximum, the width of the peak divided by the maximum of the peak and the width at which the signal exceeds the measurement range. The last feature describes the duration during which the signal is outside the measuring range. Since the extracted 42 features had too many dimensions for a graphical evaluation, they were reduced using Principal Component Analysis (PCA). For this purpose, the data was first pre-processed using a unit vector and then calculated using scikit-learn's PCA library with standard parameters [24] to calculate three principal components. Through the reduced dimension it can be determined whether clusters become apparent when the data is plotted. The loadings can then be used to identify which of the extracted features could be useful for characterising and identifying the substances and which features are obsolete or redundant. The library scikit-learn [24] with singular value decomposition as the solver was also used to perform the LDA, using the entire dataset of extracted features. Since this method belongs to the supervised methods, it is not only possible to search for substance specific clusters in the data, but also to determine a regressor function. With the regressor function, identification of unknown samples is possible. Despite the relatively small data set, the correctness of the regressor function was determined by cross-validation, using the leave-one-out cross-validation procedure. In this process, each measurement is used iteratively over all measurements as test data set. The regressor function was calculated from the rest of the dataset and the average error rate of all measurements was calculated.

5.3 Results and Discussion

5.3.1 Sensor Data

In the following chapter, a characteristic measurement for each sensor is shown for all types of explosives.

VIS Diode

The sensor responses of the VIS diode are shown in Figure 5.4. Sharp peaks can be seen in the sensor responses of lead styphnate, silver azide and lead azide, which are probably caused by a fast and violent decomposition of the sample [7, 22]. Looking at the sensor response of lead styphnate, a second, smaller and broader peak can be seen. This behaviour is frequently observed with this sample and in a wide range of intensities (Figure 9). It is also occasionally observed in measurements with azides. This is possibly due to a moderate decomposition reaction, as described by Basset et al. [5], when the sample particles are whirled up by the ball. This will be verified in future measurements using a high-speed camera. In measurements with tetrazene, there is usually no signal above the noise level.

Pyrometer

The signals of the pyrometer (Figure 5.5) are very similar to those of the VIS diode. Concerning lead styphnate, lead azide and silver azide, we also see comparatively high peaks, which are due to a fast and violent reaction of the sample [6, 7, 22]. It is noticeable that these signals take significantly more time to dissipate in comparison to those of the VIS diode. This could be explained by the vapours released during the reaction. These emit IR radiation and last longer than the emission of visible light.

It can also be seen that the signals are cut off at 5 V because the upper end of the measuring range of the Pyrometer has been reached. A second, smaller peak or tailing due to a mild side reaction is observed for the substances lead styphnate, lead azide, and silver azide. As with the VIS diode, tetrazene does not produce any signal.

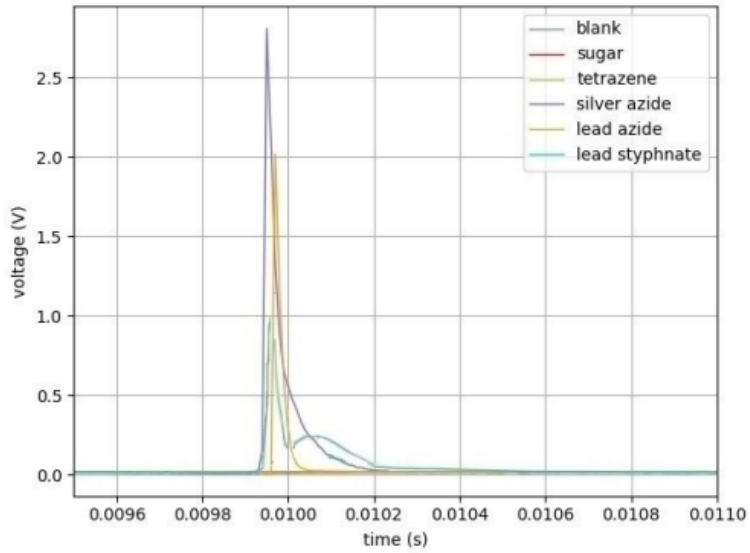


Figure 5.4: Characteristic signals of the VIS-diode of all six substances

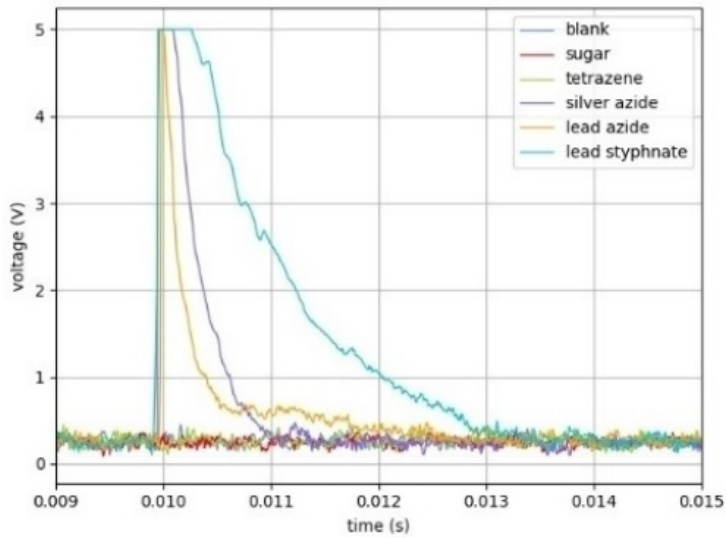


Figure 5.5: Characteristic signals of the pyrometer of all six substances

Microphone

Looking at the signals of the microphone (Figure 5.6), a signal can be detected in all samples. In the case of sugar and the blank measurement, this is generated exclusively by the impact of the ball. The signals are weakened when measured with sugar compared to the blank measurement, due to the fact that sugar mitigates the noise of impact compared to an impact between the steel ball and the ceramic plate. Signals of all explosives are clearly above those of the blank substances.

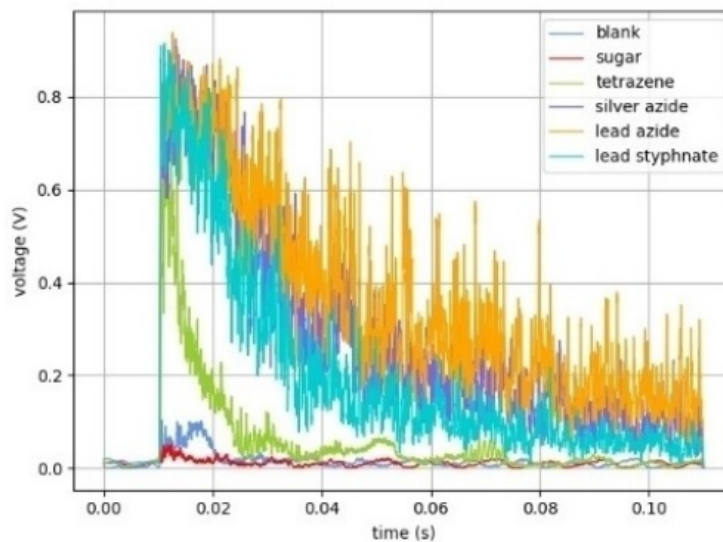


Figure 5.6: Characteristic signals of the microphone of all six substances.

As with the pyrometer, it can be seen that the measuring range of the microphone is not sufficient. At an output voltage of about 0.9 V, the microphone membrane has reached its maximum amplitude. Comparing the width of the peaks, tetrazene shows the narrowest peaks. Measurements of lead azide and silver azide show similar sensor responses, while lead styphnate shows slightly shorter signals on average.

Piezo Sensor

Figure 5.7 shows the characteristic measurement signals of the piezo crystal. Looking at the measurements of the blank samples, a signal due to the ball is also recognisable. The signal of the explosives shows a similar behaviour for all types of explosives. First, a relatively high, sharp peak can be seen, followed by a chaotic oscillating decay. This is

clearly less pronounced with tetrazene than with the other explosives investigated.

Spectrometer

The spectra of the measurements are shown in Figure 5.8. From each of the spectra shown, a blank measurement was taken immediately before the actual measurement. If one looks at the measurements of the blank substances, no peaks are recognisable. The same behaviour can be observed with tetrazene. Looking at the spectra of silver azide, peaks of the respective cations are visible (peaks silver: 256.423 nm, 466.847 nm, 519.817 nm, 546.549 nm, peaks lead: 405.780 nm, 589.562 nm, 500.541 nm, 256.423 nm [25]). However, since the wavelength is not considered in the evaluation, it is not discussed any further. Generally speaking, measurements of lead styphnate show a larger background than the spectra of the azides.

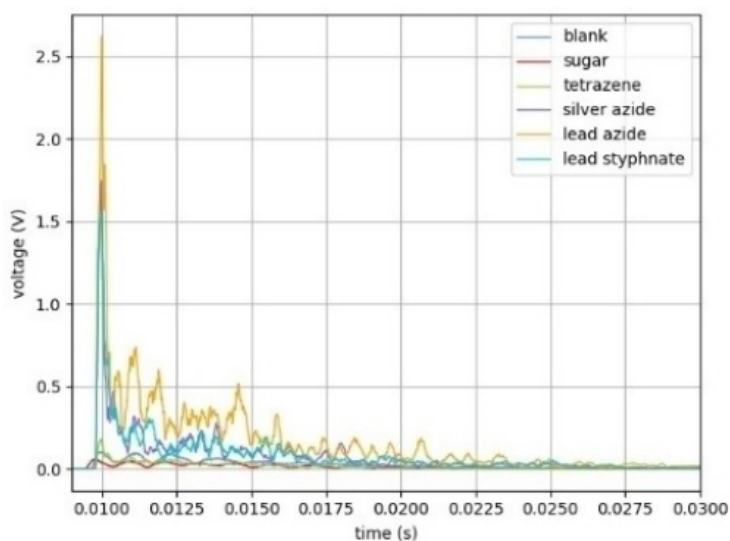


Figure 5.7: Characteristic signals of the piezo sensor of all six substances

5.3.2 Reproducibility of Lead Styphnate Measurements

If one compares the measurements from one sensor to another for an individual substance, it is noticeable that the sensor responses and signal curves are poorly reproducible. This applies to both the VIS diode and the pyrometer. Looking at the sensor responses of the VIS diode of lead styphnate (Figure 5.9), a main peak of the conversion can be identified

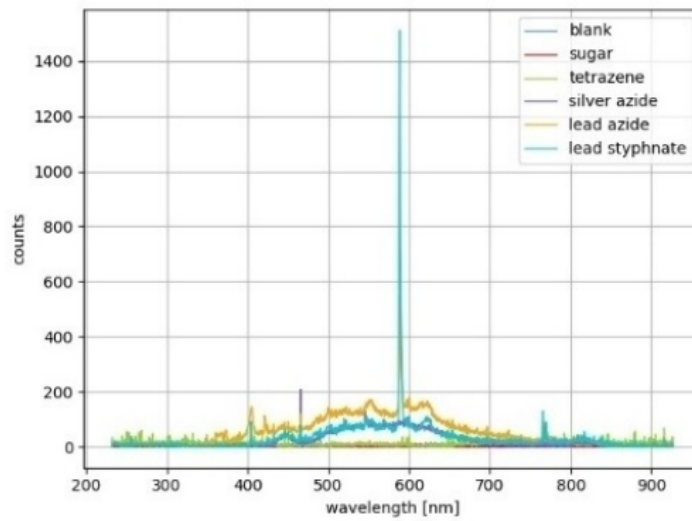


Figure 5.8: Characteristic signals of the spectrometer of all six substances.

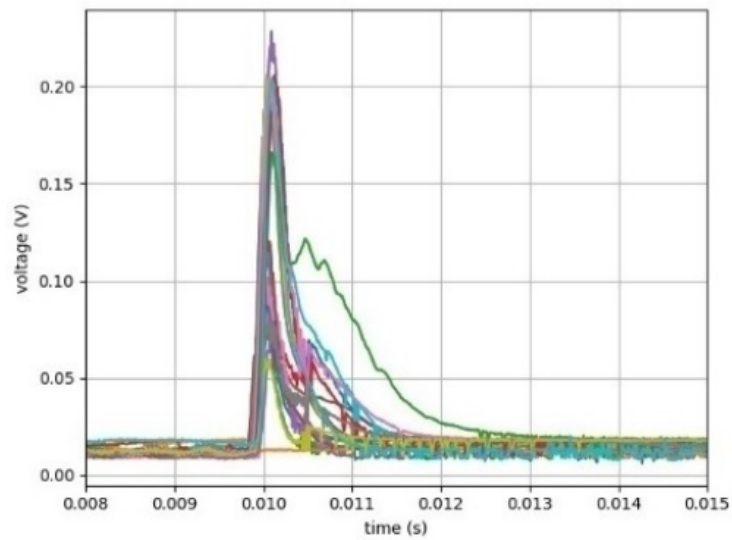


Figure 5.9: Lead styphnate - all 20 measurements, VIS-diode.

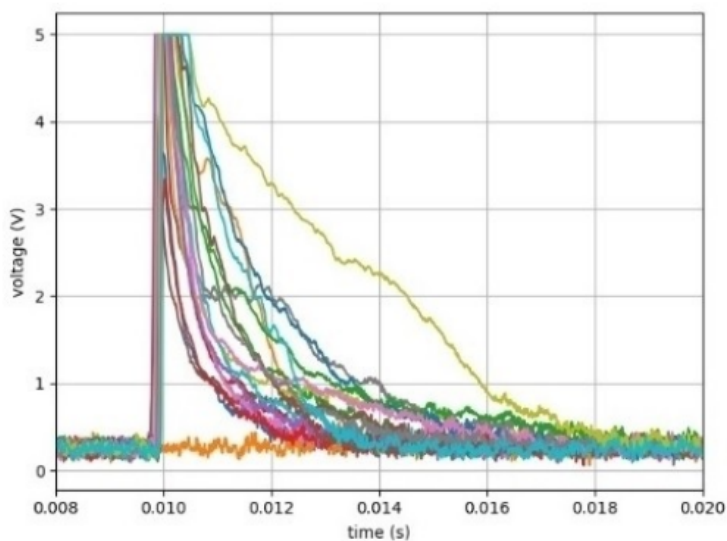


Figure 5.10: Lead styphnate - all 20 measurements, pyrometer

in each measurement. As already described, this peak is narrow and highly pronounced. The intensity of this peak varies among all measurements. This main peak is sometimes followed by a second, smaller peak or tailing, which is caused by partial conversions of the particles dispersed through the ball. These reactions vary greatly in form and intensity. The same behaviour can be observed in the signal curves of lead styphnate in the pyrometer (Figure 5.10). Here, all measurements show an initial high and comparatively narrow peak. It is noticeable that the end of the measuring range of the pyrometer is reached with almost every measurement, which makes an evaluation of the peak maximum difficult. The first peak is also partially followed by tailing caused by side reactions. The measurement ranges of the VIS diode, the pyrometer and the microphone are problematic, since the signal of the sensors is cut off in many measurements. However, a reduction in sensitivity would have the disadvantage that substances that show comparatively mild reactions (e.g., tetrazene) could no longer be detected.

5.3.3 Feature Extraction and Discrimination

Features were extracted from the data of all measurements using the described Python script. All features were statistically evaluated and compared. Figure 5.11 shows the mean values of the integral of the pyrometer signals of all substances.

Silver azide, lead azide and lead styphnate clearly stand out from the blanks and

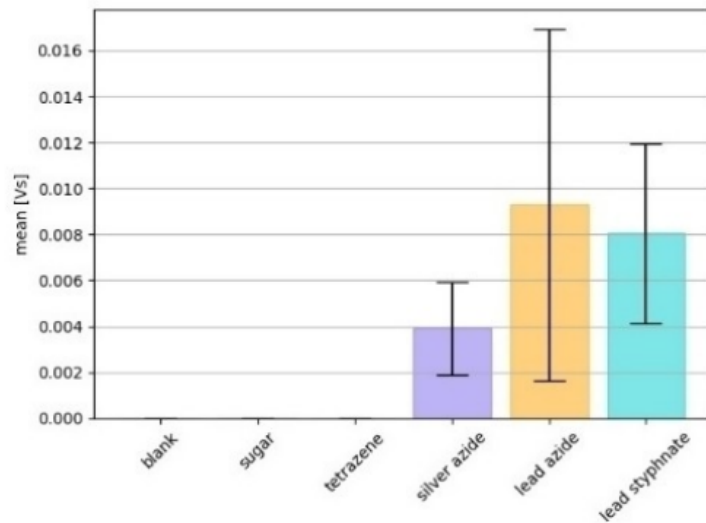


Figure 5.11: Average of the integral of the pyrometer signal, standard deviation drawn in

tetrazene. Looking at the errors, it can be seen that the values of the extracted features scatter strongly. This correlates with the observations from Figure 5.10. As already described in the literature, the samples show a high scatter in the extracted features. Although trends can be seen in the mean values, the standard deviations are high. Based on the individual extracted characteristics, substance specific trends can be recognised, but a classification on the basis of this is not possible. Looking at the pyrometer data (Figure 5.11), it is not possible to differentiate tetrazene from blank and sugar measurements. Lead azide, silver azide and lead styphnate differ significantly in their mean values, but the values are highly scattered. Looking at the average values of the integrated microphone signals of all samples (Figure 5.12), clear gradations can be seen. It is possible to distinguish the substances based on this feature, but there is a high standard deviation.

The dimensions of the entirety of the extracted data are reduced to three dimensions using PCA. The variance of these dimensions is about 65 %. Figure 5.13 plots the calculated three principal components against each other. The first principal component accounts for 48 %, the second 10 % and the third about 7 % of the total variance of the data set. The substances tend to form clusters. Sugar and blank measurements consistently show negative values for PC 1. The measurements with tetrazene are comparatively close to the blank measurements. This is probably due to the mild combustion compared to the other explosives. Looking at the lead-containing compounds, they show a much stronger scatter than all other substances. Lead styphnate shows a very large expansion of the

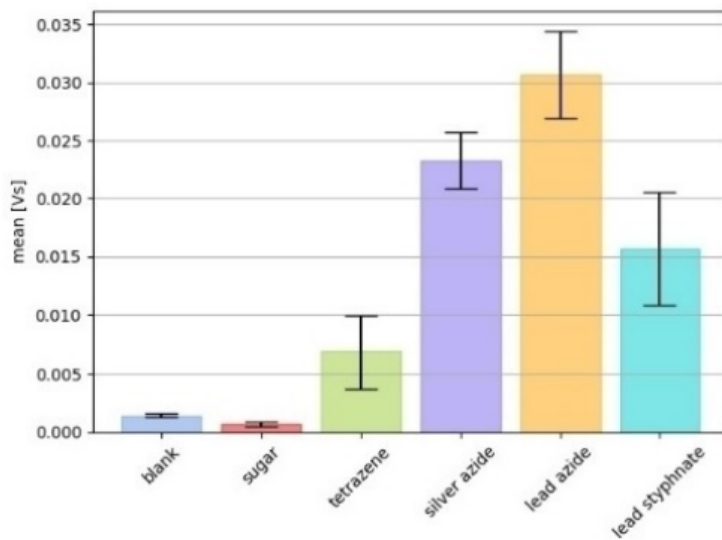


Figure 5.12: Average of the integral of the microphone, standard deviation drawn in.

point cloud. This is consistent with the observations of high variances in the raw data and the extracted features. Based on the results, it can be said that the substances are differentiable based on the reduced data set. Looking at the PCA loadings with the total variance of the individual sensors as a measure of separation (Figure 5.14), the signals from the VIS diode contribute most to the separation. The pyrometer, the microphone and the piezo crystal also contribute strongly to the separation and thus prove to be efficient for the differentiation of the measured substances. The weighting of the spectrometer is rather low. It can be omitted in future measurements. Furthermore, the dimensions of the extracted features were reduced with an LDA. Figure 5.15 shows the reduced data set. The samples form clusters so that they can be distinguished based on the reduced data. As expected, the blank measurements show a relatively low dispersion.

If we look at tetrazene, all measurements are grouped, although highly scattered. Silver azide and lead azide also form clusters. Looking at lead styphnate, there are two outliers. Their cause and occurrence must be examined in more extensive measurement series. Lead styphnate tends to form clusters but the measurements scatter strongly. This is consistent with the observation that lead styphnate (Figure 5.9) gives very diverse sensor responses. A regressor function was calculated and tested with a leave-one-out cross validation as described in chapter 2.5. The calculated error rate is 6.6 %. Figure 5.16 shows the results of the cross validation in a confusion matrix. If we consider this, all

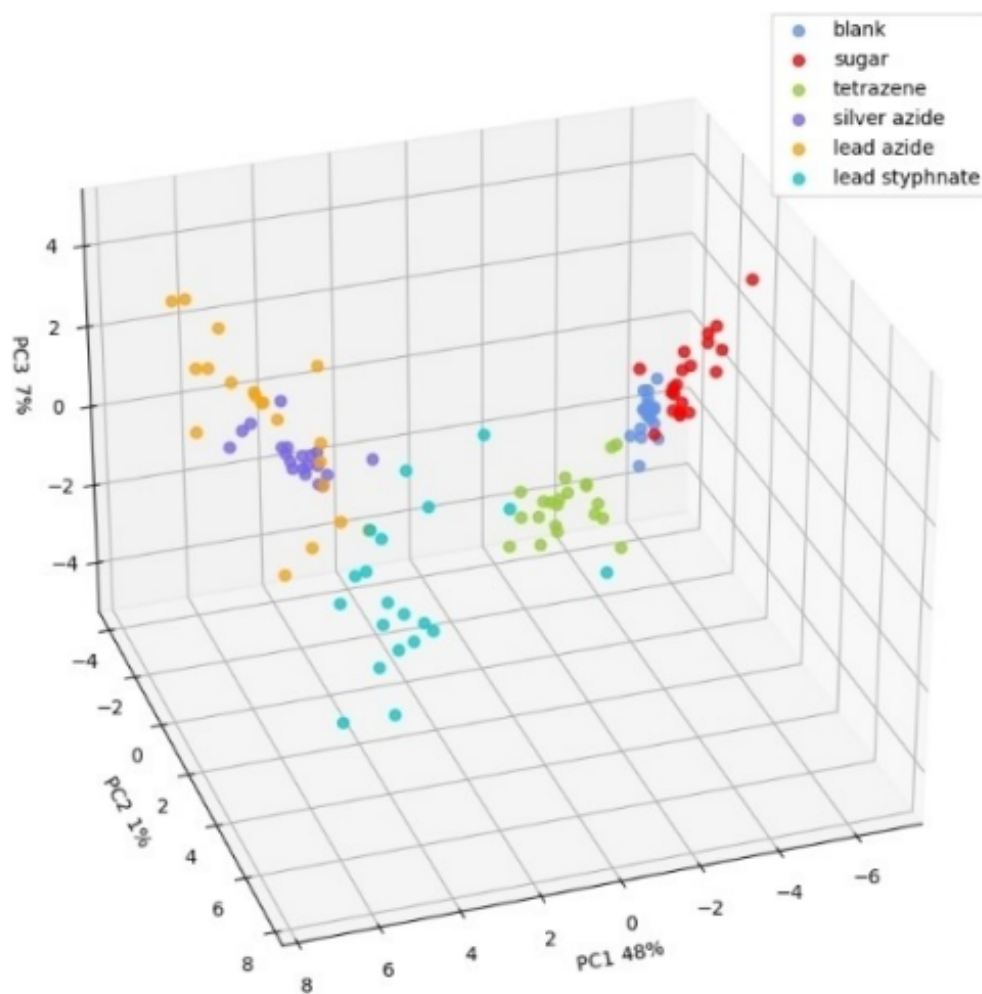


Figure 5.13: Plot of three calculated principal components.

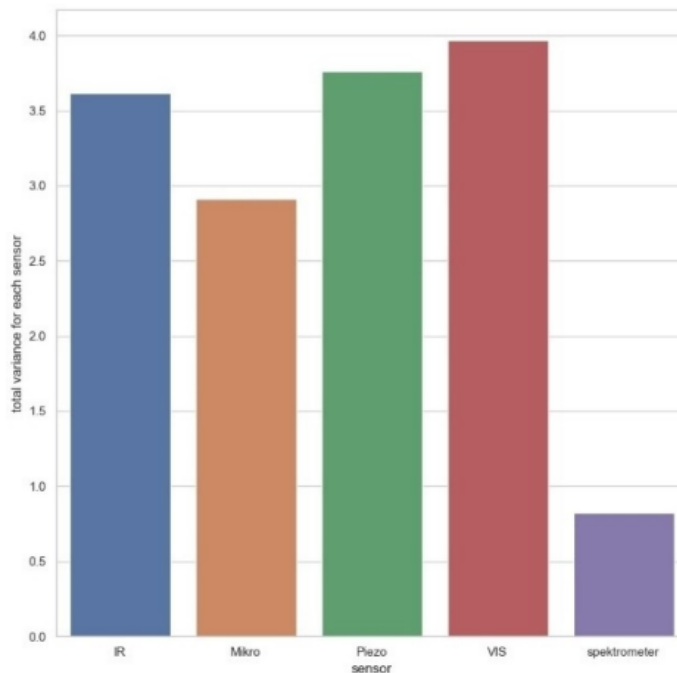


Figure 5.14: Total variance of each sensor

blank measurements as well as all measurements with lead azide were correctly assigned. For sugar and silver azide, one measurement each was incorrectly assigned. For tetrazene, two measurements were incorrectly assigned, one as a blank measurement and the other as a lead styphnate measurement. This result also correlates with the observations. Two of lead styphnate measurements were assigned to silver azide and one each to the blank measurement and tetrazene. This is consistent with the occurrence of outliers in the data reduced by LDA.

The results are a preview for future measurements where the sample size will be significantly increased. The first results show the possibility of distinguishing between different substances, so that it may also be possible to distinguish between different decomposition mechanisms of the individual substances, such as detonation and deflagration.

5.4 Conclusion

A drop hammer was built in the style of the OZM BIT. The drop mechanism and the sample plates were changed. This setup was equipped with an array of different sensors:

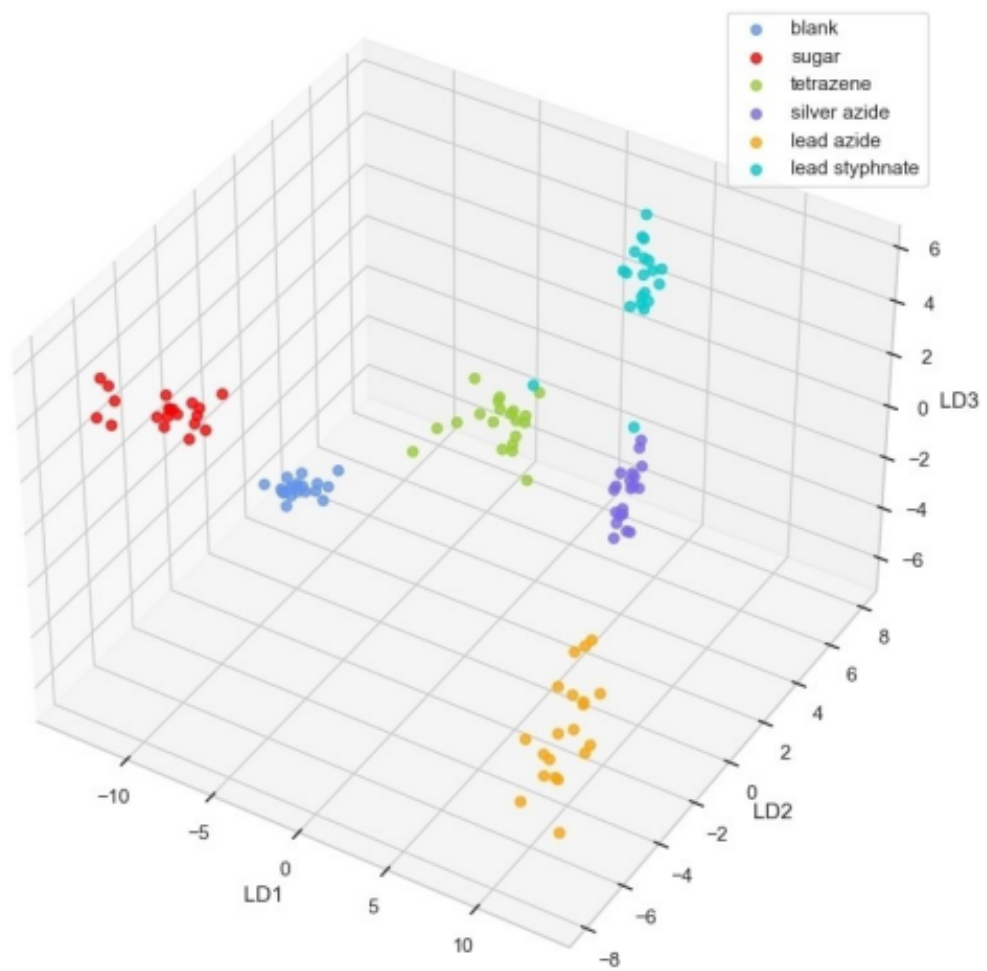


Figure 5.15: LDA of the extracted features

blank	20	0	0	0	0	0
sugar	0	19	1	0	0	0
tetrazene	1	0	18	0	0	1
silver azide	1	0	0	19	0	0
lead azide	0	0	0	0	20	0
lead styphnate	1	0	1	2	0	16
	blank	sugar	tetrazene	silver azide	lead azide	lead styphnate

Figure 5.16: Confusion matrix of a leave-one-out cross validation.

a microphone, a piezo vibration sensor, a VIS diode and a pyrometer. Four primary explosives, namely tetrazene, silver azide, lead azide and lead styphnate, were tested with this setup. The energy of the ball was selected so that all samples reacted adequately. The measurement data was first reviewed and the behaviour of the individual samples was analysed. It is noticeable that some substances show a high variance in sensor responses, especially lead styphnate. For some samples, the signals exceed the measuring range. It was not possible to counteract this issue, since other signals for substances such as tetrazene lie in the lower area of the measuring range. Thus, for future planned measurements, the dynamic range of the affected sensors will be expanded. In addition, several sensors with different measuring ranges will be used. Features from all measurements were extracted and compared. Despite strong standard deviations of the individual features, substance specific trends are recognisable. Due to only small scatter in blank measurements, the influence of the setup on the total scatter of all samples is negligible. PCA was carried out for the purpose of dimension reduction. The substances tend to form clusters. When looking at the loadings, especially the signals of the VIS diode and the pyrometer contribute a large share to the total variance. The influence of the spectrometer on the total variance is rather small - for future measurements it can be omitted. To assess whether the extracted features are suitable for classification, an additional LDA was carried out, despite the comparatively small data set. The results of the LDA show that the substances cluster and a separation of the substances could be possible by means of the extracted features. Furthermore, the data show that it might be possible to identify different decomposition mechanisms of the substances and to depict parameters that favour the respective mechanisms. For future research, measurements with significantly higher sample sizes should be carried out to increase the precision of the regressor function. In addition, samples with different impact energies of the ball as well as different ball sizes are to be used to investigate the influence of these parameters on the decomposition of the samples.

References

- [1] M. S. Gruhne, M. Lommel, M. H. H. Wurzenberger, N. Szimhardt, T. M. Klapötke, and J. Stierstorfer. "OZM Ball Drop Impact Tester (BIT-132) vs. BAM Stan-

- ard Method – a Comparative Investigation”. In: *Propellants Explos. Pyrotech.* 45 (2020), pp. 147–153. URL: <https://doi.org/10.1002/prop.201900286>.
- [2] T.M. Klapötke and C.M. Rienäcker. “Drophammer test investigations on some inorganic and organic azides”. In: *Propellants, Explosives, Pyrotechnics* 26.1 (2001), pp. 43–47. DOI: 10.1002/prop.200100073.
- [3] N. Lease, M. D. Holmes, M. A. Englert-Erickson, L. M. Kay, E. G. Francois, and V. W. Manner. “Analysis of Ignition Sites for the Explosives 3,3’-Diamino-4,4’-azoxyfurazan (DAAF) and 1,3,5,7-Tetranitro-1,3,5,7-tetrazoctane (HMX) Using Crush Gun Impact Testing”. In: *ACS Mater. Au* 1 (2021), pp. 116–129. URL: <https://doi.org/10.1021/acsmaterialsau.1c00013>.
- [4] S. M. Walley, J. E. Field, R. A. Biers, W. G. Proud, D. M. Williamson, and A. P. Jardine. “The Use of Glass Anvils in Drop-Weight Studies of Energetic Materials”. In: *Propellants Explos. Pyrotech.* 40 (2015), pp. 351–365. URL: <https://doi.org/10.1002/prop.201500043>.
- [5] Zhiwei Men, Kenneth S. Suslick, and Dana D. Dlott. “Thermal Explosions of Polymer-Bonded Explosives with High Time and Space Resolution”. In: *J. Phys. Chem. C* 122.26 (2018), pp. 14289–14295. DOI: 10.1021/acs.jpcc.8b02422.
- [6] Z. Men, K. S. Suslick, and D. D. Dlott. “Thermal Explosions of Polymer-Bonded Explosives with High Time and Space Resolution”. In: *J. Phys. Chem. C* 122 (2018), pp. 14289–14295. URL: <https://doi.org/10.1021/acs.jpcc.8b02422>.
- [7] D. M. Williamson, S. Gymer, N. E. Taylor, S. M. Walley, A. P. Jardine, A. Glauser, S. French, and S. Wortley. “Characterisation of the impact response of energetic materials: observation of a low-level reaction in 2,6-diamino-3,5-dinitropyrazine-1-oxide (LLM-105)”. In: *RSC Adv.* 6 (2016), pp. 27896–27900. URL: <https://doi.org/10.1039/C6RA03096C>.
- [8] R. M. Doherty and D. S. Watt. “Relationship Between RDX Properties and Sensitivity”. In: *Propellants Explos. Pyrotech.* 33 (2008), pp. 4–13. URL: <https://doi.org/10.1002/prop.200800201>.
- [9] C. S. Coffey and V. F. de Vost. “Impact Testing of Explosives and Propellants”. In: *Propellants Explos. Pyrotech.* 20 (1995), pp. 105–115. URL: <https://doi.org/10.1002/prop.19950200302>.

- [10] Thomas M. Klapötke. *High Energy Materials*. Berlin, New York: Walter de Gruyter, 2009. ISBN: 9783110207453.
- [11] C. A. Handley, B. D. Lambourn, N. J. Whitworth, H. R. James, and W. J. Belfield. “Understanding the shock and detonation response of high explosives at the continuum and meso scales”. In: *Applied Physics Reviews* 5 (2018), p. 031303. URL: <https://doi.org/10.1063/1.5005997>.
- [12] Josef Köhler, Rudolf Meyer, and Axel Homburg. *Explosivstoffe*. 10th revised and expanded edition. Weinheim: Wiley-VCH, 2008.
- [13] NATO Standardization Agreement (STANAG) 4489. *Explosives, Impact Sensitivity Tests (4489)*. 1999.
- [14] Ball-Drop Impact Tester BIT132. *Ball-Drop Impact Tester BIT132*. OZM Research. accessed 11 August 2022. 2022. URL: <https://www.ozmresearch.com/en/product/ball-drop-impact-tester-bit-132/>.
- [15] United States Military Standard 1751 A (MIL-STD-1751 A). *Safety and performance tests for qualification of explosives (high explosives, propellants and pyrotechnics), Method 1016*. 2001.
- [16] S. Maurer, R. Makarow, J. Warmer, and P. Kaul. “Fast testing for explosive properties of mg-scale samples by thermal activation and classification by physical and chemical properties”. In: *Sens. Actuators B: Chem.* 215 (2015), pp. 70–76. URL: <https://doi.org/10.1016/j.snb.2015.03.045>.
- [17] J. G. Reynolds, P. C. Hsu, G. A. Hust, S. A. Strout, and H. K. Springer. “Hot Spot Formation in Mock Materials in Impact Sensitivity Testing by Drop Hammer”. In: *Propellants Explos. Pyrotech.* 42 (2017), pp. 1303–1308. URL: <https://doi.org/10.1002/prop.201700115>.
- [18] P. J. Rae and P. M. Dickson. “Some Observations About the Drop-weight Explosive Sensitivity Test”. In: *J. Dyn. Behav. Mater.* 7 (2021), pp. 414–424. URL: <https://doi.org/10.1007/s40870-020-00276-2>.
- [19] Y. Wu, H. Duan, K. Yang, H. Guo, and F. Huang. “Ignition and Combustion Developments of Granular Explosive (RDX/HMX) in Response to Mild-Impact Loading”. In: *Propellants Explos. Pyrotech.* 45 (2020), pp. 1250–1268. URL: <https://doi.org/10.1002/prop.201900365>.

- [20] M. C. Phillips, B. E. Bernacki, S. S. Harilal, B. E. Brumfield, J. M. Schwallier, and N. G. Glumac. “Characterization of high-explosive detonations using broadband infrared external cavity quantum cascade laser absorption spectroscopy”. In: *J. Appl. Phys.* 126 (2019), p. 093102. URL: <https://doi.org/10.1063/1.5117306>.
- [21] H. Nefati, J.-M. Cense, and J.-J. Legendre. “Prediction of the Impact Sensitivity by Neural Networks”. In: *J. Chem. Inf. Comput. Sci.* 36 (1996), pp. 804–810. URL: <https://doi.org/10.1021/ci950223m>.
- [22] K. Konstantynowski, G. Njio, and G. Holl. “Detection of explosives – Studies on thermal decomposition patterns of energetic materials by means of chemical and physical sensors”. In: *Sens. Actuators B Chem.* 246 (2017), pp. 278–285. URL: <https://doi.org/10.1016/j.snb.2017.02.077>.
- [23] Python.org. *Download Python*. accessed 14 September 2021. 2021. URL: <https://www.python.org/downloads/>.
- [24] Scikit-learn. *Scikit-learn: Machine learning in Python*. Documentation. accessed 19 August 2021. 2021. URL: <https://scikit-learn.org/stable/>.
- [25] NIST. *Atomic Spectra Database*. accessed 14 September 2021. 2020. URL: <https://www.nist.gov/pml/atomic-spectra-database>.

Sensor-Monitored Impact Sensitivity Investigations on HMTD of Different Ageing Stages With Accompanying PTR-TOF Measurements of the Substances

by

Matthias Muhr, Emre Ünal, Phillip Raschke Thomas M. Klapötke, Peter Kaul

DOI: 10.1080/07370652.2023.2295280

as published in

Journal of Energetic Materials 2024, 42, 1-15

The work reported on in this publication was carried out together with Mr Emre Ünal. The personal contribution amounts to around 50 %. The main focus was on the production of the hardware and the sensor technology. This involved the construction and revision of the drone on the one hand and the optimisation of the sensor technology and data acquisition on the other. In addition, the planning and evaluation was carried out using multivariate statistics. The focus was on feature extraction and finding trends in the data.

Abstract: Hexamethylene triperoxide diamine (HMTD) is a commonly used homemade explosive due to its simple synthesis and availability of reactants. However, its impact sensitivity may vary significantly depending on synthesis methods and possibly substance ageing, presenting safety concerns during handling. In this study, two batches of HMTD, one stored for 3 months and one freshly synthesized, were investigated. Analytical techniques including Raman spectroscopy and PTR-ToF were utilized for the HMTD specimen. A custom-designed drop hammer based on OZM's Ball Impact Tester, equipped with optical and acoustic sensors, was employed to evaluate impact sensitivity and chemical reaction process. The setup was tested and validated with HMTD, TATP and lead azide and silver azide. Extracted features of sensor data were subjected to multivariate statistical analysis (LDA, PCA) to assess the impact of ageing to impact sensitivity and reaction characteristics. The study aimed to determine the correlation between substance composition and reaction behaviour. The results contribute to the understanding of the influence of ageing on the response and mechanical sensitivity of HMTD as well as the batch-to-batch variation.

6.1 Introduction

Although HMTD has no industrial or military use, HMTD) has been the subject of many technical and scientific studies as an organic peroxide explosive. The substance has been analysed in many studies using spectroscopic, colorimetric methods as well as sensitivity tests [1, 2, 3, 4, 5]. Good results have been obtained, which facilitate the detection and identification of the substance [3, 6, 7]. Nevertheless, this substance has been used in numerous illegal terrorist activities in recent years [8, 9]. The reason for this is the easy availability of the reactants, as well simple synthesis [10]. Due to the different synthesis routes as well as other processing methods, the resulting product can vary in its morphology and chemical composition. An important parameter for safe handling of explosives is the impact sensitivity, which is determined with the drop hammer experiment [11, 12, 13, 14]. The smallest energy required for ignition is determined by varying the energy of the drop weight by adjusting mass or height of it. The test gives a purely binary result and is dependent on the operator's perception [13]. Guhne et al. found out that good and more realistic results than conventional test device geometry can be achieved in initiation tests with the Ball Impact Tester from OZM (BIT). In this test setup, the sample is ignited

by a steel ball falling vertically on the sample [11]. Another major disadvantage is that no information is gained about the course of the reaction or the violence. The problems and issues associated with impact sensitivity have been studied in a variety of applications. Drop hammer devices were equipped with sensors. The glass anvil drop hammer was used in several publications [15, 12, 16]. With these and other measurements using high-speed cameras, spectrometers and other physical sensors, it was possible to investigate various reaction processes and the formation of hot spots. A major problem in all initiation experiments with explosives is poor reproducibility between different laboratories due to different setups [17]. For this reason, measurements were carried out with a drop hammer similar to the BIT with sensory monitoring and data evaluation using with multivariate statistics [18]. The results show that a classification is possible despite a large scattering of the data. Experiments were also carried out on the thermal initiation in which the data were evaluated using multi-variate statistics and could be classified [19]. The evaluation by means of multi-variate statistics makes it possible to determine characteristics and specific values for substances and reactions. This is a great advantage in contrast to the conventional purely binary evaluation. In this study, a drop hammer based on the ball impact tester (BIT) developed by OZM [18] was constructed and equipped with various sensors. The sensor system comprised three infrared (IR) and three visible (VIS) diodes with distinct sensitivities, along with a microphone and a piezo shock sensor. Two batches of Hexamethylene triperoxide diamine (HMTD) were synthesized and subsequently subjected to a water-methanol washing process [10, 20]. One batch was prepared three months earlier to enable measurement at different ageing stages of HMTD. The primary objective was to validate the sensor system, which involved the evaluation of four ignition substances during experimentation. Data analysis involved extracting features from the collected data and assessing them using multivariate statistics. Subsequently, the impact sensitivities of the two batches of HMTD were determined, and the corresponding sensor responses were evaluated. The study also investigated the influence of ageing on the impact sensitivity and the reaction progression. Additionally, HMTD was initiated with different spheres possessing equal energy to examine the impact type's influence on the reaction course. To monitor the samples, HMTD was measured using a Proton Transfer Reaction-Time of Flight (PTR-TOF) device. The headspace of the sample was analysed using this method. Furthermore, Raman spectroscopy was employed to measure the HMTD samples.

6.2 Experimental

6.2.1 Synthesis

HMTD

Caution. HMTD is a strong explosive compound and requires experienced personnel. HMTD was synthesized according to the methodology outlined by [21, 22]. In a three-necked flask with a magnetic stirrer, 1.40 g (10 mmol) hexamethylenetetramine was dissolved in 4.6 ml (50 %) H₂O₂ and cooled to ~0°C (ice/NaCl) in an ice bath. With stirring, 2.3 g (10.94 mmol) of citric acid monohydrate was added stepwise. The solution was further stirred for 8 hours and then stored at 24 °C in a refrigerator at 4 °C. The product was then washed first with 100 ml of distilled water and then with 50 ml of methanol using a vacuum sucker and dried. The yield was 0.58 g (~25%).

TATP

30 wt% of hydrogen peroxide was added to a flask, utilizing a small stirring rod. The flask was tightly sealed with parafilm and subsequently positioned in a tempered ice bath. Pure acetone was introduced into the flask containing the hydrogen peroxide, and the two substances were allowed to thoroughly mix for a minimum of 15 minutes. Following this, sulfuric acid was added to the mixture. The combined solution was left undisturbed for a duration of 24 hours, after which it underwent purification from DADP (Diacetone diperoxide) through treatment with hot methanol (recrystallisation). Subsequently, the substance was subjected to washing with distilled water to remove impurities [23]. The substance was checked for the presence of TATP and DADP using Raman spectroscopy (Analytical Methods).

6.2.2 Analytical Methods

Raman

To analyse the sample and to ensure that the synthesis product contains mainly HMTD and TATP including the expected by-products, Raman measurements were performed with a FirstDefemder R; RM3706. The measurements were taken with the standard parameters of the instrument and compared and evaluated with the instrument's internal substance

database. PTR-ToF For the measurements with the time-of-flight mass spectrometer with proton transfer reaction (PTR-ToF-MS), an Ionicon 2000 with a thermal desorption unit is used. This system consists of a reaction chamber, a drift tube, a time-of-flight mass spectrometer and an ion source. The thermal desorption unit is integrated into the system to facilitate the analysis of volatile compounds. The aim of the measurements is to ensure that they are HMTD and common by-products and decomposition products, as in the Raman measurements, and to determine how the ratios of the contents can be compared between the old and the new batch. For the measurements, 5 mg of the sample was filled into a vial and then enriched in the thermal desorption unit. The vial was filled and left to stand for 30 minutes to allow the volatile substances to accumulate in the gas phase. The suction tube of the device is then held in the vial and the sample is measured.

Sample Preparation

Four different explosives were tested during the measurements: TATP ($C_6H_{12}O_4$), HMTD ($C_6H_{12}N_{12}O_6$), lead azide ($Pb(N_3)_2$), and silver azide (AgN_3) were measured. The azides were purchased from DyniTec GmbH and were of industrial quality. The peroxides were synthesized according to the chapter on Synthesis. In the case of HMTD, two batches were prepared, one 3 months old at the time of measurement and the other a few days old. This serves to compare different ageing stages. Both batches were dried and stored at 30 % RH and 18 °C.

For the calibration measurements, TATP, silver azide, and lead azide were measured in addition to HMTD. Salt was also measured to investigate the influence of the ball impact on the microphone and the piezo crystal and to distinguish it from the signal of the explosive. In addition, blank measurements were carried out. Sample preparation was standardized for all substances by first storing the sample in a climate chamber at 30 % RH and 18 °C for at least 24 hours.

Drop hammer

Building upon the promising outcomes of previous investigations [18], a drop hammer based on OZM's BIT (Ball Impact Tester) was constructed. This drop hammer demonstrated suitability for testing primary explosives including sensory monitoring. The test procedure involves a steel ball of specified weight being dropped onto the sample from a predetermined height. If the kinetic energy of the ball surpasses a certain threshold,

the sample ignites, indicating a positive result. It comprises a steel base plate and a head part with an electromagnet. The electromagnet controls the release of the ball. The head part can be adjusted continuously along an aluminium rod. The sample is placed on a ceramic plate located on the base plate. An exemplary sketch of the structure can be seen in Figure 6.1.

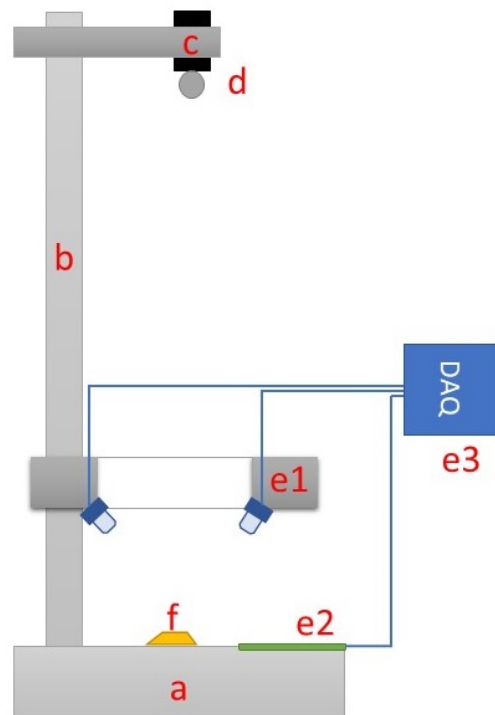


Figure 6.1: Setup drop hammer: a: baseplate, b: rod, c: electro magnet, d: ball, e1-3: sensors and data acquisition, f: sample

Distinguishing itself from the OZM BIT, this setup incorporates a ceramic base plate instead of steel. This change was made to prevent cavities from forming on the plate after repeated tests, as such cavities could potentially impact the test results. Another distinction lies in the manner of ball release. In the OZM BIT, the ball rolls over a ramp, acquiring rotation and making ignition possible through friction. Additionally, the ball experiences horizontal acceleration, making it necessary to employ camera monitoring to ensure accurate impact on the sample. In the current setup, however, the ball is secured by an electromagnet, resulting in purely vertical acceleration and eliminating ball rotation. Impact energies ranging from 4.4 mJ to 233.8 mJ can be achieved using this configuration.

Table 6.1: Used ball sizes and heights, area and dispatched volume for ball size comparison.

Ball-size [mm]	Mass [g]	Area [mm ²]	Vol. [mm ³]
6	0.88	5.37	0.82
8*	2.01	7.26	1.10
10	4.08	9.14	1.35
15	23.08	27.99	4.21

Then, according to the sample preparation of BIT [11], sample was placed on the base plate of the drop hammer. It was applied 5 mg of the sample with a measuring spoon during the preparation. The sample was then smoothed to a thickness of 0.3 mm using a slide and rail, leaving a clotted layer. Table 6.1 shows the area and displaced volume of the ball at a sample height of 0.3 mm.

6.2.3 Sensor Array

To monitor the reactions, the drop hammer was equipped with various optical and acoustic sensors. For the IR range, a pre-amplified IR sensor (PDAPC3 - Thorlabs) and two IR diodes with downstream non-inverting amplifier with different gain levels were used. For the visible range a pre-amplified sensor (PDAPC1-Thorlabs) and two additional differently amplified VIS diodes (Conrad Electronic TRU COMPONENTS 1000nm 3004M1C) were used. Due to the redundant photodiodes, both large signals, as expected for azides and the like, and small signals, as for peroxides, can be detected. The acoustic sensors used were a MEMS microphone (ELV MEMS1) for sound and a piezo shock sensor (TE Connectivity Vibration Sensor) for baseplate vibration. The analogue signals from the sensors are measured and recorded using a DAQ board (Meilhaus RedLab 1608FS-PLUS) with a sampling rate of 100 kS/s. The entire setup is shielded for noise reduction and housed in an enclosure that is shielded against interference signals and the reaction gases can be exhausted.

6.2.4 Measurement Parameters

The second series of measurements investigated the influence of ball size on ignition and reaction behaviour, using samples exclusively from the new batch of HMTD. For these experiments, measurements were conducted using two balls of different sizes (10 mm,

Table 6.2: Impact sensitivities from literature of used samples.

Compound	E50 impact sensitivity (BIT) [mJ]	E16.6 impact sensitivity (BIT) [mJ]	Impact sensitivity 1-of-6 (BAM) [mJ]
HMTD	6*	4*	60**
TATP	18*	13*	<1000*
LA	n.d.	37*	2500–4000**
SA	n.d.	29*	<1000 to 3000*

40 cm, 4.08 g; 8 mm, 80 cm, 2.01 g), with the same energy level (16 mJ) corresponding to the respective height and repeated 10 times for each configuration. The data were evaluated following the same approach as in the first series of measurements. The aim here is to find out whether there is a trend between the size of the impact body and the intensity of the reaction. The third part of the paper deals with the comparison of the impact sensitivity of the two batches of HMTD and whether or how ageing affects the impact sensitivity of the material. In addition, the characteristics of the reactions are to be compared and whether differences arise due to ageing, the type of combustion of the sample. The heights of 40 cm, 30 cm, 25 cm and 20 cm were measured with the 6 mm sphere (0.88 g) in 10 trials each. The 10 mm sphere was used, because with this weight of the sphere a large energy range as well as an exactly sufficient resolution to small energies is realisable at the construction. The resulting energies are 1.72 mJ, 2.16 mJ, 2.6 mJ, 3.5 mJ and 5.2 mJ. In addition to recording the sensor reactions, it was also documented whether the samples reacted completely, partially or not at all. Whether a sample was only partially reacted was checked by checked visually. The energy was gradually reduced until none of the 10 samples ignited. The evaluation of these measurements took into account both the raw data and the multivariate statistical analysis.

6.2.5 Pre-processing and Statistics

The measurements underwent pre-processing and analysis using a Python script [24] to obtain the sensor responses. To extract and present substance-specific characteristics from the measurements, 10 distinct features were derived from each measurement for every sensor. The features are namely the Y-position of the peak, the width of the peak at the base, the height of the peak when crossing the threshold, the height of the signal when falling below the threshold, the width of the peak, the width of the peak at half height, the half-height of the peak when rising, the half-height of the peak when falling, the integral of the peak, the slope when rising as well as when falling. Due to the excessive number of dimensions represented by the 80 extracted features, graphical analysis becomes challenging. To address this, principal component analysis (PCA) was employed to reduce the dimensions. The data was first pre-processed using a unit vector, and then three principal components were calculated using the default parameters of Scikit-learn PCA library [25]. This reduction in dimensionality helps to identify any apparent clusters within the data representation. By analysing the loadings, we can determine which extracted features are

valuable for characterising and identifying substances, and which features are redundant or unnecessary. Additionally, the Scikit-learn library [25] was utilized, employing singular value decomposition as a solver, to perform linear discriminant analysis (LDA) on the entire dataset of extracted features. LDA, being a supervised method, not only enables the exploration of substance-specific clusters in the data but also facilitates the determination of a regressor function. This regressor function allows for the identification of unknown samples. To assess the accuracy of the regressor function, cross-validation was conducted using the leave-one-out procedure. In this process, each measurement is successively used as a test dataset across all measurements, ensuring comprehensive evaluation despite the relatively small dataset.

6.3 Results and Discussion

In this section, we commence by presenting and assessing the analytical methods employed for data analysis. Subsequently, we proceed to discuss the validation measurements, ageing tests, and finally, the investigations conducted to ascertain the impact of ball size. Each of these aspects is discussed independently and in a sequential manner.

6.3.1 Analytical Methods

Raman

Figure 6.2 shows the data of the Raman measurements of old TATP (top), the new HMTD (middle) and old HMTD (bottom). Looking at the measurement of the TATP, there is a high overlap of the reference spectrum with the measured spectrum. The evaluation shows that the data are 100 % consistent with TATP. A search was also made for DADP (diacetone diperoxide), but this could not be found. When looking at the HMTD measurements, no significant differences can be seen between the old and the new batch. In both analyses, the substance is assigned 100 % as HMTD.

PTR-ToF

When analysing the PTR-ToF data, the focus was on the HMTD-relevant fragments. For both samples, the mass peaks of the relevant fragments were analysed and plotted logarithmically. In Figure 6.3, the fragments relevant for HMTD are plotted against each

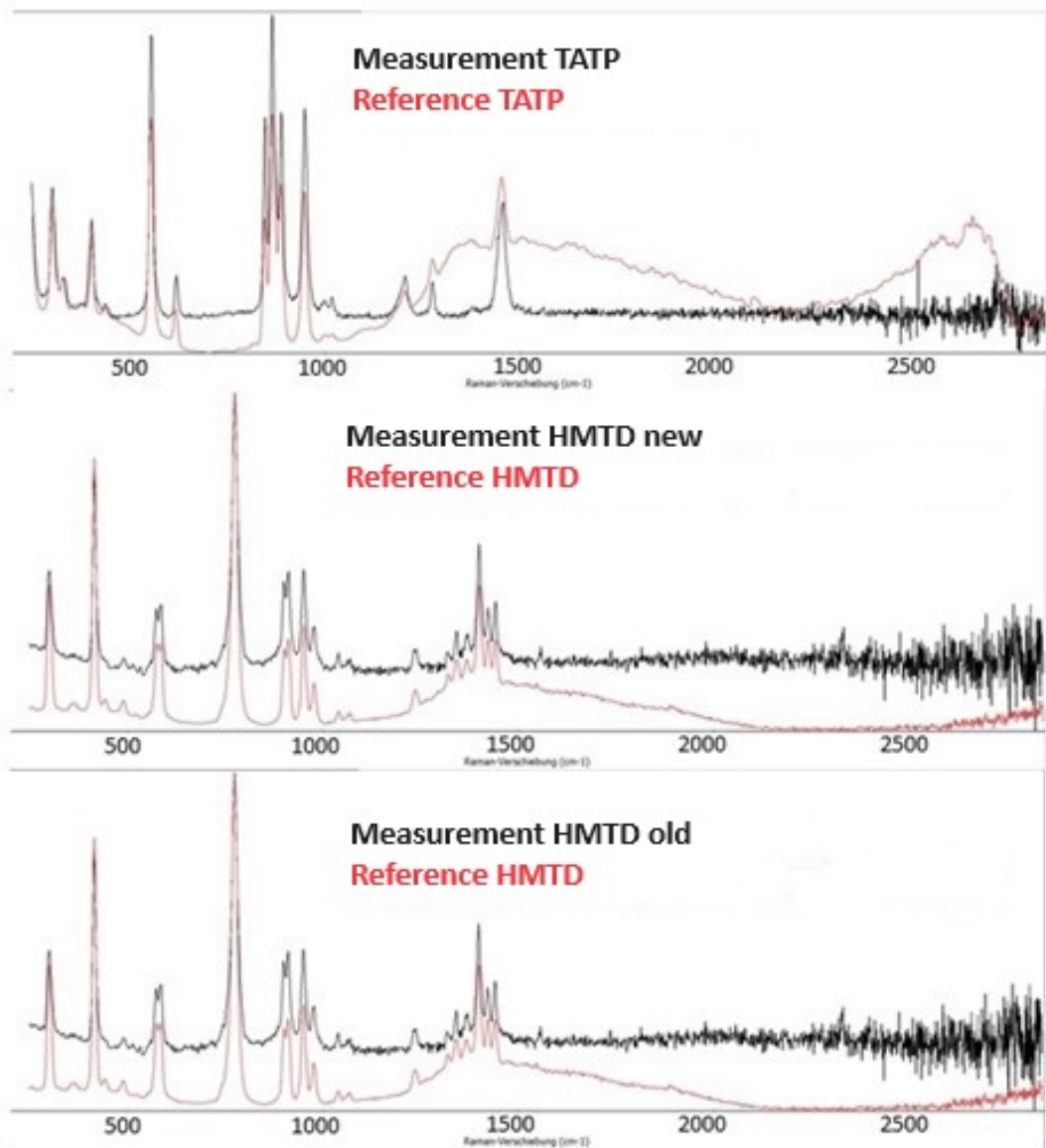


Figure 6.2: Raman spectra of TATP, old and new HMTD, the diagrams show the measured spectrum as well as the spectrum of the sought substance from the library of the instrument

Table 6.3: Predicted molecules and fragments of PTR-ToF

Fragment [m/z]	Name
46.029	Formamide
60.081	Trimethylamine
61.028	Acetic acid
74.060	Dimethylformamide
179.140	HMTD-Formaldehyde
209.077	HMTD

other. The method used only allows a limited quantitative analysis of the components, but trends in the proportions can be estimated. Table 6.3 lists the fragments with probable names of the molecules and fragments. In the old batch, the peaks of trimethylamine and dimethylformamide stand out, which indicates that this substance is formed during decomposition. This is consistent with observations from the literature. In general, it can be seen that substances that appear in measurements carried out in the literature can also be seen in these [10]. The results of the measurements show on the one hand that the synthesised substance is HMTD, and also that the composition of the substance changes over time.

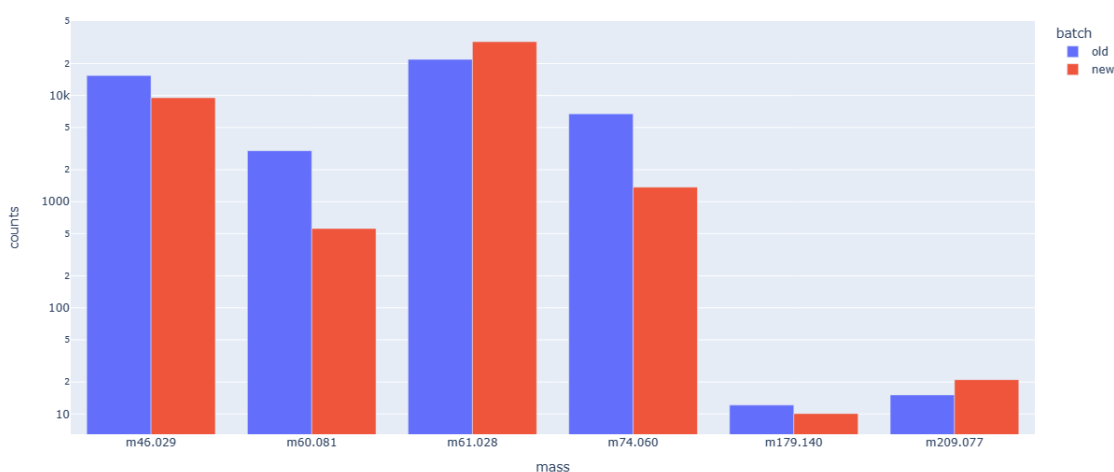


Figure 6.3: Cintegrals of selected molecular fragments of old and new HMTD, logarithmically plotted

6.3.2 Validation Measurements

In the following, the features “Micro_integral” and the feature “piezo_integral” are discussed as examples, as an evaluation of all features would go beyond the scope of this article. These features represent the integrated signal above the threshold of the respective sensors. This was extracted as in Pre-processing and Statistics. Diagrams show the mean value including standard deviation of the extracted features for each sample. The feature “Micro_integral” was analysed to assess its effectiveness in differentiating explosives. Figure 6.3 illustrates the clear signals observed for the measured explosives. The mean values for AgN_3 , HMTD, $\text{Pb}(\text{N}_3)_2$, and TATP were found to be 0.10 V, 0.23 V, 2.1 V, and 0.17 V, respectively. Conversely, the blank measurements and those with salt exhibited significantly smaller signals, with the salt measurement presenting the lowest signal intensity due to the attenuating effect of the substance. The signal from the large sphere is more pronounced due to the stronger impact on the ceramic plate. However, it is important to note that the standard deviations associated with the explosive samples were substantial, surpassing the corresponding mean values.

The feature “piezo_integral” was investigated to assess its discriminatory ability in the classification of explosives and to identify substance-specific trends. Figure 6.4 shows the analysis performed with this feature (mean values of the substances). Distinct signals were observed for the azide compounds. This phenomenon can be attributed to the higher power compared to peroxide-based explosives [13]. The structure-borne sound generated by the reactions propagates to the piezoelectric sensor and leads to the detected signals. However, the peroxides, especially TATP and HMTD, had relatively low signals whose intensities hardly differed from the blank measurements. This can be attributed to the nature of their reactions, which lead to less pronounced transmission of structure-borne sound.

Interestingly, the blank measurements had comparatively high signals. This can be attributed to the fact that the ball hits the base plate without encountering any resistance or braking effect. On the other hand, the presence of salt resulted in the smallest mean value of all substances examined. This can be attributed to the dampening effect of the substance, which softens the impact and reduces the resulting signal intensity.

When analysing the standard deviations related to the feature “piezo_integral”, it can be seen that the values are smaller compared to features such as the “microphone_integral”, but still too high to prevent an effective classification based on this

feature alone. Therefore, additional features or complementary analytical methods are needed to improve the accuracy and reliability of explosives classification using the entire dataset.

When evaluating the features of the optical sensors, it becomes apparent that the azides produce clear optical signals through away. However, the emission of light during the decomposition of the peroxides is very sporadic. This greatly increases the standard deviation of these features and shows that none of these features are suitable for denoting the substances.

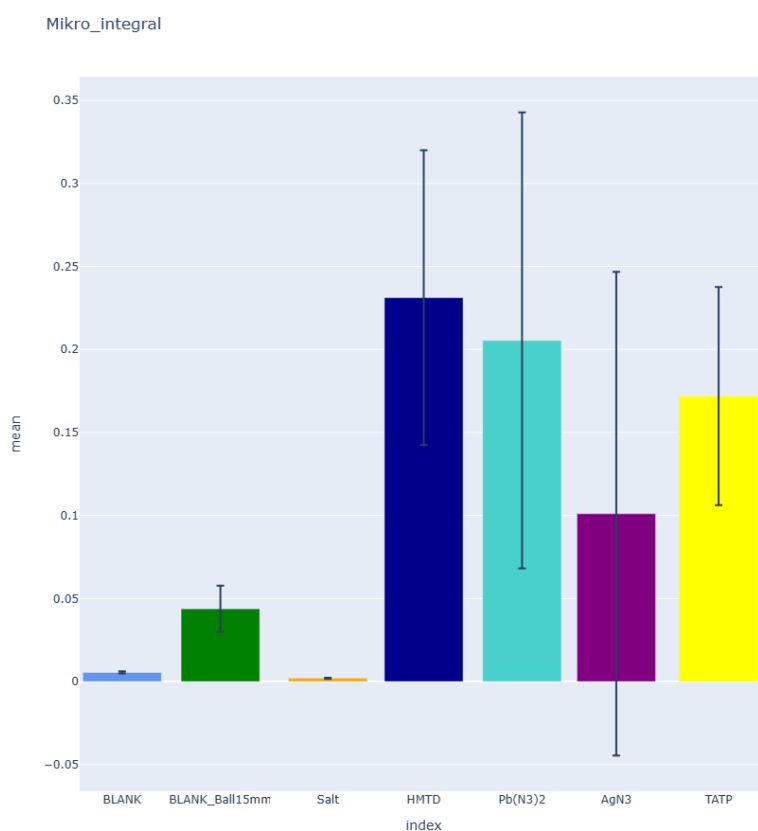


Figure 6.4: Mean of the Mikro_integral feature for every sample including standard deviation for validation measurements

Principal Component Analysis (PCA) was utilized to derive three principal components from the initial set of 80 features. As an unsupervised method, PCA enables the reduction of data dimensions and offers insights into data separability. Figure 6.3 illustrates a plot of the three principal components obtained. Upon examining the plot, it

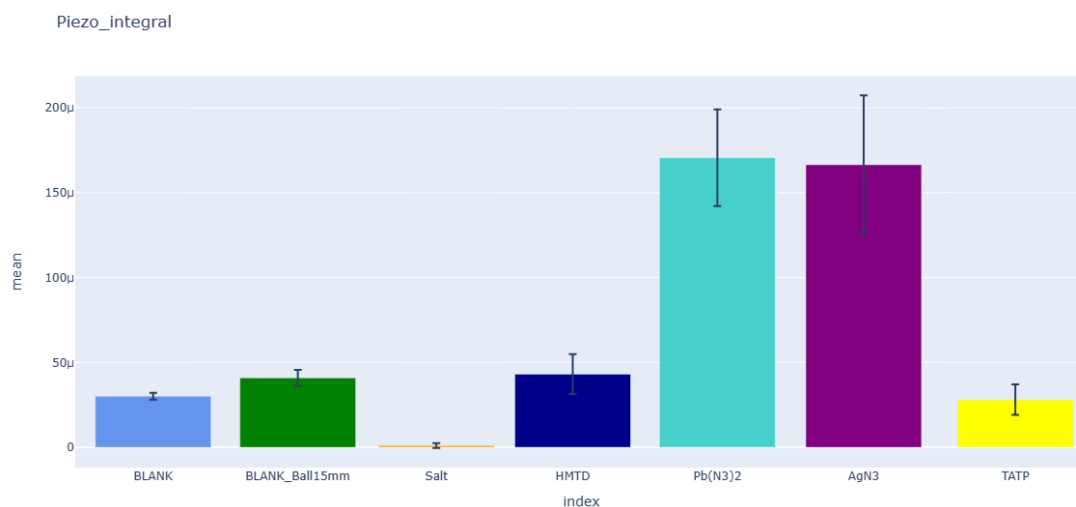


Figure 6.5: Mean of the piezo_integral feature for every sample including standard deviation for validation measurements

becomes apparent that the point clouds corresponding to HMTD and TATP measurements exhibit overlap. This suggests that the classification of these substances is limited within the series of measurements conducted. Notably, TATP displays a notably smaller scattering range compared to HMTD, aligning with the observations made regarding the average micro_integral feature values. When considering the blank measurements and those involving salt, distinct and well-defined clusters are observed. These clusters indicate clear separability between these groups, reflecting their distinctive characteristics.

The point clouds associated with the azide compounds are particularly striking. They exhibit substantial scattering, consistent with the observations made regarding the extracted features. Notably, the azide measurements distinctly separate from all other point clouds, emphasizing their unique characteristics. Overall, the PCA analysis provides valuable insights into data separability and clustering patterns. The results highlight the challenges in accurately classifying HMTD and TATP based on the measured substances while demonstrating the distinct clustering of blank measurements, those involving salt and azide compounds. These findings align with the observations made regarding the feature analyses.

If we look at the scree plot (Figure 6.7), we can clearly see that the first main component already covers about 60 % of the total variance, the second still provides 15 % and

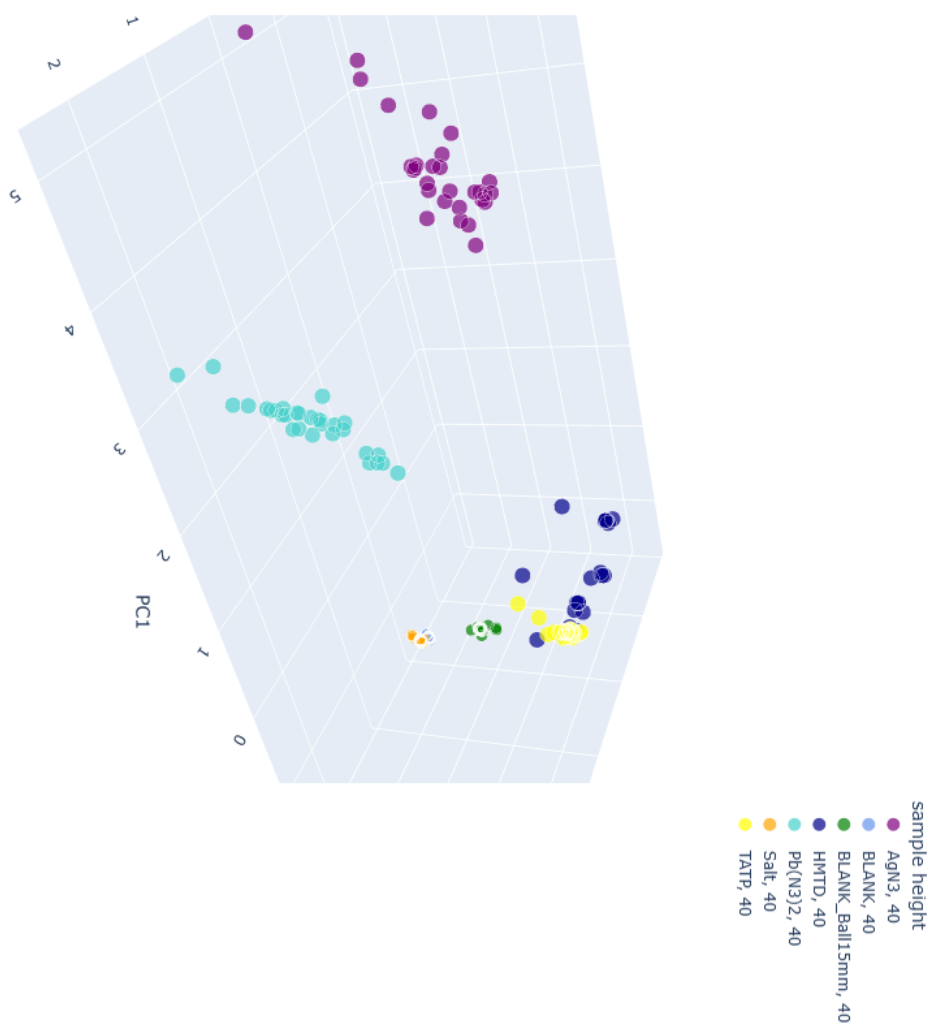


Figure 6.6: PCA-plot of the calculated three components of validation measurements

more values, and the third about 8 %.

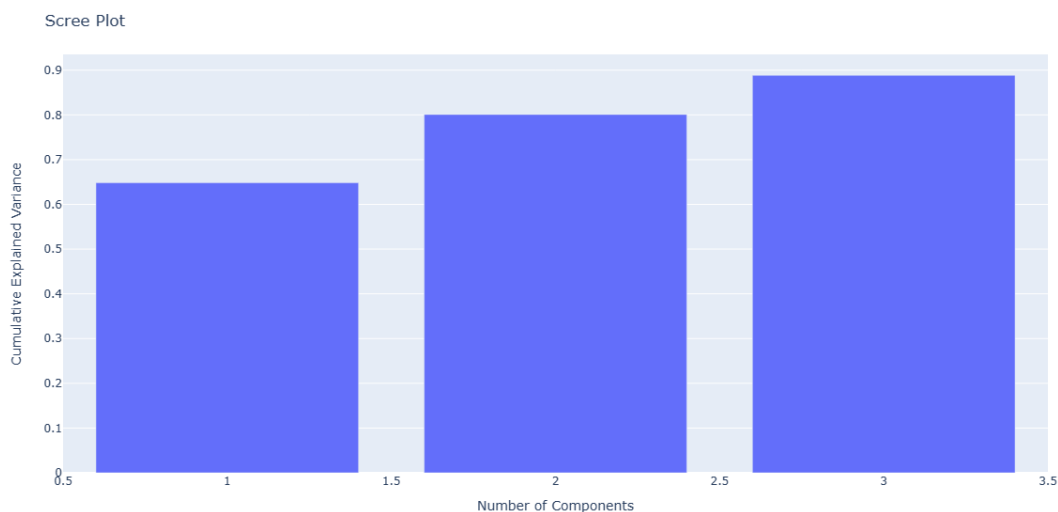


Figure 6.7: Cumulative scree plot of first three PCA components

The LDA is a supervised method, thus characteristics that differentiate the classes from each other are weighted more heavily. Figure 6.8 shows the data reduced by LDA. As in the PCA-reduced data, it is evident that most of the compounds form clusters that are distinct from each other. However, if the peroxides TATP and HMTD are considered, it is evident, as in the raw data and PCA, that the clusters overlap and classification is not possible or only possible to a very limited extent.

To validate the LDA, a leave-one-out cross-validation was performed and a predictor function was created. Iteratively, each measurement was used once as a test measurement and the others as training data. The results of this cross-validation are shown in Figure 6.9 in a heat plot. It can be seen that HMTD was assigned 8 times as TATP and TATP 8 times to HMTD. However, this is sufficient, since a better separation can be expected when differentiating different peroxides by means of LDA without strongly deviating azides.

6.3.3 Influence of the ball size

In order to rule out the influence of the ball masses as the sole cause of the observed trends in the sensor signals, blank measurements were performed as part of the experimental protocol. In particular, the microphone and piezo signals were examined during these blank measurements (where no optical emission was expected). Through this analysis, it was

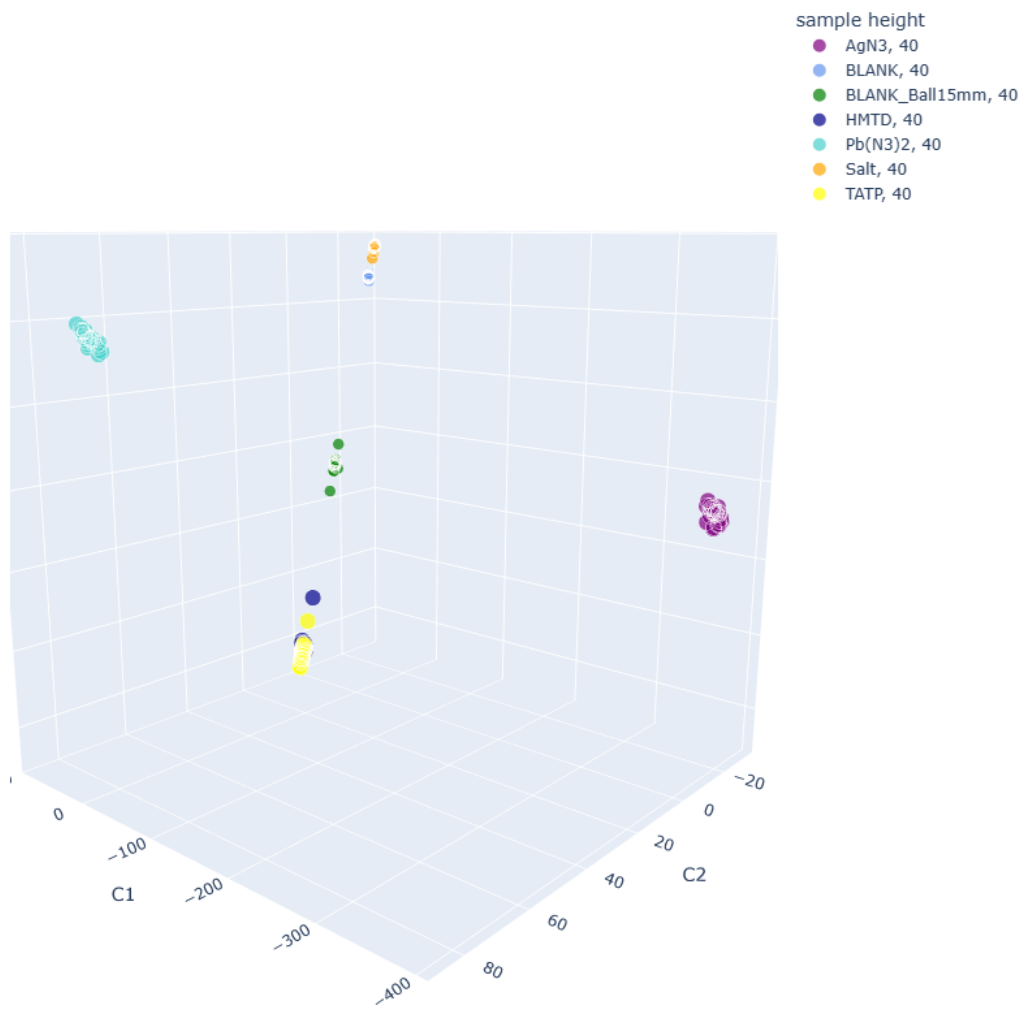


Figure 6.8: LDA-plot of the calculated three components of validation measurements

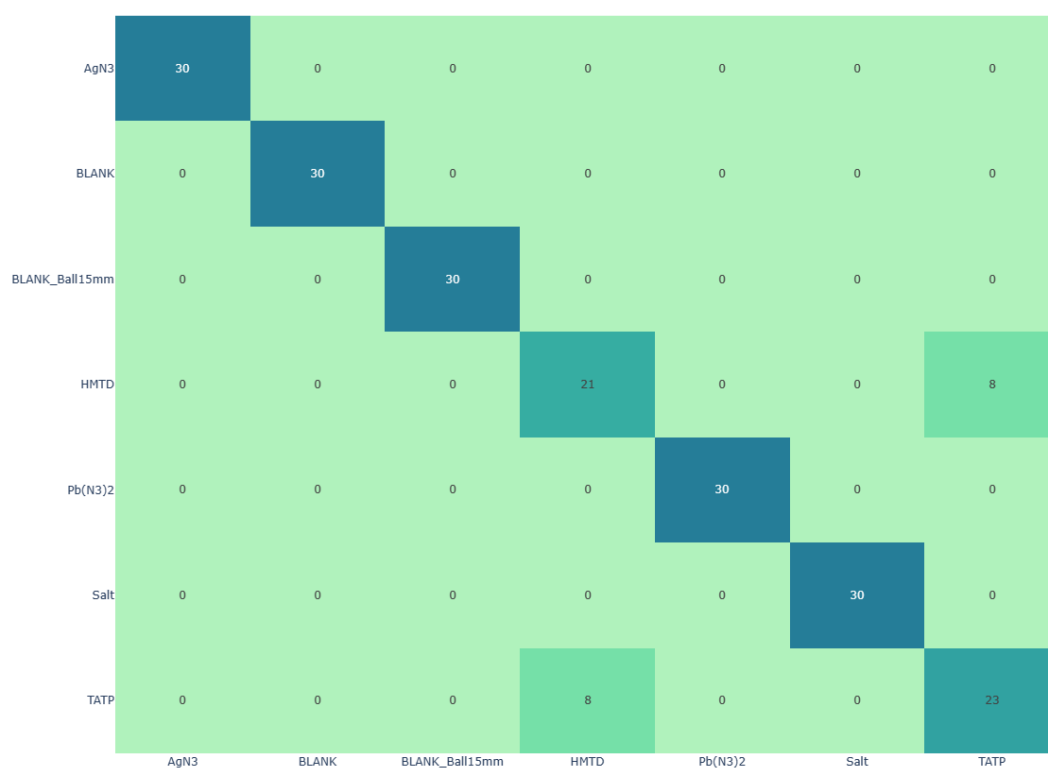


Figure 6.9: Heatplot of the via LDA predicted data from validation measurements

confirmed that the intensities of the blank measurements differed from each other. However, it should be noted that the intensities of the blank measurements were significantly lower compared to the signals from the measurements with HMTD and thus do not have a confounding effect on the results. When analysing the results from the comparison measurements, which were performed with different sphere sizes but the same initiation energy, it can be seen that the extracted features show similar behaviour to the validation measurements. To further evaluate the properties of these features, an illustrative example is discussed. In the first example (Figure 6.10), the integral of the piezoelectric sensor response is plotted against the ball size/height. The plot shows that the signal resulting from the responses to the larger sphere is more pronounced compared to the signals from the measurements with a small ball. However, similar to the validation measurements, it can be seen that the values have a high standard deviation. Consequently, a clear distinction between the different measurements is not possible when relying only on this one feature. Other features in this series of measurements also confirm the trend that initiation with the larger ball tends to elicit more violent responses. The reason for this is presumably the larger surface area and ergo a higher attenuation of the sample [11]. This makes fast and complete reaction of the sample more likely. The extracted features of this measurement series were also evaluated using multivariate statistics. Since there are only two parameter sets in this measurement series, an evaluation via LDA is not possible. In Figure 6.11, the features reduced by PCA are plotted. In spite of the fact that PCA is a non-supervised method, it can be seen that clouds of points of the two ball sizes are formed which are separated from each other. It can be seen that the measurements with the large sphere scatter significantly more. This is consistent with the observation that these measurements have a higher standard deviation in many features (Figure 6.10).

Comparison of the ageing stages

The evaluation of this series of measurements is carried out without taking into account the influence of the sphere size, as only one type of sphere was used. In Figure 6.12, the relationship between the frequency of ignitions and impact energy, as well as substance type, is visually represented. The left portion of the figure illustrates the ignition probability per measurement plotted against energy. Notably, at an energy level of 5.19 mJ, all samples, including both the new and old batches, exhibit a 100% ignition rate. The data results in an E_{10} value of around 2.2 J. However, if these results are compared with

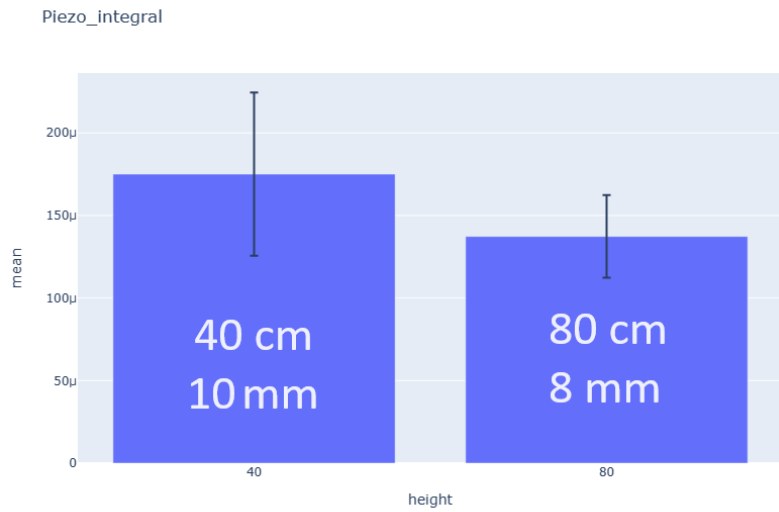


Figure 6.10: Mean of the Piezo integral feature for every sample including standard deviation for ball size measurements

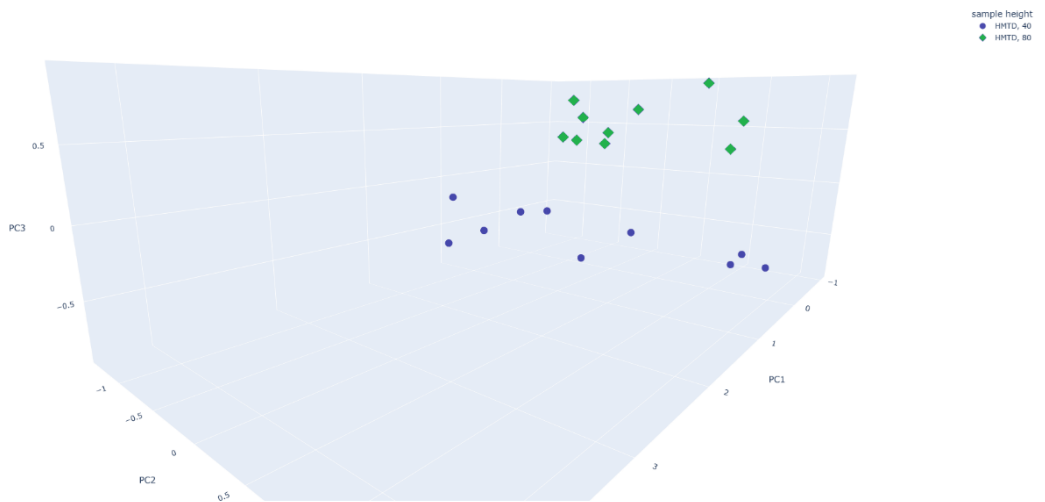


Figure 6.11: PCA-plot of the calculated three components of ball size measurements

the existing literature of 6 mJ [11], it is noticeable that the value determined is lower than the value given in the literature. This is remarkable, as ignition due to friction can be ruled out in our setup. The value determined with the BAM drop hammer is also significantly higher than ours at 60 mJ [13]. It should also be noted that these values can fluctuate depending on factors such as crystal modification and water content [11]. Despite the uniform design, synthesis, and handling of the samples, the results presented do not indicate a firm correlation between the course of the reaction and impact sensitivity in connection with the ageing of the substance, but rather show the possibility that a correlation exists.

By examining the ignition probability of the new HMTD, it becomes evident that all samples ignite even at a lower energy level of 3.46 mJ, with the probability decreasing as the energy decreases. In contrast, the behaviour of the old batch HMTD differs. The probability of ignition does not exhibit a consistent decline with increasing energy. For instance, at 3.46 mJ, the ignition probability is only 90%, while at 2.59 mJ, it returns to 100%. At an energy level of 1.73 mJ, no further conversions occur with the old HMTD.

Analysing the frequency of partial conversions for both substances (Figure 6.12, centre), it is evident that no partial reactions are observed at an energy level of 5.19 mJ. The highest likelihood of partial reactions occurs at an energy level of 2.16 mJ, with the old substance demonstrating a tendency towards partial reactions in 50% of the measurements, compared to approximately 30% for the new substance. Moreover, considering that the old HMTD does not undergo any conversion at an

In the course of this series of measurements, additional information was extracted from the collected data and analysed using multivariate statistical methods. To illustrate this process, the feature known as `micro_integral` (Figure 6.13) was selected as an example. Looking at the data, it is evident throughout all heights and also samples that all measurements, as with those of the validation measurements, show a high standard deviation. For measurements at 20 cm, no ignition occurred for the old HTMD, ergo no signal is seen. Apart from the value for new HMTD at 20 cm, the mean values increase with increasing height, that is, as the energy increases, the violence of the response increases. It is clear to see that the mean values of new HMTD consistently have a higher value, indicating that it responds more violently compared to the old batch. This trend is consistent across almost all of the features extracted. Although differences in the mean values can be seen in almost all features, the substances cannot be discriminated due to the large standard deviation.

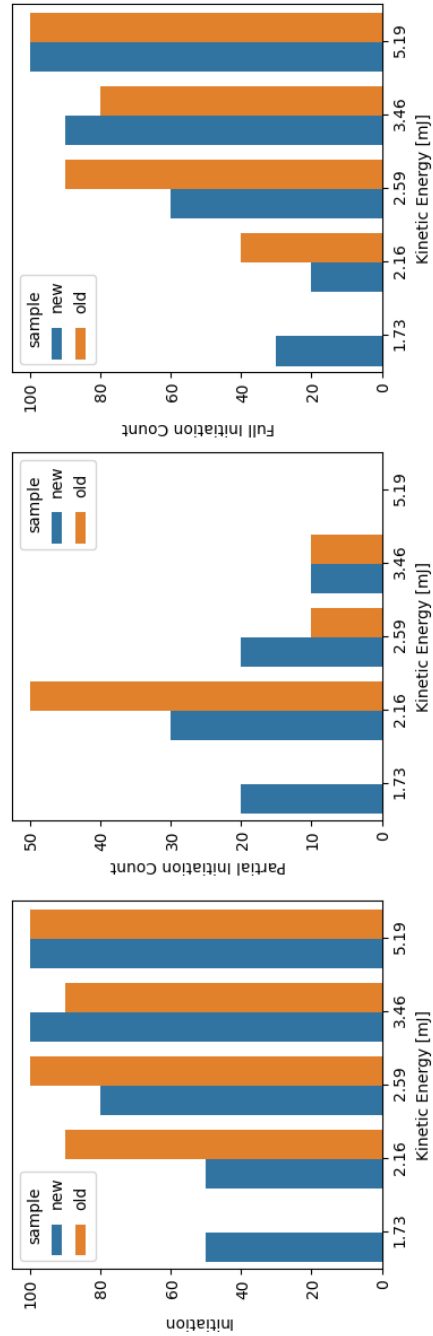


Figure 6.12: Probability of conversion versus impact energy of old and new HMTD. Left: all combustions, middle: only partial combustions, right: only complete combustions

The results show that the aged HMTD is more insensitive to impact and shows a milder decomposition reaction compared to the freshly produced product. The reason for this could be that HMTD ages rapidly. In this aging process, the substance decomposes into smaller, non-reactive parts. These are deposited on and in the crystals, which can interrupt the continuation of the reaction front [11]. Other impurities, which can also vary from batch to batch, can have a similar effect. Furthermore, the net explosive amount of the sample decreases, which means that quantitatively less material is present that can react.

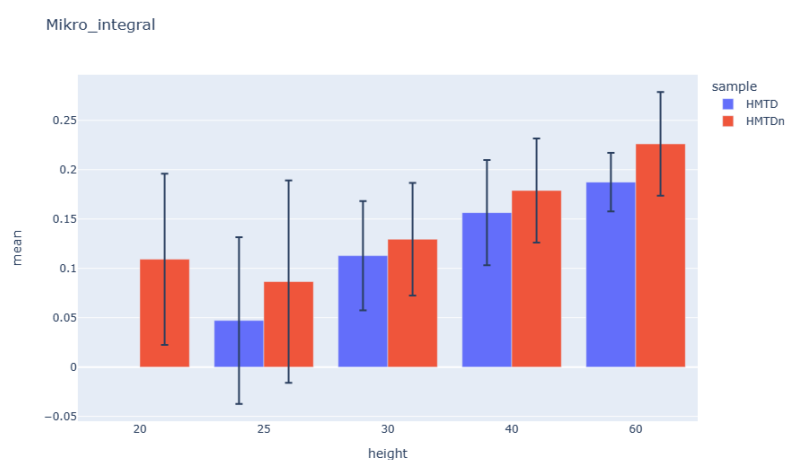


Figure 6.13: Mean of the Mikro integral feature for all combusted samples and heights including standard deviation for impact sensitivity measurements

Due to the limited number of measurements (10 per parameter set) and the fact that not all measurements resulted in ignition, a comprehensive analysis of class-specific characteristics becomes challenging. Nonetheless, the dataset encompassing all measurements leading to sample conversion, including the validation measurements, underwent a thorough evaluation utilizing multivariate statistical techniques. Out of the 100 measurements conducted in this series, a total of 76 yielded full or partial combustion. These measurements were subjected to Linear Discriminant Analysis (LDA) and subsequently reduced to three dimensions, as depicted in Figure 6.14. Distinct HMTD batches are denoted by various colours, while different symbols represent varying heights. When looking at the plotted points, it is clear that the point clouds of the two samples separate on the axis of the first components, when intersections also occur. Comparing the measurements of the individual heights (marked with different symbols), a trend can also be seen. Thus, on

average, the values of the points on components 1 and 2 increase with increasing height. Basically, it can be seen that the points of the measurements of the old HMTD show a larger scatter, whereby the height-dependent trend, which can be seen well with the new HMTD, is only weakly developed. The reason for this is presumably the changed morphology and composition of the sample due to aging. Batch to batch variation must also be taken into consideration. In principle, however, it seems possible to discriminate measurements from batches of HMTD of different ages on the basis of the sensor response of the decomposition reaction. In order to validate the possibility of assigning measurements, cross-validation was performed, as was done for the validation measurements (Figure 6.15). In the heat plot shown, the true values of the measurements are plotted on the Y-axis and the predicted values are plotted on the X-axis. All measurements in the red marked area show measurements of the new HMTD, those in the blue those of the old one. Measurements that are not in any of the boxes are incorrectly predicted. Measurements that are within the marked fields are partially predicted to the wrong height, but to the correct substance. It is worth noting that these values can exhibit variations depending on factors such as crystal modification and water content [11]. Despite the uniform design, synthesis and handling of the samples, the results presented do not indicate a firm correlation between the course of the reaction and impact sensitivity in connection with the ageing of the substance, but rather show the possibility that a correlation exists.

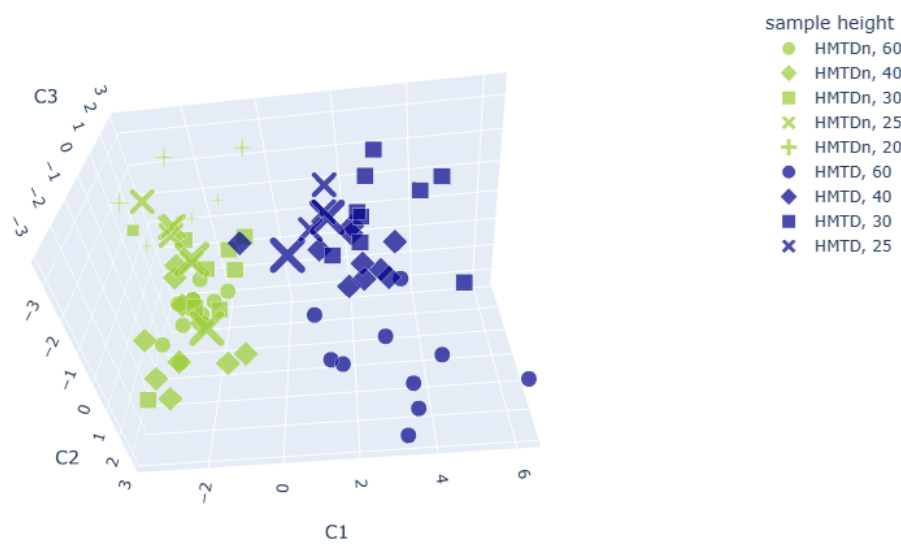


Figure 6.14: LDA-plot of the calculated three components of impact sensitivity measurements

6.4 Conclusion

In conclusion, a drop hammer apparatus resembling the OZM Ball Impact Tester, equipped with optical and acoustic sensors, was utilized for the evaluation of impact sensitivity and response of four distinct initial explosive materials: HTMD, TATP, silver azide and lead azide. The peroxides were synthesized, and two batches of HMTD with different ages were prepared. The substances underwent controlled energy-induced conversions to validate their distinctive characteristics and ensure differentiation capability. Extracting 80 features from each measurement, followed by multivariate statistical analysis and dimensionality reduction, facilitated the differentiation process. Cross-validation yielded a predictor function accuracy of 93 %, confirming the suitability of the setup for distinguishing ignition substances. In the subsequent segment of this research, the reaction behaviour of HTMD was examined at different ball sizes and heights, maintaining a constant energy level as in the initial phase. The objective was to assess the impact of sphere size on the reaction process. Statistical evaluation results indicated that the severity of the reaction increases with larger ball sizes, highlighting the dependency on the impact area rather than the ball velocity. Future experiments will explore this influence with different substances. In the final phase of the study, the impact sensitivities of two differently aged batches of material were determined and the response curves observed. The analytical methods confirmed the ageing phenomena described in the literature [26, 27, 22, 10]. The experiments were performed with energies between 1.73 mJ and 5.19 mJ, and the number of ignitions per height and substance was evaluated as 1 out of 10 [14]. The static evaluation showed that ageing could influence the impact sensitivity. In addition, the statistical analysis revealed that aged materials have a higher tendency to partial combustions. Overall, this study provides insights into the differentiation of igniters, the impact sensitivity of aged materials and the influence of ball size on reaction behaviour. Future studies will include measurements of several batches with different ages in order to exclude batch to batch variations and to obtain more comprehensive and accurate results. It would also be useful to measure the substances at more than just two ageing stages. In future, more comprehensive series of measurements will also have to be carried out for experiments with different sphere sizes. On the one hand, a larger repertoire of spheres and, if necessary, also different substances must be measured.

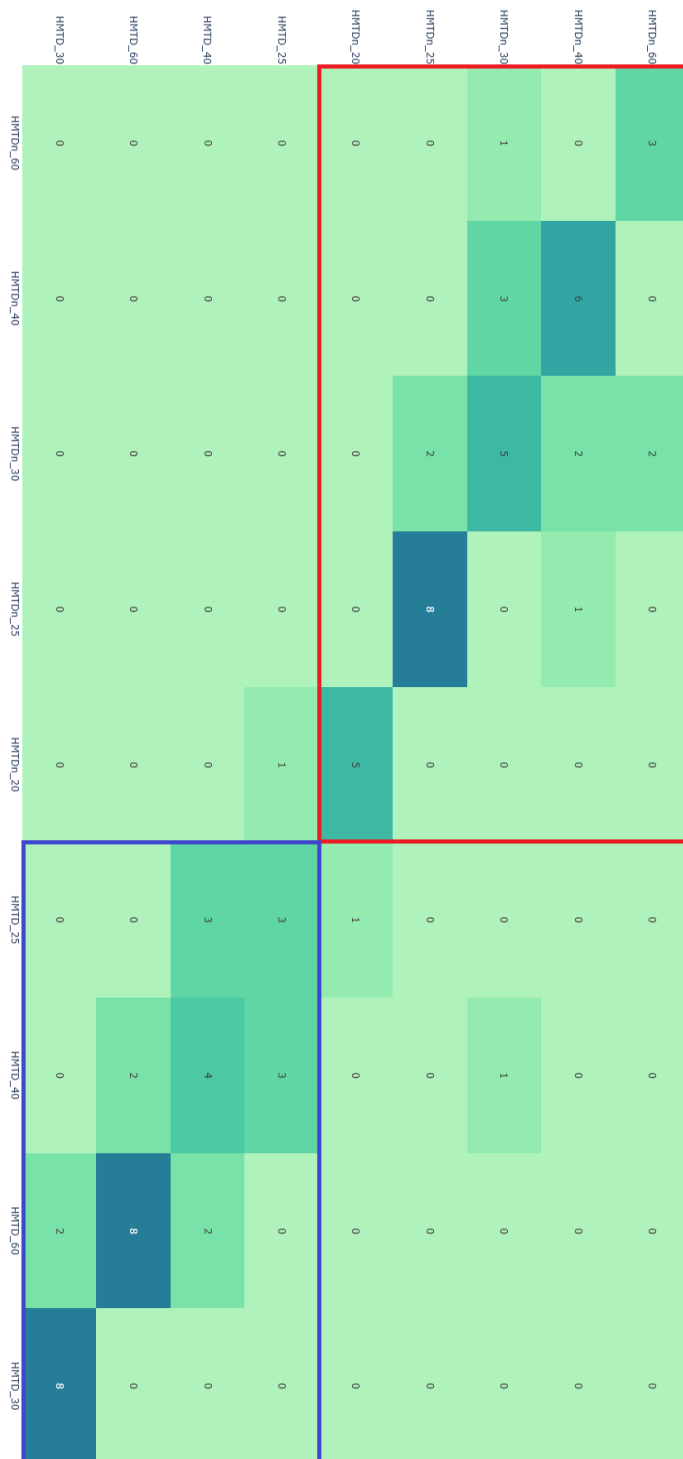


Figure 6.15: Confusion matrix of the cross-validation of the impact sensitivity tests. Z axis true values, x axis predicted values

References

- [1] Lindsay McLennan, James L. Smith, and Jimmie C. Oxley. “A new polymorph of HMTD”. In: *Journal of Energetic Materials* 39.3 (2021), pp. 361–376. DOI: 10.1080/07370652.2020.1802630.
- [2] Kevin Colizza, Alexander Yevdokimov, Lindsay McLennan, James L. Smith, and Jimmie C. Oxley. “Using Gas Phase Reactions of Hexamethylene Triperoxide Diamine (HMTD) to Improve Detection in Mass Spectrometry”. In: *Journal of the American Society for Mass Spectrometry* 29.4 (2018), pp. 675–684. DOI: 10.1007/s13361-017-1879-5.
- [3] Lauryn E. DeGreeff, Michelle M. Cerreta, and Christopher J. Katilie. “Variation in the headspace of bulk hexamethylene triperoxide diamine (HMTD) with time, environment, and formulation”. In: *Forensic Chemistry* 4 (2017), pp. 41–50. DOI: 10.1016/j.forc.2017.03.001.
- [4] Zheng Li, Will P. Bassett, Jon R. Askim, and Kenneth S. Suslick. “Differentiation among peroxide explosives with an optoelectronic nose”. In: *Chemical Communications* 51.83 (2015), pp. 15312–15315. DOI: 10.1039/c5cc06221g.
- [5] Jirí Pachmán, Jakub Selesovský, and Robert Matyás. *New Trends in Research of Energetic Materials (NTREM '14)*. 2014.
- [6] M. O. Salles, G. N. Meloni, W. R. de Araujo, and T. R. L. C. Paixão. “Explosive colorimetric discrimination using a smartphone, paper device and chemometrical approach”. In: *Anal. Methods* 6.7 (2014), pp. 2047–2052. DOI: 10.1039/C3AY41727A.
- [7] Derek F. Laine and I. Francis Cheng. “Electrochemical detection of the explosive, hexamethylene triperoxide diamine (HMTD)”. In: *Microchemical Journal* 91.1 (2009), pp. 125–128. DOI: 10.1016/j.microc.2008.08.015.
- [8] J.C. Oxley, J.L. Smith, W. Luo, and J. Brady. “Determining the vapor pressures of diacetone diperoxide (DADP) and hexamethylene triperoxide diamine (HMTD)”. In: *Propellants, Explosives, Pyrotechnics* 34.6 (2009), pp. 539–543. DOI: 10.1002/prop.200800073.

- [9] A.G. Simon and L.E. DeGreeff. “Variation in the headspace of bulk hexamethylene triperoxide diamine (HMTD): Part II. Analysis of non-detonable canine training aids”. In: *Forensic Chemistry* 13 (2019), p. 100155. DOI: 10.1016/j.forc.2019.100155.
- [10] Jimmie C. Oxley, James L. Smith, Matthew Porter, Lindsay McLennan, Kevin Colizza, Yehuda Zeiri, et al. “Synthesis and Degradation of Hexamethylene Triperoxide Diamine (HMTD)”. In: *Propellants, Explosives, Pyrotechnics* 41.2 (2016), pp. 334–350. DOI: 10.1002/prep.201500151.
- [11] M. S. Gruhne, M. Lommel, M. H. H. Wurzenberger, N. Szimhardt, T. M. Klapötke, and J. Stierstorfer. “OZM Ball Drop Impact Tester (BIT-132) vs. BAM Standard Method – a Comparative Investigation”. In: *Propellants Explos. Pyrotech.* 45 (2020), pp. 147–153. URL: <https://doi.org/10.1002/prep.201900286>.
- [12] C. S. Coffey and V. F. de Vost. “Impact Testing of Explosives and Propellants”. In: *Propellants, Explosives, Pyrotechnics* 20.3 (1995), pp. 105–115. DOI: 10.1002/prep.19950200302.
- [13] Josef Köhler, Rudolf Meyer, and Axel Homburg. *Explosivstoffe*. 10th revised and expanded edition. Weinheim: Wiley-VCH, 2008.
- [14] NATO. *STANAG 4489, 1999 (4489)*. 1999.
- [15] David M. Williamson, Sue Gymer, Nicholas E. Taylor, Stephen M. Walley, Andrew P. Jardine, Annette Glauser, et al. “Characterisation of the impact response of energetic materials: observation of a low-level reaction in 2,6-diamino-3,5-dinitropyrazine-1-oxide (LLM-105)”. In: *RSC Advances* 6.33 (2016), pp. 27896–27900. DOI: 10.1039/C6RA03096C.
- [16] P. J. Rae and P. M. Dickson. “Some Observations About the Drop-weight Explosive Sensitivity Test”. In: *Journal of Dynamic Behavior of Materials* 7.3 (2021), pp. 414–424. DOI: 10.1007/s40870-020-00276-2.
- [17] Zhiwei Men, Kenneth S. Suslick, and Dana D. Dlott. “Thermal Explosions of Polymer-Bonded Explosives with High Time and Space Resolution”. In: *J. Phys. Chem. C* 122.26 (2018), pp. 14289–14295. DOI: 10.1021/acs.jpcc.8b02422.
- [18] M. Muhr, T.M. Klapötke, and G. Holl. “Sensory monitoring of drop hammer experiments with multivariate statistics”. In: *Propellants, Explosives, Pyrotechnics* 47.11 (2022). DOI: 10.1002/prep.202200025.

- [19] S. Maurer, R. Makarow, J. Warmer, and P. Kaul. “Fast testing for explosive properties of mg-scale samples by thermal activation and classification by physical and chemical properties”. In: *Sens. Actuators B: Chem.* 215 (2015), pp. 70–76. URL: <https://doi.org/10.1016/j.snb.2015.03.045>.
- [20] William P. Schaefer, John T. Fourkas, and Bruce G. Tiemann. “Structure of hexamethylene triperoxide diamine”. In: *Journal of the American Chemical Society* 107.8 (1985), pp. 2461–2463. DOI: 10.1021/ja00294a043.
- [21] Andrzej Wierzbicki, E. Alan Salter, Eugene A. Cioffi, and Edwin D. Stevens. “Density Functional Theory and X-ray Investigations of P- and M-Hexamethylene Triperoxide Diamine and Its Dialdehyde Derivative”. In: *Journal of Physical Chemistry A* 105.38 (2001), pp. 8763–8768. DOI: 10.1021/jp0123841.
- [22] Jimmie C. Oxley, James L. Smith, Matthew Porter, Lindsay McLennan, Kevin Colizza, Yehuda Zeiri, Ronnie Kosloff, and Faina Dubnikov. *Synthesis and Degradation of Hexamethylene Triperoxide Diamine (HMTD)*. 2015. DOI: 10.1002/prep.201500151.
- [23] Jimmie C. Oxley, James L. Smith, Patrick R. Bowden, and Ryan C. Rettinger. “Factors Influencing Triacetone Triperoxide (TATP) and Diacetone Diperoxide (DADP) Formation: Part I”. In: *Propellants, Explosives, Pyrotechnics* 38.2 (2013), pp. 244–254. DOI: 10.1002/prep.201200116.
- [24] M. Muhr. *mattmatt91/Promotion_process*. https://github.com/mattmatt91/Promotion_process. Accessed: 2022-03-25. 2022.
- [25] Fabian Pedregosa, Gaël Varoquaux, Alexandre Gramfort, Vincent Michel, Bertrand Thirion, Olivier Grisel, Mathieu Blondel, Peter Prettenhofer, Ron Weiss, Vincent Dubourg, et al. “Scikit-learn: Machine learning in Python”. In: *Journal of machine Learning research* 12 (2011), pp. 2825–2830.
- [26] R. González-Méndez et al. “Use of rapid reduced electric field switching to enhance compound specificity for proton transfer reaction-mass spectrometry”. In: *Analytical Chemistry* 90.9 (2018), pp. 5664–5670. DOI: 10.1021/acs.analchem.7b05211.

- [27] R. González-Méndez et al. “Development and use of a thermal desorption unit and proton transfer reaction mass spectrometry for trace explosive detection: Determination of the instrumental limits of detection and an investigation of memory effects”. In: *International Journal of Mass Spectrometry* 385 (2015), pp. 13–18. DOI: 10.1016/j.ijms.2015.05.003.

Part IV

Results and Discussion: Laser Initiation

Sensory Monitoring and Analytical Study of Laser Initiated Graphite-Coated TATP Using PTR-ToF-MS and Microphone

by

Emre Ünal, Matthias Muhr, Jennifer Braun, Thomas M. Klapötke, Peter Kaul

Accepted for publication in

Journal of Energetic Materials, Taylor & Francis, Open Select

The work reported on in this publication was carried out together with Mr Emre Ünal. The personal contribution amounts to around 50 %. The main focus was on the production of the hardware and the sensor technology. This involved optimising the sensors and data acquisition and synchronising them with the laser system. In addition, the planning and evaluation using multivariate statistics was overhauled. The focus was on feature extraction and finding trends and correlations in the data.

Abstract: Triacetone triperoxide (TATP) is a significant threat due to its use in improvised explosive devices (IED), attributed to its simple synthesis and readily available precursors. TATP exhibits high sensitivity to impact, friction, and heat. This study investigates detection methodologies focusing on the effects of various laser beam parameters on TATP. By applying coatings with known absorption coefficients, energy can be coupled in a controlled manner without prior knowledge of the substance. This allows for controlled local initiation, preventing mass detonation. In our setup, graphite-coated TATP is irradiated with laser radiation, analysed and controlled using PTR-ToF-MS and a sensitive microphone.

7.1 Introduction

Triacetone triperoxide (TATP) is a highly unstable and sensitive explosive, known for its hazardous nature. Even in small quantities, TATP is prone to detonation from minimal stimuli, such as friction, impact, or changes in temperature. This sensitivity makes it extremely dangerous to handle and transport. TATP's volatility and unpredictability have made it one of the most challenging explosives to manage safely, highlighting the significant risks associated with its presence. The simplicity of its synthesis, coupled with the ready availability of its reactants, makes TATP a popular yet dangerous explosive among terrorist circles, presenting considerable challenges to civil security pattern [1, 2, 3, 4]. Unlike many explosives, TATP contains neither metallic elements nor nitro groups, complicating detection with traditional spectroscopic methods [5, 6, 7, 8, 9, 10, 11, 12]. The significance of this research lies in the fact that TATP represents a major threat to public safety due to its extreme instability and susceptibility to detonation. Developing reliable and safe detection methods for TATP is crucial to preventing its use and mitigating its dangers. In particular, non-destructive detection methods that do not require mechanical sampling are of utmost importance, as traditional approaches are often unreliable or pose safety risks. This research contributes to the exploration of new laser-based detection methods that address the specific challenges posed by TATP and offers a valuable contribution to enhancing civilian security measures. Due to TATP's high sensitivity and the dangerous nature of substance transformation, non-destructive detection methods and those without mechanical sampling are clearly advantageous in identifying the material. Laser supported techniques such as Raman spectroscopy have been employed, with no-

table successes [13, 14]. In fact, several commercialized systems now utilize Raman spectroscopy for TATP detection, developed by companies like Pendar Technologies, Thermo Fisher Scientific, and Detectachem [15, 16]. Pendar's X10 handheld Raman spectrometer is capable of identifying hazardous materials, including highly sensitive explosives like TATP, at standoff distances up to six feet, offering enhanced safety and efficiency in field operations. Similarly, Thermo Fisher's FirstDefender and TruNarc systems are widely used by law enforcement and military agencies for rapid identification of explosives, leveraging both Raman and FTIR technologies to detect TATP and other hazardous substances. These systems exemplify the successful transition from research to practical, deployable solutions in enhancing security. In addition to commercial systems, several academic studies have validated the effectiveness of Raman spectroscopy in detecting TATP. For example, Fan et al. demonstrated that Raman spectroscopy could be successfully employed to identify TATP, even at trace levels, making it a robust technique for explosive detection [7]. Bulatov et al. further explored the advantages of Raman spectroscopy in distinguishing between different peroxide-based explosives, highlighting its selectivity and sensitivity [5]. The use of portable Raman systems in real-world environments has also been discussed by Zapata et al., emphasizing their utility in explosive detection [17]. These studies support the view that Raman spectroscopy, particularly in its commercialized handheld forms, is both effective and reliable for TATP detection. For instance, Pendar X10 has been recognized for its ability to detect dangerous materials, including black powders and dark explosives, while minimizing the risk of ignition, thanks to its innovative design that disperses laser heat over a larger area [15]. Thermo Fisher's FirstDefender RM and TruDefender also offer non-contact chemical identification, crucial for safe and efficient handling of explosives like TATP in real-time scenarios [16]. Additionally, the potential for laser initiation of explosive substances has been explored, where a short ignition time is typically the goal [18, 19, 20, 21, 22]. In the field of analysing TATP using MS methods, especially with PTR-ToF-MS, a number of results have been achieved. This technique has been particularly successful in the detection of very low concentrations [12, 23, 24]. A major advantage of this is the extremely short analysis time of the device, which can be regarded as real time analysis. This makes the measuring method very suitable for live monitoring of processes and reactions [25, 26, 27]. However, the local and controlled initiation of energetic materials using laser radiation comes with a range of problems, particularly for primary explosives. For these, the ignition thresholds are comparatively low, and complete conversion of the sample is

likely [18, 20, 28]. The use of coatings in the context of laser processing was investigated [18, 29]. The results show that the energy required to achieve the desired effects can be significantly reduced by using coatings. In this context, the controlled coupling of energy through laser radiation, using coatings, into the materials under investigation is of great interest for the monitoring of the reaction, especially without knowledge of their specific absorption coefficients. One approach is the coating of substances with materials that have a known and significantly higher absorption coefficient than that of the explosive. The desired effect of the coating is to determine laser parameters and conditions at which no conversion of the entire explosive mass occurs, particularly with highly sensitive substances, and at which non-critical quantities (e.g. individual crystals) are initiated simultaneously. For this publication, TATP was synthesized and subjected to photonic radiation. The samples were exposed to power levels ranging from 25 mW to 100 mW, and a set of the samples was coated with graphite to investigate the influence on the processing and decomposition of the substance. The purity of TATP was initially assessed using PTR-ToF-MS and Raman spectroscopy. PTR-ToF-MS was used to analyse the reaction gases. In addition, measurements were taken using a microphone. As a sensor, this can provide a certain amount of information about the degree and intensity of decomposition and, if necessary, about partial decomposition. [30, 31, 32]. The objective of this study is to investigate the relationship between the behaviour of TATP under photonic irradiation and the applied power levels. Furthermore, the influence of highly absorptive coatings on the decomposition of the substance will be examined, as well as the extent to which these coatings promote partial reactions at lower power levels.

7.2 Experimental Section

7.2.1 Synthesis of TATP

A 30% aqueous solution of hydrogen peroxide was carefully dispensed into a reaction vessel using a slender mixing rod for stirring. The vessel was securely sealed with parafilm to prevent any contamination or evaporation and then placed within an ice bath to maintain a low reaction temperature. Afterward, an aliquot of anhydrous acetone was added to the vessel already containing the hydrogen peroxide solution. The two reagents were mixed for at least 15 minutes to ensure uniform distribution. Concentrated sulfuric acid was then slowly introduced to the homogenous solution. The obtained mixture was left

to stand undisturbed at a low temperature for a full 24- hour period. Following this incubation period, the reaction mixture was subjected to a purification process to separate Diacetone diperoxide (DADP), using heated methanol as the purification agent. The final product was further cleansed with distilled H₂O to eliminate residual contaminants as reported by Oxley et al. [33]. Verification of TATP and DADP within the sample was performed employing Raman spectroscopic techniques, as outlined in Analytical Methods. The synthesis of TATP involves the reaction of hydrogen peroxide with acetone under acidic conditions, with concentrated sulfuric acid acting as the catalyst, as described in the method adapted from Oxley et al. One of the key aspects of this reaction is the formation of various peroxide species, including diacetone diperoxide (DADP), which necessitates further purification to isolate TATP. Acetone is tracked and measured as a critical decomposition product of TATP, as its formation is indicative of the breakdown of the peroxide bond structure within TATP molecules. The identification and monitoring of DADP, along with acetone, are crucial for confirming the purity of the synthesized TATP, since the presence of DADP may complicate the decomposition behavior of TATP in subsequent experiments. This provides a more thorough validation of the experimental data and ensures that the TATP used is not contaminated by significant amounts of other peroxides.

7.2.2 Sample Preparation

Ahead of conducting the experimental measurements, the prepared samples were placed in a climatic chamber and left undisturbed for a minimum duration of 48 hours at a controlled relative humidity of 20 % and a temperature of 18 °C. For the experimental analysis, each sample was transferred into cylindrical metallic tubes of 2 mm diameter and gently pressed by hand. The fill level was set at 5 mm, yielding an average sample mass of 10 mg. For the coated samples, a layer of graphite was applied. The graphite coating was administered using an aerosol technique, employing an airbrush at a consistent distance of 10 cm and a spray duration of 500 ms. Figure 7.1 shows a prepared coated and an uncoated sample as an example.

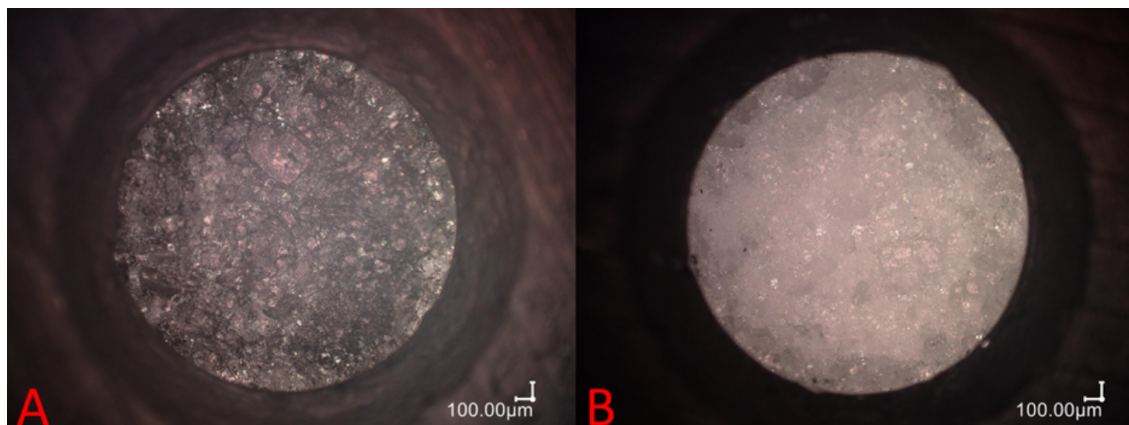


Figure 7.1: Image of the prepared TATP samples, coated on the left (a), uncoated on the right (b)

7.2.3 Analytical Methods

Microphone

A MEMS microphone (ELV MEMS1) was used for acoustic monitoring of the experiments under laser processing. The data was recorded using a DAQ card (Meilhaus Redlad FS 1208) with a sampling rate of 10 kHz.

Raman

The synthesized sample was subjected to analytical scrutiny to confirm the predominance of TATP and its anticipated by-products within the product mix. This was achieved through Raman spectroscopic analysis utilizing a First Defender R device. Instrumental readings were conducted following the standard operating parameters of the device. The resulting spectral data were then cross-referenced and assessed against the device's built-in chemical substance library for verification.

PTR-ToF-MS

A Proton Transfer Reaction Time-of-Flight Mass Spectrometer (PTR-ToF-MS), particularly the Ionicon 2000 model, was utilized for the characterization of synthesized triacetone triperoxide (TATP). This included confirming its identity and detecting prevalent by-products and decomposition compounds. The PTR-ToF-MS comprises an ion source, reaction chamber, drift tube, and a time-of-flight mass spectrometer. For analysis, a 5 mg

sample of TATP was placed in a sample vessel and left undisturbed for 60 minutes to facilitate the accumulation of volatile compounds in the gas phase. Subsequently, the PTR-ToF-MS's suction tube was introduced into the vessel to collect the gas sample, using an ionization voltage of 80 Townsend. The same protocol was adhered to during laser experiment measurements [34, 35].

Laser

The samples were irradiated using a laser system developed by Laser Zentrum Hannover e.V. This system is based on a pulsed neodymium-doped yttrium aluminum garnet (NdYAG) laser, with its output wavelength shifted to 532 nm via a frequency conversion crystal. The laser operates at a maximum power of 5 W and a pulse repetition rate of 2000 Hz. Each burst delivers exactly 10 pulses, with each pulse providing 2.5 mJ of energy and lasting for 10 nanoseconds. A 250 mm focal length converging lens is integrated to focus and enhance the optical power. Additionally, a polarization filter is utilized for fine-tuning the laser output. The laser power was measured using a power meter, revealing fluctuations of approximately ± 1 mW during adjustments. Measurements of optical power and stability were taken in 1-minute intervals. A shutter was used to precisely control the timing and duration of irradiation.

Setup

For the experiments, the samples were irradiated with laser. The irradiation was controlled with a shutter, which was opened for 15 s per measurement. The microphone and the hose for aspirating the sample for the PRT-ToF-MS are located in front of the sample. A schematic sketch of the setup is shown in Figure 7.2.

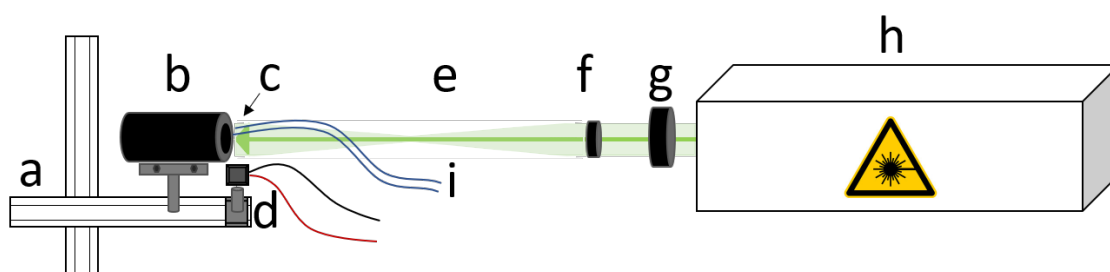


Figure 7.2: Experimental setup: a: yz-stage, b: sample holder, c: sample surface, d: microphone, e: laser beam, f: lens, g: shutter, h: laser system, i: PTR-ToF-MS

Experiments

The experiments were organised as follows: 3 sets without coating (25 mW, 50 mW, 100 mW), one with coating (25 mW) and in total 10 measurements per set were carried out. The shutter opened for 15 seconds. During the each experiment the spot of the beam was defocused on the surface of the sample, to a ratio of 500 μm . Here 5 measurements per parameter set were carried out. Various power levels with and without coating were tested in preliminary trials. Power levels of up to 100 mW proved to be useful for uncoated samples. Power levels above this have led to ignitions in many cases. As conversion inevitably leads to oversaturation of the PTR-ToF and this is undesirable, measurements with higher power were not carried out. In measurements with coating, ignitions frequently occur above 25 mW. Here too, measurements with higher power were not carried out.

7.3 Results and Discussion

Raman

Figure 7.3 shows the Raman measurement of the TATP, the spectra were corrected with the internal software of the measuring device and plotted against a reference spectrum (here in red). The analysis shows that the substance is TATP and that the proportion of DADP (diacetone diperoxide) is negligible.

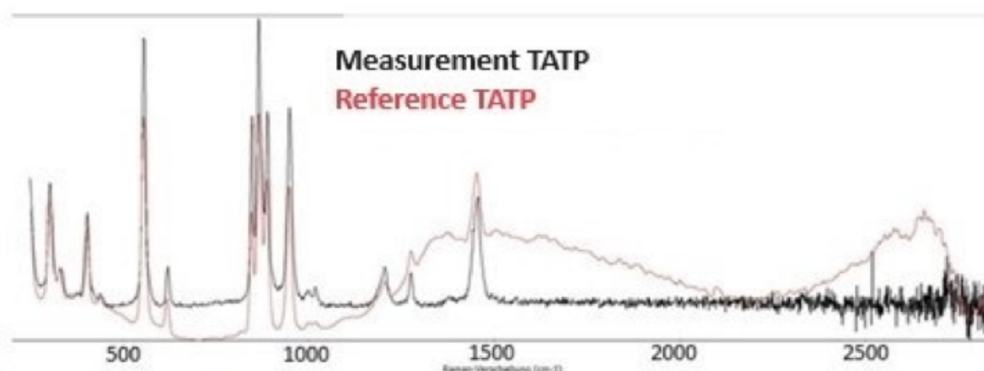


Figure 7.3: Raman spectrum of TATP highlighting the characteristic peaks

Data PTR-ToF-MS

Figure 7.4 shows the mass peaks relevant for the identification of TATP. Due to the protonation of the fragments with a proton, the mass is always 1 g/mol higher than the expected fragment. The peak at 59.049 can be assigned to acetone and the peak at 223.240 to TATP. Mass peaks that are visible in our measurement such as m/z 59.049, 74.000, 75.000, 91.000 are also described in the literature and are typical for TATP [36].

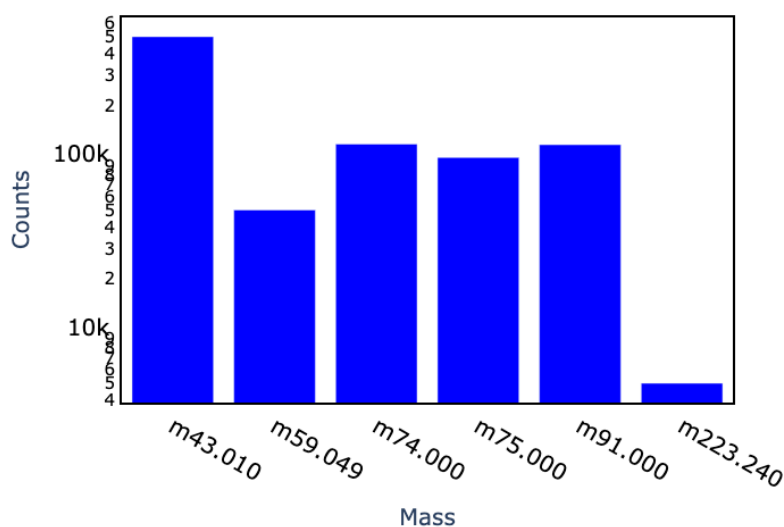


Figure 7.4: Relevant mass peaks of the PTR-ToF-MS measurement of TATP

The masses given below for TATP and acetone each contain the additional mass of a proton due to ionisation in the PTR-ToF-MS. The following section presents representative measurements for each class and the investigated mass traces of acetone (59 g/Mol) and TATP (223 g/Mol), as a comprehensive discussion of all data would exceed the scope of this paper. Figure 7.5 illustrates measurements for the mass of acetone. The shutter opens at 10 seconds and remains open for a duration of 15 seconds. Observing the representative measurement of the uncoated sample at 25 mW (oG 25 mW), it is evident that the concentration of acetone slightly increases at around 25 seconds, which can be attributed to a gradual heating of the sample. The power is insufficient to significantly convert TATP into acetone, or to evaporate existing acetone. The measurement at 50 mW (oG 50 mW) exhibits a comparatively stronger increase, with the peak reaching about 75k counts. Here, too, there is a noticeable delay between the opening of the shutter and the detection of acetone, suggesting that the sample is likely being heated slowly rather

than being instantaneously vaporized or decomposed. The highest peaks are observed in the 100 mW uncoated class (oG 100 mW), with top values just under 300k counts. It is notable that the signal begins to rise at approximately 12 seconds. Taking into account the offset sampling time of the PTR-ToF-MS, it can be deduced that acetone is immediately transferred to the gas phase upon laser impact. Additionally, the concentration continues to rise after about 20 seconds, which may also be a result of the comparatively slow heating of the sample. When analysing the signal from the coated sample at 25 mW (mG 25 mW), an initial increase is also visible at around 12 seconds. The presence of graphite at this energy level is apparently sufficient to cause immediate decomposition and vaporisation of the sample. Similar to the 100 mW measurements, the concentration starts to increase more significantly after 20 s. In our experimental setup, acetone is closely monitored because it is one of the primary decomposition products of TATP, formed during its thermal decomposition or photodecomposition. The mass peak at m/z 59.049 corresponds to acetone, while m/z 223.240 corresponds to TATP, both of which are crucial in confirming the decomposition dynamics. The measurement and tracking of these mass peaks provide valuable insight into the integrity of TATP during heating processes. As shown in figure 7.5, the gradual increase in acetone concentration across the power classes suggests that TATP is undergoing slow decomposition at lower power levels, with more rapid breakdown at higher power levels. This correlation between acetone formation and TATP degradation is further supported by figure 7.6, which tracks the behavior of TATP fragments at different power levels. Notably, the delayed signal rise of TATP compared to acetone indicates that TATP decomposes in a more staggered manner, releasing acetone as a primary byproduct. The presence of acetone and the corresponding decrease in TATP signals provide strong evidence of TATP decomposition, with the acetone concentration serving as a marker for the extent of the reaction.

Figure 7.6 showcases representative traces of TATP from the PTR-ToF-MS measurements. For each class, a single measurement is depicted. Initially, it is evident that the counts for TATP are significantly lower than those for acetone, and the signal-to-noise ratio is also poorer. Examining the measurement from the uncoated series at 25 mW (oG 25 mW), no discernible increase in TATP concentration is observed in relation to the opening of the shutter. The class oG 50 mW exhibits an increase to just over 50 counts around 25 seconds. Here, the delay between the shutter opening and the signal rise is greater than that observed for acetone (the reason for this discrepancy remains to be explored). The signals are difficult to distinguish from noise. Looking at the oG 100 mW class measure-

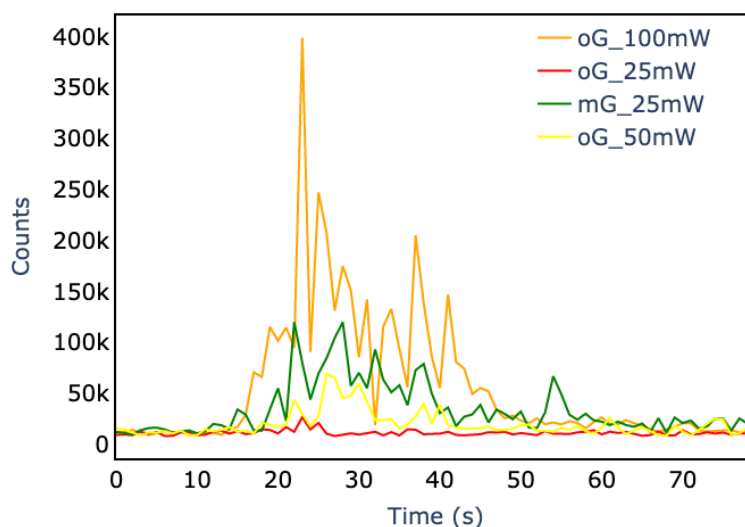


Figure 7.5: Exemplary measurements, one per class, of the acetone (59 g/mol) traces in the PTR-ToF-MS

ment, a clear TATP signal is detectable, peaking at around 65 counts. As with acetone, the delay between the signal and the shutter opening is shorter, yet longer than that for acetone (approximately at 22 seconds). The class with the strongest signals is mG 25 mW. Similar to the oG 100 mW, a clear signal is noticeable, with a timing that mirrors the 100 mW measurements. In the measurement shown, the signal rises to over 75 counts. In both the oG 100 mW and mG 25 mW cases, an energy threshold appears to have been reached where vaporization occurs suddenly, not through comparatively slow heating. Additionally, the throw out of TATP from the borehole by minor partial decompositions could have locally increased the concentration.

For the subsequent analysis of acetone and TATP traces, the measurements were integrated and the average value per class was determined. Figure 7.7 presents the average values of the integrated data per class for acetone. Consistent with the integrated microphone data, it is apparent that the class oG 25mW shows the smallest value (1 M counts). This is followed by class oG 50 mW with approximately 1.7 M counts. The class oG 100 mW yields the highest value at 4.5 M counts. The class mG 25 10 mW is around 3 M counts. This trend is in line with the results from the microphone data evaluation. However, the average value of the integrals per class for the TATP trace exhibits a different pattern (figure 7.8). Here, the value for class mG 25 mW, at just about 2500 counts, is

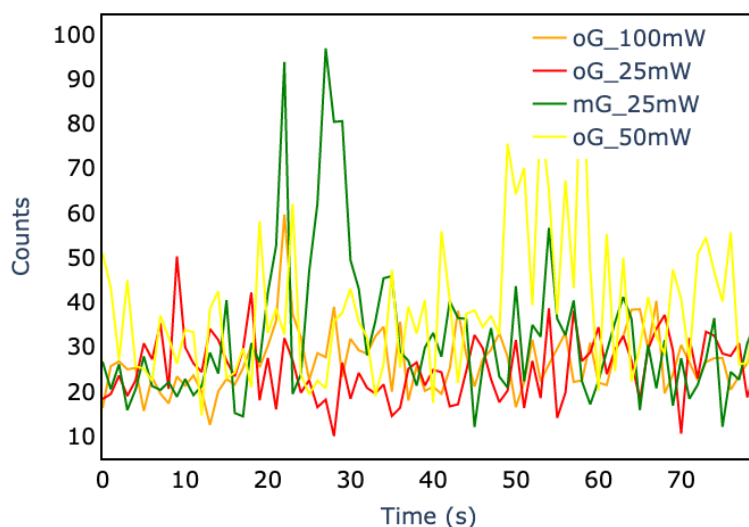


Figure 7.6: Exemplary measurements, one per class, of the TATP (223 g/mol) traces in the PTR-ToF-MS

higher than that for the oG 100 mW series (approximately 2200 counts). The reason for this behaviour is presumably that although continuous decomposition and evaporation of TATP takes place in the oG 100 mW class, partial decomposition tends to occur sporadically. In the mG 25 mW class, hotspots are formed by the graphite, which lead to partial decompositions. These eject TATP particles from the sample into the air, increasing the concentration. The value for class oG 25 mW is the smallest, with the value for oG 50 mW being slightly higher.

Data Microphone

The raw microphone data is discussed here first. Figure 7.9 shows an example measurement of the microphone data for each category (as the amplitudes of the signals are very different, different y axes are used). Absolute values were used and corrected for their offset. Looking at the measurements without graphite at 25 mW (red), the shutter opening at about 0.75 V is clearly visible. The values do not indicate that significant partial reactions take place. At a power of 50 mW (oG 50 mW, yellow) it can be seen that the signals are significantly stronger than at 25 mW. Here, a signal usually does not exceed 0.4 V. This trend continues at 100 mW (oG 100 mW, orange), where signals of up to 2 V are observed, some even higher. Such peaks could indicate small partial reactions in the TATP, as short

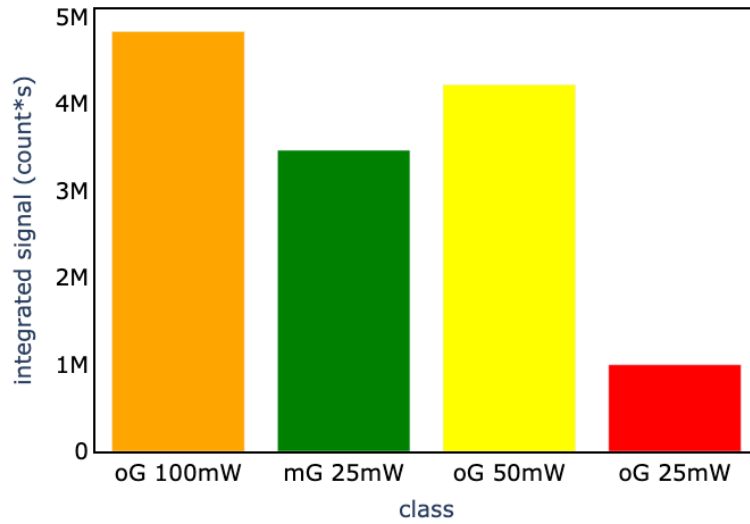


Figure 7.7: Mean value of the integral of the mass traces of acetone (59 counts) per class

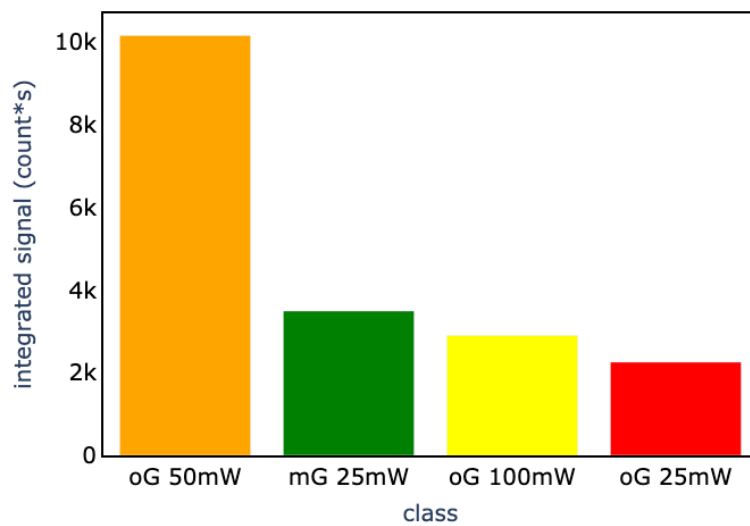


Figure 7.8: Mean value of the integral of the mass traces of TATP (223 counts) per class

and strong pressure increases are typical for explosives. However, the data suggest regular processing without many irregularities. Examination of the signal from the coated sample shows that the signal is more uneven. Most peaks are around 0.5 V, some are over 1 V. The signals indicate that smaller partial reactions could also take place here. It can be seen that the course of the data at the beginning of the measurement is more irregular and has more large peaks. This could indicate that at the beginning of the measurement there is a stronger interaction with the graphite, which erodes over time and is carried into the sample. Many irregularities are also recognisable during the measurement, which indicate partial conversions. Upon closer examination of the data (figure 7.10), the laser pulse packet is discernible within the measurements. For the oG 25 mW measurement, the peaks caused by the laser are barely distinguishable from noise. At 50 mW, these become clearer, and at 100 mW, they are distinctly visible. The interaction of the radiation with the sample is also clearly visible in the mG 25 mW measurement. Looking at the shape of the peaks, it is generally observed that there is an initial “main peak” caused by the laser, followed by further reactions from the sample, especially at oG 100 mW and mG 25 mW, resulting in small shoulders or subsequent peaks. These are significantly more intense in the 100 mW measurement compared to the coated 25 mW sample. The measurements from all categories were integrated between the opening and closing of the shutter. To account for slight variations in the opening times, the integrated values were then normalized by the duration of the shutter being open. An overview of the maximum values of the respective measurements shown can be seen in table 7.1.

Sample Class	Signal Amplitude Range (V)
oG 25 mW	up to 0.75 V
oG 50 mW	up to 0.4 V
oG 100 mW	up to 2 V
mG 25 mW	0.5 V (some over 1 V)

Table 7.1: Summary of Signal Amplitude Range for Each Category

Subsequently, the average values for each category were calculated and are displayed in figure 7.11. Upon examining the data, it is noticeable that the measurements from the uncoated 25 mW (oG 25 mW) samples exhibit the lowest value, approximately 0.4 V. This is followed by the uncoated 50 mW (oG 50 mW) samples showing around 0.45 V. The uncoated 100 mW (oG 100 mW) measurements reach a value of about 1.15 V. The coated 25 mW (mG 25 mW) measurements are positioned between these values,

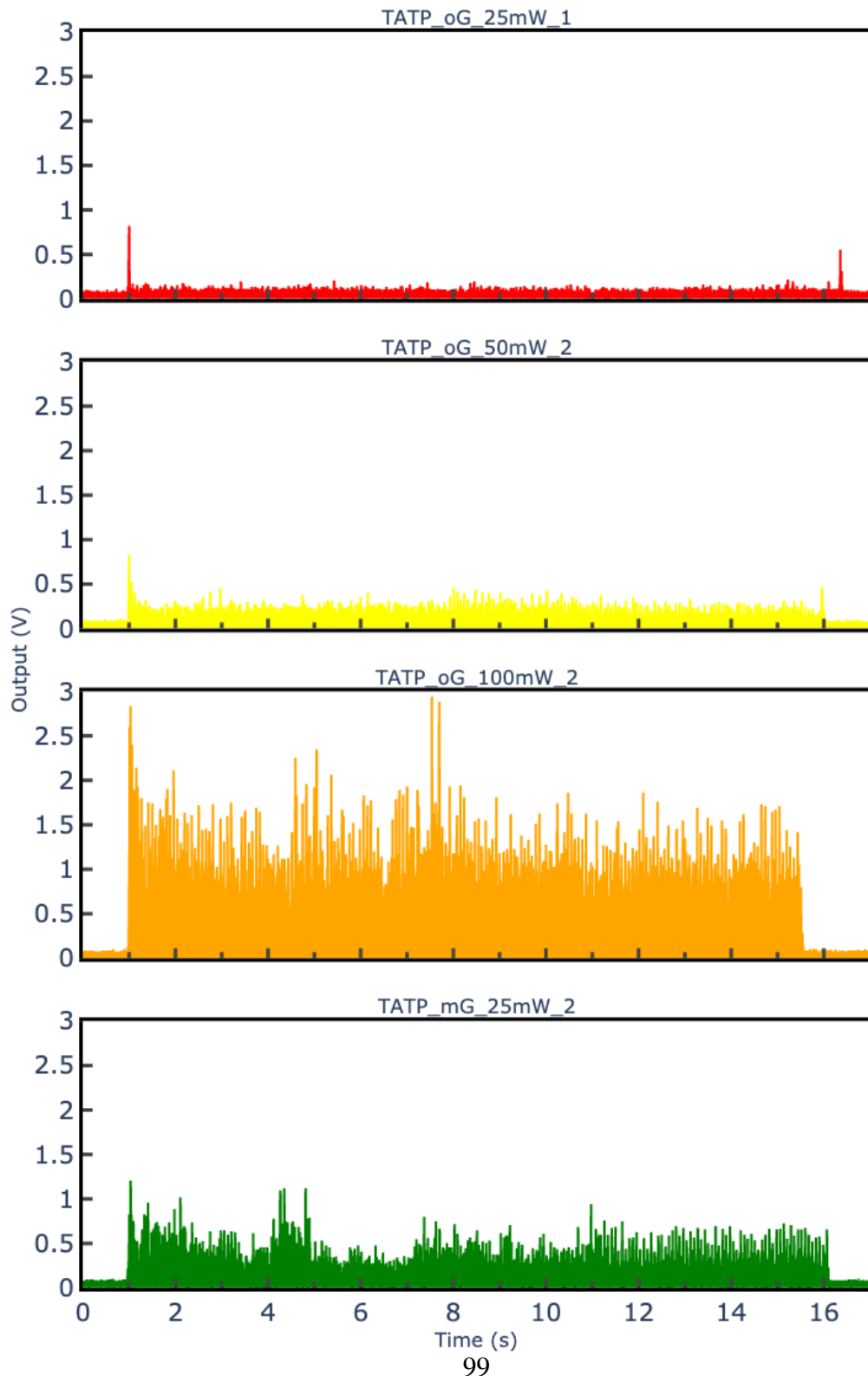


Figure 7.9: Raw data from one measurement per class of microphone

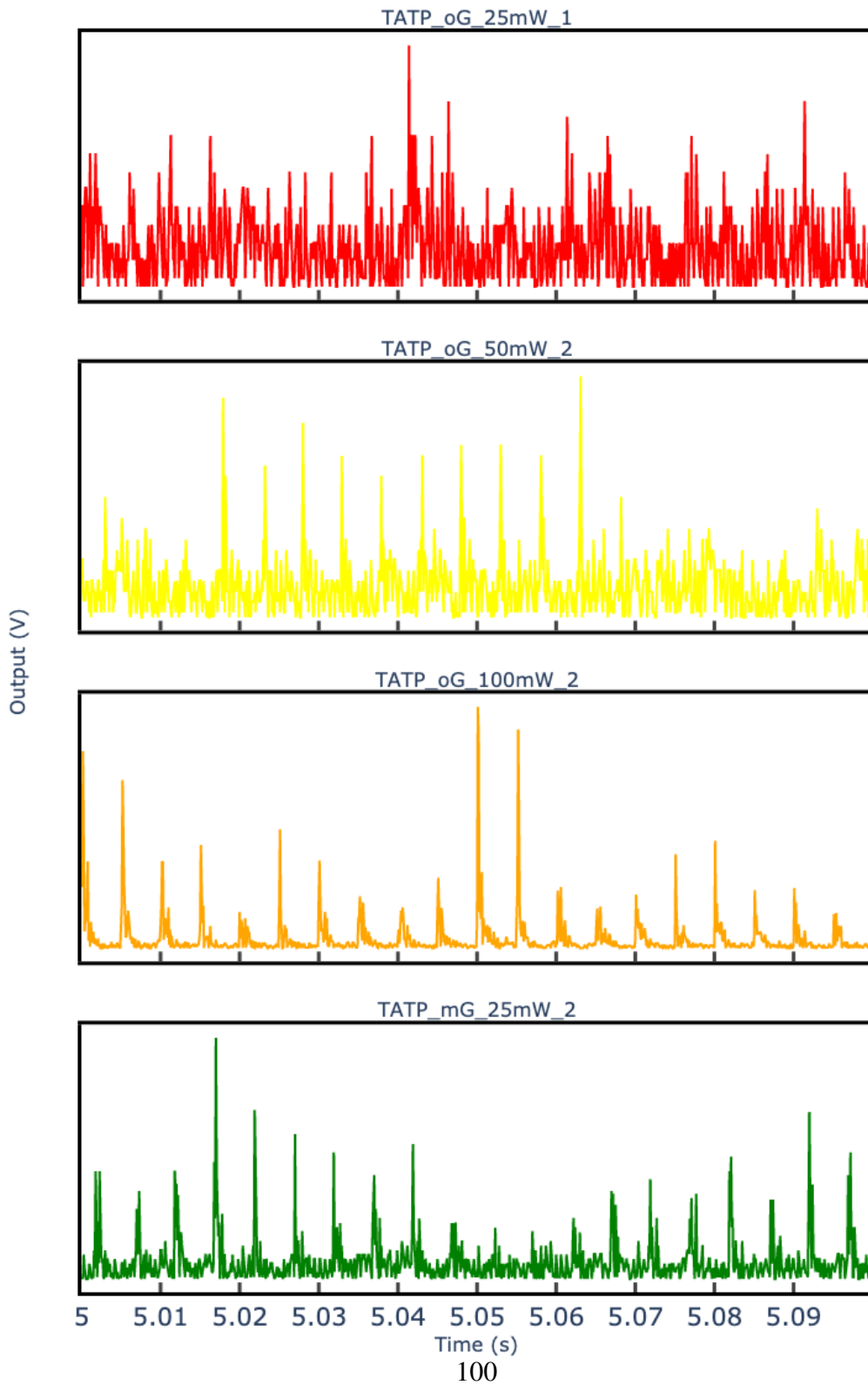


Figure 7.10: Raw data from one measurement per class of microphone, zoomed in

aligning with observations made from the raw data. The relationship between the emitted acoustic signal and the power appears to be exponential for uncoated samples, given the available data. In order to obtain more accurate and statistically relevant results, larger measurement volumes will be used in future work.

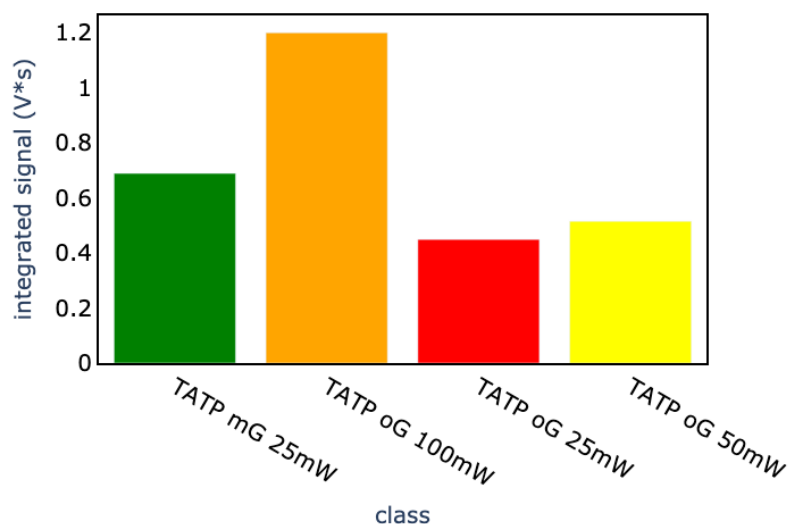


Figure 7.11: Mean values of the integral of all measurements per class of microphone data divided by the shutter opening time

7.4 Conclusion and Outlook

This investigation has demonstrated the successful initiation of triacetone triperoxide (TATP), both graphite-coated and uncoated, using laser irradiation, with analytical emphasis placed on proton-transfer-reaction time-of-flight mass spectrometry (PTR-ToF-MS). The results highlight PTR-ToF-MS as the superior analytical technique, offering highly sensitive and precise quantification of reaction intermediates and products. This method provided critical insights into the reactivity and energetic thresholds of TATP under varying laser parameters, particularly concerning the influence of the graphite coating.

The application of the graphite coating was found to significantly modulate the energetic response of TATP, increasing reproducibility and enhancing control over partial initiation events. These findings suggest that the coating facilitates localized energy absorption, likely leading to the formation of hot spots that induce crystal reorganization

and reaction without full detonation. The graphite layer, by virtue of its high absorption coefficient, appears to play a critical role in mediating the energy transfer dynamics, enabling partial initiation at lower, non-hazardous laser powers—conditions conducive to controlled analytical study.

In contrast, acoustic monitoring via microphone, while capturing sound phenomena during laser initiation, does not offer the same level of precision or direct analytical value as PTR-ToF-MS. Although the microphone provided supplementary data on initiation events, it does not meet the stringent criteria required for robust analytical metrics in energetic material studies. Thus, its utility in this context is limited to secondary, qualitative observations rather than quantitative analysis.

In conclusion, PTR-ToF-MS has proven to be an indispensable tool for the precise monitoring and analysis of laser-induced initiation in sensitive energetic materials like TATP, offering clear advantages over acoustic monitoring in terms of specificity and analytical rigor. Future research will focus on further characterizing the role of various coatings in modulating initiation behavior and enhancing detection sensitivity, as well as optimizing the interplay between laser parameters and material response. Further measurements with different explosives are also planned, so that a basis for a broader data and thus stronger scientific statement on the methods and initiation mechanism can be made.

7.5 Declarations

Data will be made available on a reasonable request.

References

- [1] DER STANDARD. *Moscheenanschlag in hernalds: Selber sprengstoff wie in london verwendet*. Available at: <https://www.derstandard.at/story/2637639/moscheenanschlag-in-hernalds-selber-sprengstoff-wie-in-london-verwendet>. Accessed: 13-11-2023. 2007.
- [2] G.M. Segell. "Terrorism on london public transport". In: *Defense & Security Analysis* 22.1 (2006), pp. 45–59. DOI: 10.1080/14751790600577132.

- [3] Merkur. *Sprengstoff-Brief an Gauck abgefangen*. Available at: <https://www.merkur.de/politik/sprengstoffverdaechtiger-brief-bundespraesidialamt-zr-2861520.html>. Accessed: 13-11-2023. 2023.
- [4] C.A. Mayhew et al. “Applications of proton transfer reaction time-of-flight mass spectrometry for the sensitive and rapid real-time detection of solid high explosives”. In: *International Journal of Mass Spectrometry* 289.1 (2010), pp. 58–63. DOI: 10.1016/j.ijms.2009.09.006.
- [5] V. Bulatov et al. “Time-resolved, laser initiated detonation of TATP supports the previously predicted non-redox mechanism”. In: *Physical Chemistry Chemical Physics* 15.16 (2013), pp. 6041–6048. DOI: 10.1039/C3CP44662J.
- [6] F. Dubnikova et al. “Novel approach to the detection of triacetone triperoxide (TATP): Its structure and its complexes with ions”. In: *The Journal of Physical Chemistry A* 106.19 (2002), pp. 4951–4956. DOI: 10.1021/jp014189s.
- [7] W. Fan et al. “Fast detection of triacetone triperoxide (TATP) from headspace using planar solid-phase microextraction (PSPME) coupled to an IMS detector”. In: *Analytical and Bioanalytical Chemistry* 403.2 (2012), pp. 401–408. DOI: 10.1007/s00216-012-5878-x.
- [8] S. Fan et al. “Solid-state fluorescence-based sensing of TATP via hydrogen peroxide detection”. In: *ACS Sensors* 4.1 (2019), pp. 134–142. DOI: 10.1021/acssensors.8b01029.
- [9] C. Fischer et al. “TATP stand-off detection with open path: FTIR techniques”. In: *Optics and Photonics for Counterterrorism, Crime Fighting, and Defence VIII*. Ed. by C. Lewis and D. Burgess. Vol. 8546. Proceedings of SPIE. SPIE, Edinburgh, United Kingdom, 2012, p. 85460. DOI: 10.1117/12.974592.
- [10] Y. Li et al. “Rapid and selective on-site detection of triacetone triperoxide based on visual colorimetric method”. In: *Journal of Chemical Research* 46.4 (2022), p. 174751982211174. DOI: 10.1177/17475198221117409.
- [11] D. Nascimento Correa et al. “Direct detection of triacetone triperoxide (TATP) in real banknotes from ATM explosion by EASI-MS”. In: *Propellants, Explosives, Pyrotechnics* 42.4 (2017), pp. 370–375. DOI: 10.1002/prop.201600046.

- [12] C. Shen et al. “Triacetone triperoxide detection using low reduced-field proton transfer reaction mass spectrometer”. In: *International Journal of Mass Spectrometry* 285.1-2 (2009), pp. 100–103. DOI: 10.1016/j.ijms.2009.04.007.
- [13] X. Fang and S.R. Ahmad. “Detection of explosive vapour using surface-enhanced Raman spectroscopy”. In: *Applied Physics B* 97.3 (2009), pp. 723–726. DOI: 10.1007/s00340-009-3644-3.
- [14] F. Zapata, M. López-López, and C. García-Ruiz. “Detection and identification of explosives by surface enhanced Raman scattering”. In: *Applied Spectroscopy Reviews* 51.3 (2016), pp. 227–262. DOI: 10.1080/05704928.2015.1118637.
- [15] Pendar Technologies. *Pendar X10 Handheld Raman Spectrometer*. <https://www.pendar.com/introducing-pendar-x10/>. Accessed: 2024-09-05. 2024.
- [16] Thermo Fisher Scientific. *FirstDefender RM and TruDefender Handheld Raman Systems*. <https://www.thermofisher.com/us/en/home/industrial/spectroscopy-elemental-isotope-analysis/portable-analysis-material-id/raman-spectrometers.html>. Accessed: 2024-09-05. 2024.
- [17] F. Zapata et al. “Portable Raman spectroscopy for explosive detection: Field testing and applications”. In: *Sensors* 16.3 (2016), p. 352. DOI: 10.3390/s16030352.
- [18] N.K. Bourne. “On the laser ignition and initiation of explosives”. In: *Proceedings of the Royal Society of London. Series A: Mathematical, Physical and Engineering Sciences* 457.2010 (2001), pp. 1401–1426. DOI: 10.1098/rspa.2000.0721.
- [19] M.D Bowden. “Laser initiation of energetic materials: a historical overview”. In: *Optical Technologies for Arming, Safing, Fuzing, and Firing III*. Ed. by J.W.J. Thomes and F.M. Dickey. SPIE Proceedings. SPIE. 2007, p. 666208. DOI: 10.1117/12.734225.
- [20] J.G. Du, H.H. Ma, and Z.W. Shen. “Laser initiation of non–primary explosive detonators”. In: *Propellants, Explosives, Pyrotechnics* 38.4 (2013), pp. 502–504. DOI: 10.1002/prop.201200132.
- [21] X. Fang and W.G. McLuckie. “Laser ignitibility of insensitive secondary explosive 1,1-diamino-2,2-dinitroethene (FOX-7)”. In: *Journal of Hazardous Materials* 285 (2015), pp. 375–382. DOI: 10.1016/j.jhazmat.2014.12.006.

- [22] Y. Wang et al. “Laser ignition of energetic complexes: impact of metal ion on laser initiation ability”. In: *New Journal of Chemistry* 45.28 (2021), pp. 12705–12710. DOI: 10.1039/d1nj02345d.
- [23] P. Sulzer et al. “Designer drugs and trace explosives detection with the help of very recent advancements in proton-transfer-reaction mass spectrometry (PTR-MS)”. In: *Future Security*. Ed. by N. Aschenbruck et al. Vol. 318. Communications in Computer and Information Science. Springer Berlin Heidelberg. Berlin, Heidelberg, 2012, pp. 366–375.
- [24] Q. Zhang et al. “Ammonia-assisted proton transfer reaction mass spectrometry for detecting triacetone triperoxide (TATP) explosive”. In: *Journal of the American Society for Mass Spectrometry* 30.3 (2019), pp. 501–508. DOI: 10.1007/s13361-018-2108-6.
- [25] I. Khomenko et al. “Non-invasive real time monitoring of yeast volatilome by PTR-TOF-MS”. In: *Metabolomics* 13.10 (2017), p. 118. DOI: 10.1007/s11306-017-1259-y.
- [26] F. Wieland et al. “Online monitoring of coffee roasting by proton transfer reaction time-of-flight mass spectrometry (PTR-TOF-MS): towards a real-time process control for a consistent roast profile”. In: *Analytical and Bioanalytical Chemistry* 402.8 (2012), pp. 2531–2543. DOI: 10.1007/s00216-011-5401-9.
- [27] L. Zhu et al. “Real-time monitoring of emissions from monoethanolamine-based industrial scale carbon capture facilities”. In: *Environmental science & technology* 47.24 (2013), pp. 14306–14314. DOI: 10.1021/es4035045.
- [28] R. Akhmetshin et al. “Effect of laser radiation wavelength on explosives initiation thresholds”. In: *Journal of Physics: Conference Series* 552 (2014), p. 012015. DOI: 10.1088/1742-6596/552/1/012015.
- [29] F. Dausinger et al. “Energy coupling in surface treatment processes”. In: *Journal of Laser Applications* 2.3 (1990), pp. 17–21. DOI: 10.2351/1.4745263.
- [30] X. Chen et al. “Standoff photoacoustic detection of explosives using quantum cascade laser and an ultrasensitive microphone”. In: *Applied optics* 52.12 (2013), pp. 2626–2632. DOI: 10.1364/AO.52.002626.

- [31] T.M. Klapötke and C.M. Rienäcker. “Drophammer test investigations on some inorganic and organic azides”. In: *Propellants, Explosives, Pyrotechnics* 26.1 (2001), pp. 43–47. DOI: 10.1002/prop.200100073.
- [32] M. Muhr, T.M. Klapötke, and G. Holl. “Sensory monitoring of drop hammer experiments with multivariate statistics”. In: *Propellants, Explosives, Pyrotechnics* 47.11 (2022). DOI: 10.1002/prop.202200025.
- [33] Jimmie C. Oxley, James L. Smith, and H. Chen. “Decomposition of a Multi-Peroxidic Compound: Triacetone Triperoxide (TATP)”. In: *Propellants, Explosives, Pyrotechnics* 27.4 (2002), pp. 209–216. DOI: 10.1002/prop.200290019.
- [34] R. González-Méndez et al. “Development and use of a thermal desorption unit and proton transfer reaction mass spectrometry for trace explosive detection: Determination of the instrumental limits of detection and an investigation of memory effects”. In: *International Journal of Mass Spectrometry* 385 (2015), pp. 13–18. DOI: 10.1016/j.ijms.2015.05.003.
- [35] R. González-Méndez et al. “Use of rapid reduced electric field switching to enhance compound specificity for proton transfer reaction-mass spectrometry”. In: *Analytical Chemistry* 90.9 (2018), pp. 5664–5670. DOI: 10.1021/acs.analchem.7b05211.
- [36] Jimmie C. Oxley, James L. Smith, Patrick R. Bowden, and Ryan C. Rettinger. “Factors Influencing Triacetone Triperoxide (TATP) and Diacetone Diperoxide (DADP) Formation: Part I”. In: *Propellants, Explosives, Pyrotechnics* 38.2 (2013), pp. 244–254. DOI: 10.1002/prop.201200116.

Investigation of laser initiation of graphite-coated TATP and HMTD with regard to the influence of coating thickness accompanied by sensor-safe surveillance using a microphone

by

Emre Ünal, Matthias Muhr, Thomas M. Klapötke*, Peter Kaul

Accepted for publication in

Propellants, Explosives, Pyrotechnics

The work reported on in this publication was carried out together with Mr Emre Ünal. The personal contribution amounts to around 50 %. The main focus was on the production of the hardware and the sensor technology. This involved optimising the sensors and data acquisition and synchronising them with the laser system. In addition, the planning and evaluation using multivariate statistics was overhauled. The focus was on feature extraction and finding trends and correlations in the data.

Abstract: Triacetone triperoxide (TATP) and Hexamethylene triperoxide diamine (HMTD), known for their propensity towards use in improvised explosive devices due to facile synthesis from readily accessible precursors, present a considerable security challenge. Their sensitivity to mechanical stimuli, such as impact and friction, as well as to thermal input, necessitates the development of advanced detection methodologies. This study is dedicated to evaluate the influence of varied laser beam parameters during radiation on these peroxide-based energetic materials. A novel approach for the controlled energy delivery to substances under investigation involves the application of coatings with predefined absorption coefficients. This technique, coupled with the careful selection of laser parameters, enables the controlled local initiation of reaction in the energetic material without reaching the threshold for mass combustion, thereby avoiding detonation or deflagration. The experimental setup involves the laser irradiation of defined quantities of graphite-coated TATP and HMTD, with the subsequent laser processing being monitored using a sensitive microphone. This set-up enables a detailed investigation of the physical phenomena that manifest themselves during the interaction and thus contributes to the state of knowledge about the safe handling and detection of these energetic materials.

8.1 Introduction

Triacetone triperoxide (TATP) and Hexamethylene triperoxide diamine (HMTD) are highly dangerous explosives due to their extreme sensitivity to accidental ignition and propensity for spontaneous detonation [1, 2]. Their acute sensitivity to accidental ignition and likelihood of spontaneous detonation make them especially challenging to handle and detect safely [3, 4, 5, 6, 7]. The simplicity of their synthesis and the accessibility of their reactants have made them explosives of choice among terrorist groups, posing significant challenges to civil security [8, 9, 10, 11]. Unlike many explosives, TATP and HMTD lack metallic elements and nitro groups, which complicates their detection through traditional spectroscopic techniques [12]. Consequently, non-destructive detection methods, especially those that do not require mechanical sampling, are preferred for identifying these materials. Techniques such as Raman spectroscopy, supported by laser technology, have achieved notable success in this area [13, 14]. Furthermore, approaches from the combination of microphone and the detection of explosives and vapours by means of acoustical spectroscopy have been tested and have produced promising results [15, 16].

Furthermore, the exploration of laser initiation of these explosives, aiming for a brief ignition time, has been a focus of research [17]. However, the use of laser radiation for the local and controlled initiation of energetic materials presents challenges, especially with primary explosives that have relatively low ignition thresholds and are likely to undergo complete combustion [15]. The application of coatings in laser processing has been studied to reduce the energy required for desired effects [18]. This approach involves coating substances with materials that possess a significantly higher absorption coefficient than the explosives themselves. The goal is to identify laser parameters and conditions that prevent the combustion of the entire explosive mass, especially with highly sensitive substances, while simultaneously initiating non-critical quantities, such as individual crystals. In this study, TATP and HMTD were synthesized and exposed to photonic radiation at power levels from 12.5 mW to 100 mW. The effect of graphite coatings of varying thicknesses on the processing and decomposition of these substances was investigated. Raman spectroscopy assessed the purity of the substances, while a microphone served as a reliable sensor for detecting partial conversions. This research aims to explore the behavior of TATP and HMTD under photonic irradiation, the impact of graphite coating on their decomposition, and how these coatings facilitate partial reactions at lower power levels.

8.2 Experimental

8.2.1 Synthesis of TATP

Caution. TATP is a strong explosive compound and requires experienced personnel. The synthesis was carried out according to Oxley et al. [19]. Hydrogen peroxide at a concentration of 30 % was carefully added to a reaction vessel. The vessel was then sealed with parafilm to prevent any contamination or evaporation and placed in an ice bath to keep the reaction temperature low. Anhydrous acetone was then added to the vessel containing the hydrogen peroxide solution. The components were stirred for at least 15 minutes to ensure good mixing. Concentrated sulphuric acid was then gradually added to the homogeneous solution. The mixture was left undisturbed for 24 hours at a reduced temperature. The reaction mixture was purified with methanol to remove DADP. The final product was then rinsed with distilled water to remove any remaining impurities.

8.2.2 Synthesis of HMTD

Caution. HMTD is a strong explosive compound and requires experienced personnel. For the synthesis, hexamine was added to a aqueous solution of formaldehyde in an ice bath. Subsequently, a hydrogen peroxide solution was gradually added. The reaction mixture was further treated addition of citric acid. Precipitation of HMTD was observed within two hours, a significant reduction from the 5-6 hours normally required in the absence of formaldehyde. The reaction was allowed to run overnight while the temperature of the ice bath gradually increased to room temperature. The crude HMTD product was isolated by vacuum filtration, washed with distilled water to remove residual acid and then washed methanol to facilitate drying. The product was dried at room temperature [2, 20].

8.2.3 Sample Preparation

Ahead of conducting the experimental measurements, the prepared samples were placed in a climate chamber and left undisturbed for a minimum duration of 48hours at a controlled relative humidity of 20 % and a temperature of 18 °C. In the experimental setup, each specimen was placed into cylindrical metallic tubes with a diameter of 2 mm. The tubes were filled to a height of 5 mm and gently pressed manually with a suitable metal rod, which corresponds to an approximate sample mass of 10 mg. This type of sample preparation creates a surface that is not microscopically planar, which can increase the variability of the results. After filling, the samples were carefully sealed. For the preparation of coated samples, a mono or bilayer graphite deposition was executed, ensuring the complete drying of the initial layer prior to the application of the subsequent one. The graphite layers were administered using an aerosolised delivery method, facilitated by an airbrush apparatus positioned at a fixed distance of 10 cm from the target, with a spray exposure time precisely controlled at 500ms. The particle size of the graphot was between 1 and 10 µm. Figure 8.1 shows specimens that have been prepared exemplary. A is an uncoated sample, B is a single-coated sample and C is a double-coated sample. In the follow- ing, samples are mostly labelled with abbreviations. oG stands for uncoated, mG for single-coated and 2mG for double-coated. The power and the consecutive number of the parameter set are given below. For example, TATP_mg_50mW_2 is the second measurement of single-coated TATP and a power of 50 mW.

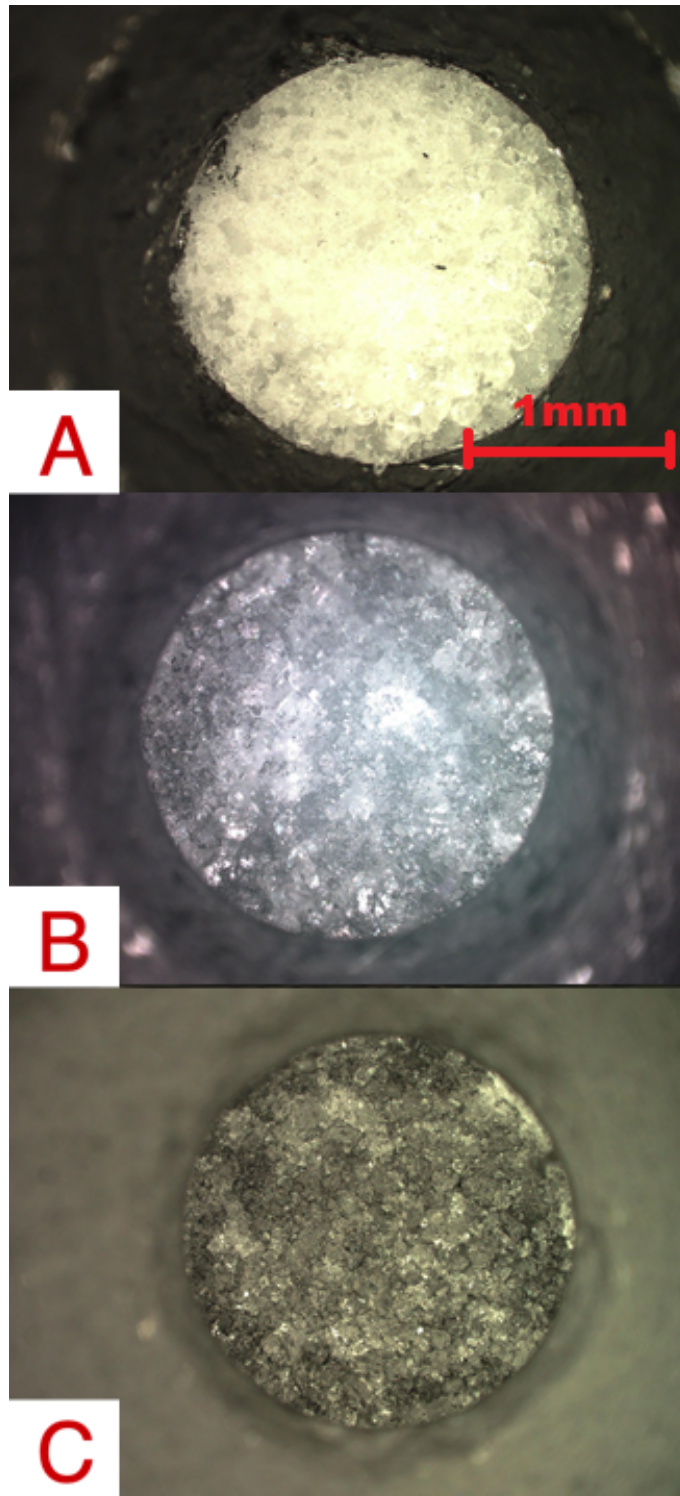


Figure 8.1: Preparation and coating of TATP samples (magnification: 100x): A: uncoated, B: single-coated, C: double-coated

8.2.4 Analytical methods

RAMAN

Samples were analysed for purity and the presence of by-products by Raman spectroscopy using a First Defender R by Thermo Fischer. The measurements were performed according to the standard operating procedures of the instrument. The spectral data subsequently obtained were compared to the instrument's inbuilt chemical library and analysed for confirmation.

Microphone

During laser processing experiments, acoustic monitoring was carried out using a MEMS microphone (ELV MEMS1). Output voltage was captured via a DAQ card (Meilhaus Redlab FS 1208) set to a sampling 10 kHz.

Laser

For the experiments, the samples were irradiated with a laser constructed by Laser Zentrum Hannover e.V.. The laser used is a pulsed neodymium-doped yttrium aluminium doped laser (NdYAG). Its output wavelength is converted to 532 nm using a conversion crystal. The system has a maximum output power of 5 W and a pulse frequency of 2000 Hz. Each burst consists of exactly 10 pulses with a single-pulse energy of 2.5 mJ, with each pulse having a duration of 10 nanoseconds. A converging lens with a focal length of 250 mm is integrated into the system to refine and concentrate the optical power. A polarisation filter is used to precisely adjust the laser power. The power was checked using a power meter. The power fluctuations during adjustment are around ± 1 mW. The optical power and fluctuations were checked using a power meter in a time interval of about 1 min. The regulation of the irradiation was precisely controlled with the aid of a shutter programmed for an exposure time of 15 seconds per measurement cycle.

8.2.5 Experiments

TATP and HMTD samples were investigated. These were each coated with graphite a different number of times and irradiated with the laser at different laser power and constant irradiation time. The basic influence of the graphite coating was analysed in order to be

able to make a comparison with inert and explosive materials. As an organic reference material, sugar, also coated and uncoated, was analysed in the same structure and with the same parameters. All samples were irradiated with 12.5, 25, 50 and 100 mW for 15 s each at a distance of about 20 mm from the focus. The focus was located behind the sample so that the laser spot was defocused on the surface to a ratio of 500 μm . With the exception of HMTD, all tests were repeated three times. A schematic sketch of the structure is shown in Figure 8.2. Measurements with HMTD with two graphite layers and power $\geq 50\text{mW}$ and TATP with power of 100 mW were omitted, as this always led to complete combustion of the sample. Data acquisition was performed using a DAQ card with a sampling 10 kHz, followed by moving average and envelope smoothing which is explained in detail in 8.2.6.

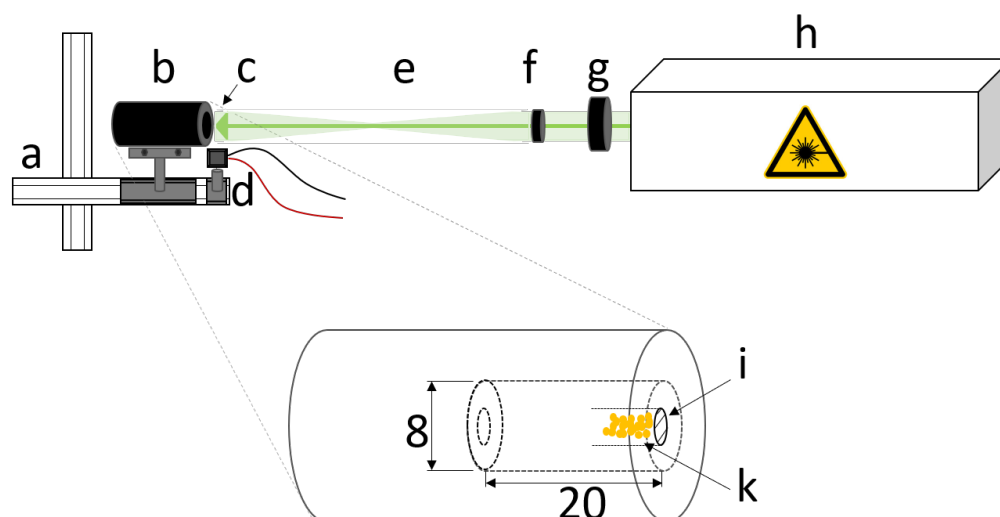


Figure 8.2: Schematic sketch of the set-up - a: x-y stage, b: sample container, c: sample container; sample, d: microphone, e: laser beam, f: converging lens, g: shutter, h: laser system, i: sample container; coating (enlarged), k: sample (enlarged)

8.2.6 Preprocessing

The preprocessing script for analogue microphone data involves cleaning the data by subtracting the mean of the first 1000 points to remove baseline drift and taking the absolute value to ensure all positive values [21]. An upper envelope is created by applying a rolling maximum over 1000 points, which highlights the data peaks and smooths short-term fluctuations.

tuations. Subsequently, a rolling mean is calculated over 100 points to further smooth the data, followed by downsampling to reduce data size and emphasize overall trends. These steps ensure the data are clean, smooth, and ready for accurate analysis by reducing noise and highlighting key features.

8.3 Results and Discussion

8.3.1 Raman Measurements

The spectra were acquired using the integrated software of the employed device and plotted against existing reference spectra. The spectra confirm that the substances used are indeed TATP and HMTD, with no significant impurities or competing products detected.

8.3.2 Microphone Measurements

The data recorded by the microphone are discussed below. The presented plots are representative and illustrate the trends observed for each substance. The voltage output from the microphone was captured, and the following plots display measurements for each substance at a specific power level with all coating variations. To facilitate data analysis, pre-processing was conducted. Specifically, the absolute values of the signals were utilized, as a significant signal can be identified at the start of each plot.

Data discussion

The following section presents and discusses the preprocessing voltage output of the microphone from measurements with varying coating and power. Measurements with HMTD with two graphite layers and power ≥ 50 mW and TATP with power of 100 mW were omitted, as this always led to complete combustion of the sample.

Figure 8.3 shows the test results for a laser power of 25 mW and all three coatings as examples of HMTD measurements. At the beginning of each graph, a strong high signal can be seen, caused by the first impact of the laserbeam on the sample. This can be observed in all measurements and is generally stronger the higher the laser power. For the measurement without graphite coating, the microphone signal is around 0.8 V (Figure 8.3). Subsequently, a low, noisy signal can be recognised, which indicates a low level of processing (interaction of the laserbeam and the investigated material). There is no

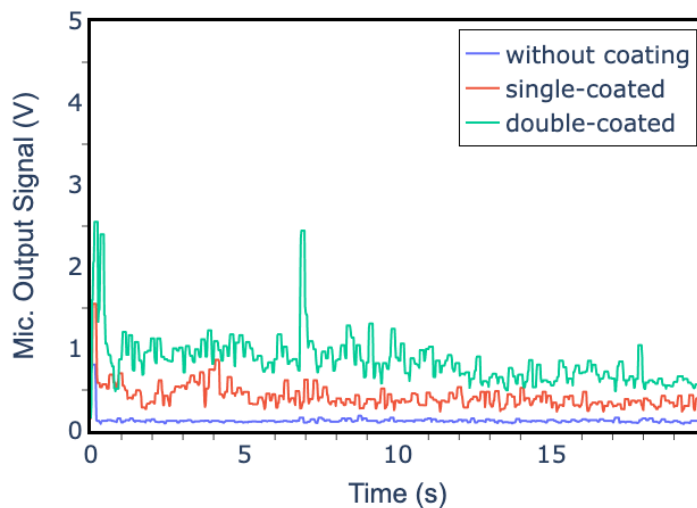


Figure 8.3: Exemplary preprocessed microphone data of HMTD - 25 mW - all coatings

significant variation in intensity over time. The signal does not exceed 0.2 V after the laser has been applied for the first time. The exemplary measurement of the single coated HMTD sample shows a significantly stronger signal. The opening of the shutter can also be recognised here, whereby the signal is around 1.5 V. The signal then shows some irregularities, with smaller peaks of up to 0.7 V. The peaks that occur are presumably caused by smaller partial combustions in the sample, which do not lead to complete combustion of the sample. It can be seen that the occurrence of these peaks decreases with time. This can be caused by the removal of the graphite layer or the pushing of the graphite particles into the depth of the explosive sample. This trend continues in the measurements with a double graphite layer. The first impact of the laser on the sample is also clearly visible here. This is higher than in the other two measurements and is around 2.5 V. Here too, the signal tends to be rather irregular, which indicates a partial decomposition of the sample. One peak directly after opening the shutter and another at around 7 seconds are particularly noticeable. It can also be seen here that the occurrence and intensity of these peaks decrease with time.

Figure 8.4 shows exemplary measurements with all three coatings at 50 mW for TATP. The measurement without graphite shows, with the exception of the first impact of the laser, similar to HMTD, only very weak signals whose intensity remains constant over time and does not exceed 0.2 V. At the first impact of the laser, the signal is about 0.5 V

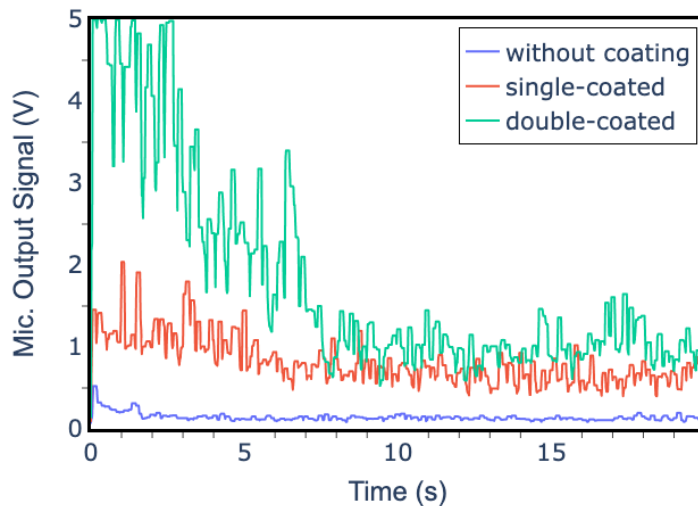


Figure 8.4: Exemplary preprocessed microphone data of TATP - 50 mW - all coatings

high. The data show that the sample is processed without coating, but no significant partial conversion takes place. The measurement shown with a graphite coating shows more irregular peaks, which could be caused by partial conversions. The signals reach levels of up to 2 V. It can be seen that the intensity decreases with time, which is presumably caused by removing or pressing the graphite particles into the sample. If this is compared with the double-coated sample, it is noticeable that the latter has very strong peaks in the signal. The first impact of the laser is comparatively small in this measurement, but this is not the rule for these parameters. The signals sometimes exceed the microphone's dynamic range of 5 V. It is noticeable that the signal decreases sharply and almost falls to the level of the single-coated sample. This is also due to the removal of the graphite particles or the introduction of the graphite particles into the sample, which increases the adsorption.

Exemplary measurements for sugar with 50 mW with all coating variations are shown in Figure 8.5. Looking at the measurement without graphite coating, the first impact of the laser on the sample with an amplitude of approximately 0.3 V is clearly recognisable. Otherwise, this measurement shows little deflection, which indicates that the sample is not or only very slightly processed. The signal does not exceed 0.1 V. If one compares the measurements with the simple graphite layer, significantly stronger signals can be seen. When the laser hits the sample for the first time, the signal reaches over 2.5 V.

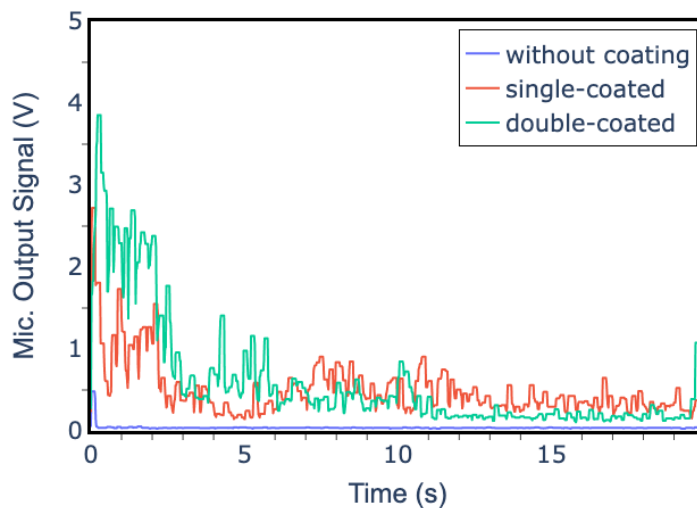


Figure 8.5: Exemplary preprocessed microphone data of combusted samples - 50 mW - double coated

The subsequent signal curve shows many smaller peaks, which indicate processing. The peaks are smaller than with the explosives, which is due to the fact that the decomposition is not self-propagating and only small amounts of the sugar are decomposed. It is also noticeable that the signal intensities decrease with time, which indicates that the graphite particles are being driven into the sample or removed. Compared to the single-coated measurement, however, the signals are higher. When the laser strikes the graphite layer, a signal of just under 4 V is generated.

Figure 8.6 also shows some examples of data from samples where processing via laser led to complete combustion of the sample. As these would falsify the statistical analysis, these data were not taken into account. It is noticeable that when a sample is combusted, this happens in most cases directly after opening the shutter. This is probably due to the initially high amount of graphite which increases the formation of hot spots.

If one compares the exemplary measurements of all three substances in Figure 8.7, you can see that all substances show a clear signal. It can be seen that all samples also generate signals that exceed the dynamic range of the 5 V microphone. Over time, it is noticeable that the signal decreases for all samples. The reason for this is that the graphite particles have been removed or are being driven into the sample. Compared to the other samples shown in this plot, the measurement of sugar shows fewer and also

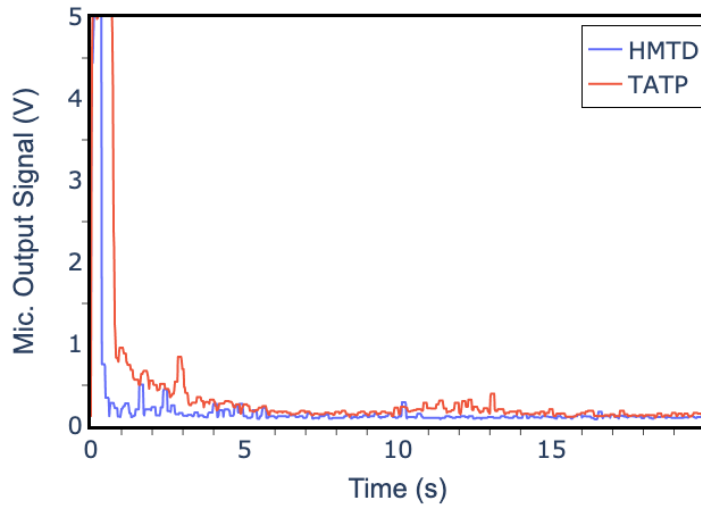


Figure 8.6: Exemplary preprocessed microphone data of combusted samples - 50 mW - double coated

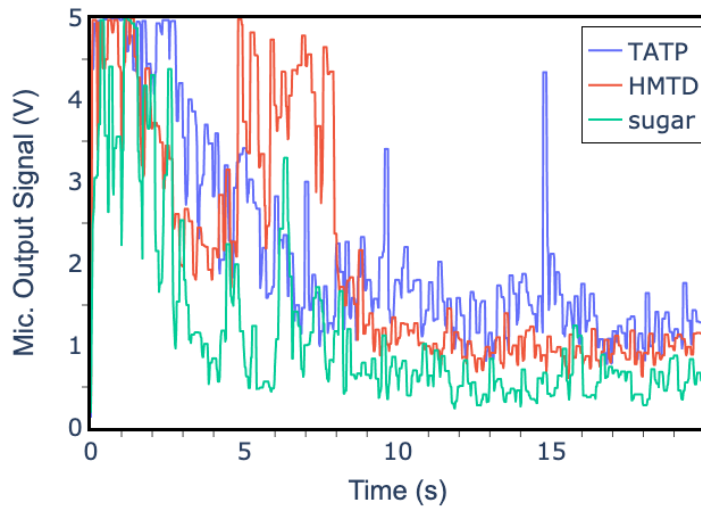


Figure 8.7: Exemplary measurement for TATP, HMTD and sugar with single graphite coating at 100 mW

smaller peaks above the signal, which are caused by the decomposition of the sugar. The measurement with TATP shows high, narrow peaks over the entire measurement, whereby their frequency decreases over time. This is characteristic for measurements with TATP. It is also noticeable that a high basic low level of the signals can be recognised at the beginning of the measurement. This is due to partial redistribution of the material and a high availability of graphite at the beginning of the measurement. The observable partial combustion of the sample, as well as the general mechanism of decomposition, are probably triggered by hotspots, in which a graphite particle is heated by the strong adsorption of the laser radiation and initiates the decomposition [22, 23, 24]. If this behaviour is compared with that of the HMTD sample, a high baseline of the signal can be seen here, particularly at the start of processing. This decreases in the course of the measurement. In contrast to TATP, HMTD shows a stronger accumulation of peaks during the measurement. It appears that the partial reactions are more intense here at the same laser power. This is also consistent with the observations that HMTD tends to react faster in the double-coated samples. In general, the microphone signal of the measurements with HMTD is not significantly higher than that of TATP, which may indicate that HMTD tends to react more strongly once a hotspot is created.

Statistical Evaluation

In order to quantitatively analyze the data of the measurements, the data of all measurements with the same parameters (i.e. sample, reading and coating) were integrated and averaged over the groups. In the following, the data are shown in bar plots. Each plot represents the data of a substance at all powers and different coatings. The standard deviation is shown as an error bar.

Figure 8.8 shows the extracted integrals of the microphone data of all HMTD measurements. Looking at the mean values of the integrals over the different powers (Figure 8.8), it is clear to see that the amount of noise emissions generated by processing and partial decomposition increases with number of graphite layers applied. The uncoated sample shows a slight increase in the integral, with values increasing from 0.12 Vs at 12.5 mW to 0.31 Vs at 100 mW. It can be assumed that the values observed are dependent on the laser power. This is also shown by the HMTD measurements with a graphite layer. Here the values increase from 0.17 Vs at 12.5 mW to 1.42 Vs at 100 mW, too. Such an increase can also be seen in the measurements with two layers of graphite. The values here are

approximately 0.19 Vs at 12.5 mW to 0.60 Vs at 25 mW. For future investigations, it could be determined whether there is an acoustic threshold above which a sample tends towards complete combustion.

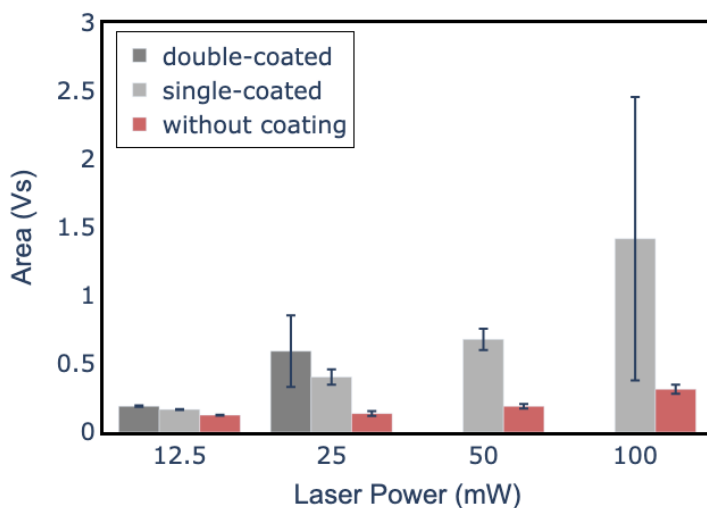


Figure 8.8: Integral of the microphone signal of the HMTD measurements averaged over all measurements with all coating types

Looking at the data situation for TATP (Figure 8.9), the picture is similar. Here, too, it is clear that the noise emissions increase with increasing power. The values 0.09 Vs at 12.5 mW rise to 0.35 Vs at 100 mW. It is noticeable that the values for TATP in the section are more power-dependent than those of the HMTD. This trend is also confirmed in the measurements with a single graphite layer. These range from 0.24 Vs at 12.5 mW to 2.04 Vs at 100 mW, which is higher than the value for HTMD. Looking at the plots for double coated samples, it can be seen that these are at 0.19 Vs at 12.5 mW and increase to 1.66 Vs at 50 mW. Again, this confirms the trend that the dependence of noise emissions on conductivity increases with increasing coating thickness. It is striking that the values of the single-coated samples at 12.5 and 25 mW are higher than those of the double-coated samples.

Looking at the statistically analysed data for sugar (Figure 8.10), there are differences to those for explosives. Basically, it can also be recognised here that the noise emissions increase with increasing laser power, but this is not as clear as with the explosives. For example, the emission of uncoated samples increases from 0.023 Vs at 12.5 mW to

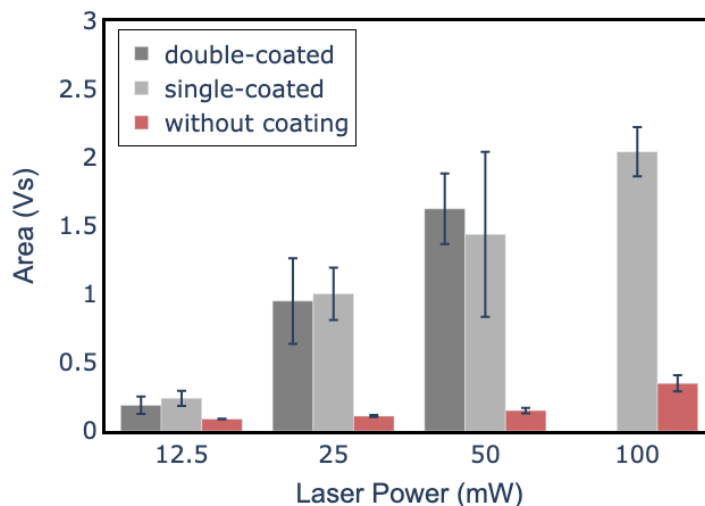


Figure 8.9: Integral of the microphone signal of the TATP measurements averaged over all measurements with all coating types

0.045 Vs at 25 mW, but no further increase can be observed thereafter. However, both the single-coated sample and the double-coated sample with graphite show an increase. The values for single-coated samples and 12.5 mW range from 0.17 Vs to 1.4 Vs at 100 mW. What is striking about this substance is that the integrals of the signals for the single-coated sample are higher than those of the double-coated sample for three out of four lines. However, the differences are small compared to the differences between the single and double coated samples for the explosives, as can be seen from the standard deviations in the plots (TATP in Figure 8.9 and HMTD in Figure 8.8). The reason for this could be that the amount of graphite is relatively large and is not thrown out of the hole by smaller amounts, as could be the case with the explosives.

Optical Evaluation

Figure 8.11 shows a single-coated TATP sample after treatment with 50 mW. The focus point of the laser is marked with a red cross. It can be seen that the processing has created a cavity. This has a diameter of about 600 μm . This is significantly larger than the beam diameter in the area where the laser hits the sample. The reason for this is that gas is produced during the processing of the sample, which flows out through the drill hole. This effect is intensified by the occurrence of small partial reactions that take place in

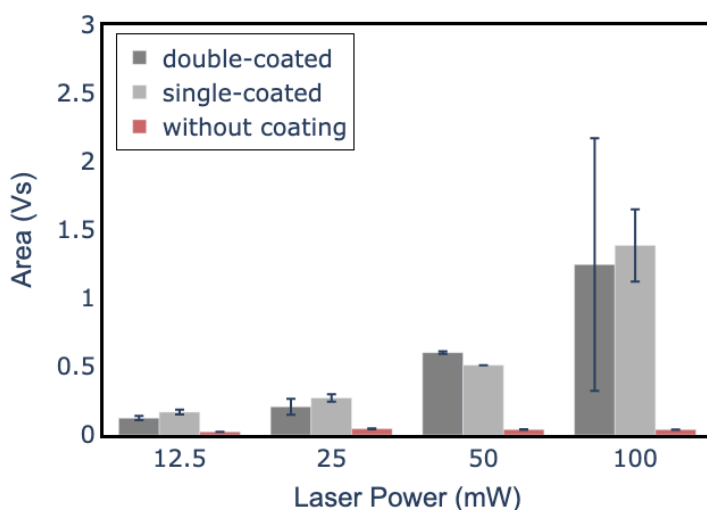


Figure 8.10: Integral of the microphone signal of the sugar measurements averaged over all measurements with all coating types

explosives under laser irradiation. This observation is consistent with the fact that the intensity of the treatment decreases over time and that graphite is lost due to the partial over-expansion of the sample.

8.4 Conclusion and Outlook

In this work we have analysed the behaviour of energetic materials under photonic irradiation. In experiments, HMTD, TATP and sugar with one, two and no graphite coatings were processed with a pulsed laser system at different power levels. The resulting acoustic signals were recorded and analysed using a MEMS microphone. On the one hand, the data show that the processing noise increases as expected with increasing power; this is basically independent of the material. It is noticeable that the increase in noise emissions as a function of power is dependent on the coating, particularly in the case of explosives. The processing noise per power increases the least without coating and the most with two coatings. The results suggest that the graphite particles increase the absorption of light and thus the energy absorption of the particles. This leads to an increase in the formation of hotspots [22, 23]. This in turn leads to partial conversion, which does not result in complete combustion of the sample, at least up to a certain value. The final threshold

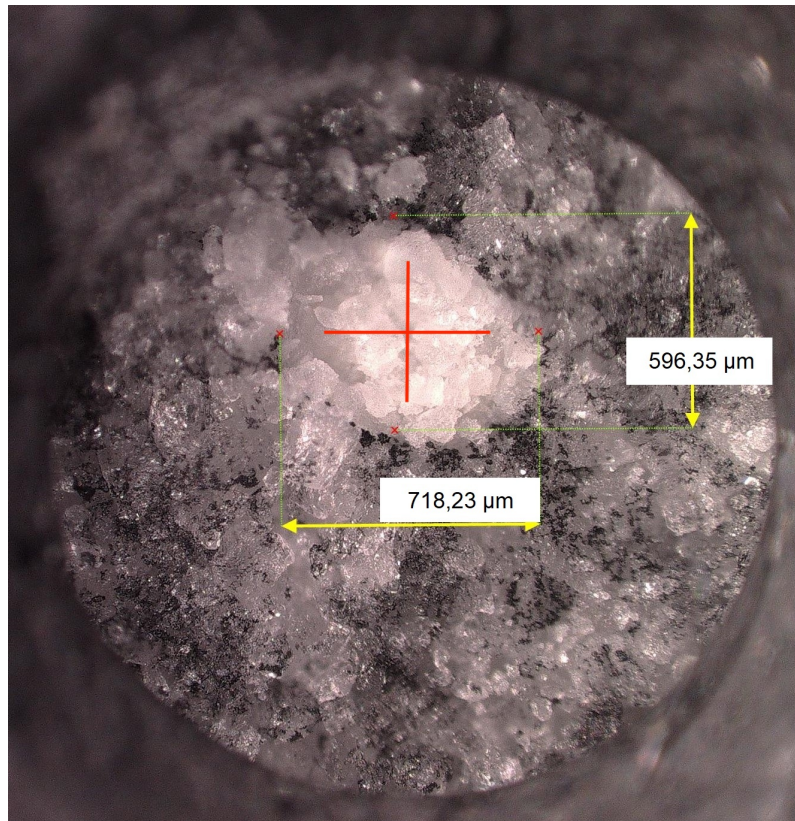


Figure 8.11: Processed single-coated TATP sample ,the focus point of the laser is marked with a red cross

for HMTD is lower than that for TATP, which may indicate that HMTD, once initiated, is more likely to result in complete combustion than TATP. One reason for this could be the higher total specific energy release of HMTD, which favours a continuation of the reaction. This is 2.80 kJ/g for TATP and 5.08 kJ/g for HMTD [25].

Another reason for this could be that different substances adsorb light of different wavelengths to different degrees. In experiments with other wavelengths, the values could vary. The nature of the sample also plays a role. The reaction behaviour can vary due to grain sizes and geometries [23]. In the case of sugar, the influence of the graphite layer is significantly less. In particular, there is hardly any difference between single and double coating. It is also noticeable that the graphite is removed or particles are pushed into the sample over time. Another possibility is that the graphite is oxidised by the high energy input. This reduces the adsorption of light over time and the colouration decreases. In particular, there is hardly any difference between single and double coating, the reason for this could be that with a layer of graphite there is already a kind of saturated layer. This means that the particles do not react so violently and also do not self-propagate, which means that fewer particles are transported away from the reaction zone, although some particles are still driven into the sample. Another possibility is that the graphite is oxidised by the high energy input. This reduces the adsorption of light over time and the colouring decreases. One factor that can significantly influence the results is the quality of the layers. For the series of measurements carried out, the quality of the layers was checked under a microscope, and the results can vary due to irregularities and defects, as the surface of the samples is not completely flat despite pressing.

To summarize, the coating of samples combined with laser processing offers a method for decomposing or partially converting explosives in a more controlled manner and at lower power levels. Possibilities include both the targeted decomposition of substances and the transfer of decomposition products into the gas phase, as well as individual particles of the substance, and subsequent sampling for rapid identification of the substances. For future measurements, the substances should first be better characterised regarding particle size. A further step is to visualise the absolute optical sensitivities of the substances.

8.5 Data Availability Statement

The data that support the findings of this study are available from the corresponding author upon reasonable request.

References

- [1] J.C. Oxley, J.L. Smith, W. Luo, and J. Brady. “Determining the vapor pressures of diacetone diperoxide (DADP) and hexamethylene triperoxide diamine (HMTD)”. In: *Propellants, Explosives, Pyrotechnics* 34.6 (2009), pp. 539–543. DOI: 10 . 1002/prop.200800073.
- [2] Jimmie C. Oxley, James L. Smith, Matthew Porter, Lindsay McLennan, Kevin Colizza, Yehuda Zeiri, Ronnie Kosloff, and Faina Dubnikov. *Synthesis and Degradation of Hexamethylene Triperoxide Diamine (HMTD)*. 2015. DOI: 10 . 1002/prop.201500151.
- [3] A.G. Simon and L.E. DeGreeff. “Variation in the headspace of bulk hexamethylene triperoxide diamine (HMTD): Part II. Analysis of non-detonable canine training aids”. In: *Forensic Chemistry* 13 (2019), p. 100155. DOI: 10 . 1016 / j . forc . 2019.100155.
- [4] V. Bulatov et al. “Time-resolved, laser initiated detonation of TATP supports the previously predicted non-redox mechanism”. In: *Physical Chemistry Chemical Physics* 15.16 (2013), pp. 6041–6048. DOI: 10 . 1039/C3CP44662J.
- [5] F. Dubnikova et al. “Novel approach to the detection of triacetone triperoxide (TATP): Its structure and its complexes with ions”. In: *The Journal of Physical Chemistry A* 106.19 (2002), pp. 4951–4956. DOI: 10 . 1021/jp014189s.
- [6] W. Fan et al. “Fast detection of triacetone triperoxide (TATP) from headspace using planar solid-phase microextraction (PSPME) coupled to an IMS detector”. In: *Analytical and Bioanalytical Chemistry* 403.2 (2012), pp. 401–408. DOI: 10 . 1007/s00216-012-5878-x.
- [7] S. Fan et al. “Solid-state fluorescence-based sensing of TATP via hydrogen peroxide detection”. In: *ACS Sensors* 4.1 (2019), pp. 134–142. DOI: 10 . 1021 / acssensors.8b01029.

- [8] DER STANDARD. *Moscheenanschlag in hernalds: Selber sprengstoff wie in london verwendet*. Available at: <https://www.derstandard.at/story/2637639/moscheenanschlag-in-hernalds-selber-sprengstoff-wie-in-london-verwendet>. Accessed: 13-11-2023. 2007.
- [9] G.M. Segell. "Terrorism on london public transport". In: *Defense & Security Analysis* 22.1 (2006), pp. 45–59. DOI: 10.1080/14751790600577132.
- [10] Merkur. *Sprengstoff-Brief an Gauck abgefangen*. Available at: <https://www.merkur.de/politik/sprengstoffverdaechtiger-brief-bundespraesidialamt-zr-2861520.html>. Accessed: 13-11-2023. 2023.
- [11] Ilya Dunayevskiy, Alexei Tsekoun, Manu Prasanna, Rowel Go, and C. Kumar N. Patel. "High-sensitivity detection of triacetone triperoxide (TATP) and its precursor acetone". In: *Applied Optics* 46.25 (2007), pp. 6397–6404. DOI: 80372.
- [12] Martin Amani, Yun Chu, Kellie L. Waterman, Caitlin M. Hurley, Michael J. Platek, and Otto J. Gregory. "Detection of triacetone triperoxide (TATP) using a thermodynamic based gas sensor". In: *Sensors and Actuators B: Chemical* 162.1 (2012), pp. 7–13. DOI: 10.1016/j.snb.2011.11.019. URL: <https://doi.org/10.1016/j.snb.2011.11.019>.
- [13] X. Fang and S.R. Ahmad. "Detection of explosive vapour using surface-enhanced Raman spectroscopy". In: *Applied Physics B* 97.3 (2009), pp. 723–726. DOI: 10.1007/s00340-009-3644-3.
- [14] F. Zapata, M. López-López, and C. García-Ruiz. "Detection and identification of explosives by surface enhanced Raman scattering". In: *Applied Spectroscopy Reviews* 51.3 (2016), pp. 227–262. DOI: 10.1080/05704928.2015.1118637.
- [15] Aleksej M. Rodin, Jonas Sarlauskas, Jelena Tamuliene, and Augustinas Petrulėnas. "Detection of Explosives by Ultrasonic Spectrum upon Pulsed Laser Initiation". In: *Proceedings of SPIE Security + Defence, 2020, Counterterrorism, Crime Fighting, Forensics, and Surveillance Technologies IV*. Vol. 11542. SPIE. 2020, 115420E. DOI: 10.1117/12.2573678. URL: <https://doi.org/10.1117/12.2573678>.
- [16] Sara Wallin, Anna Pettersson, Henric Östmark, and Alison Hobro. "Laser-based standoff detection of explosives: a critical review". In: *Analytical and Bioanalytical Chemistry* 395 (2009), pp. 259–274. DOI: 10.1007/s00216-009-2844-3. URL: <https://doi.org/10.1007/s00216-009-2844-3>.

- [17] M.D Bowden. “Laser initiation of energetic materials: a historical overview”. In: *Optical Technologies for Arming, Safing, Fuzing, and Firing III*. Ed. by J.W.J. Thomes and F.M. Dickey. SPIE Proceedings. SPIE. 2007, p. 666208. DOI: 10 . 1117/12 . 734225.
- [18] Maria Isabel Sierra-Trillo, Ralf Thomann, Ingo Krossing, Ralf Hanselmann, Rolf Mülhaupt, and Yi Thomann. “Laser Ablation on Isostatic Graphite—A New Way to Create Exfoliated Graphite”. In: (2023).
- [19] Jimmie C. Oxley, James L. Smith, Patrick R. Bowden, and Ryan C. Rettinger. “Factors Influencing Triacetone Triperoxide (TATP) and Diacetone Diperoxide (DADP) Formation: Part I”. In: *Propellants, Explosives, Pyrotechnics* 38.2 (2013), pp. 244–254. DOI: 10 . 1002/prop . 201200116.
- [20] Andrzej Wierzbicki, E. Alan Salter, Eugene A. Cioffi, and Edwin D. Stevens. “Density Functional Theory and X-ray Investigations of P- and M-Hexamethylene Triperoxide Diamine and Its Dialdehyde Derivative”. In: *Journal of Physical Chemistry A* 105.38 (2001), pp. 8763–8768. DOI: 10 . 1021/jp0123841.
- [21] M. Muhr, T.M. Klapötke, and G. Holl. “Sensory monitoring of drop hammer experiments with multivariate statistics”. In: *Propellants, Explosives, Pyrotechnics* 47.11 (2022). DOI: 10 . 1002/prop . 202200025.
- [22] Thomas M. Klapötke. *High Energy Materials*. Berlin, New York: Walter de Gruyter, 2009. ISBN: 9783110207453.
- [23] Josef Köhler, Rudolf Meyer, and Axel Homburg. *Explosivstoffe*. 10th revised and expanded edition. Weinheim: Wiley-VCH, 2008.
- [24] Will P. Bassett, Belinda P. Johnson, Nitin K. Neelakantan, and Dana D. Dlott. “Shock initiation of explosives: High temperature hot spots explained”. In: *Applied Physics Letters* 111.6 (2017), p. 061902. DOI: 10 . 1063/1 . 4985593.
- [25] Ashot Nazarian and Cary Presser. “Thermochemical analysis of improvised energetic materials by laser-heating calorimetry”. In: *Thermochimica Acta* 707 (2022), p. 178971. DOI: 10 . 1016/j . tca . 2022 . 178971.

Part V

Appendix

List of Abbreviations

Table 8.1: List of Abbreviations

Abbreviation	Meaning
AgN ₃	Silver Azide
BIT	Ball Impact Tester
CO ₂	Carbon Dioxide (Laser)
DAQ	Data Acquisition
DSC	Differential Scanning Calorimetry
DTA	Differential Thermal Analysis
DDT	Deflagration-Detonation Transition
ECC	Energetic Coordination Compound
EM	Energetic Material
ESD	Electrostatic Discharge
FS	Friction Sensitivity
FTIR	Fourier Transform Infrared Spectroscopy
HMTD	Hexamethylene Triperoxide Diamine
HNS	Hexanitrostilbene
IED	Improvised Explosive Device
IR	Infrared
LDA	Linear Discriminant Analysis
LIBS	Laser-Induced Breakdown Spectroscopy
MEMS	Micro-Electro-Mechanical Systems
Nd:YAG	Neodymium-Doped Yttrium Aluminium Garnet (Laser)
PCA	Principal Component Analysis
PETN	Pentaerythritol Tetranitrate
Pb(N ₃) ₂	Lead Azide
PTR-ToF-MS	Proton Transfer Reaction - Time-of-Flight Mass Spectrometry
RDX	Cyclotrimethylene Trinitramine
SNR	Signal-to-Noise Ratio
TATP	Triacetone Triperoxide
VIS	Visible Spectrum

List of Publications

8.6 Publications

1. Matthias Muhr, Thomas M. Klapötke, Gerhard Holl, “Sensory Monitoring of Drop Hammer Experiments with Multivariate Statistics”
DOI: 10.1002/prop.202200025
as published in
Propellants, Explosives, Pyrotechnics 2022, 47, 1-10
2. Matthias Muhr, Emre Ünal, Phillip Raschke, Thomas Klapötke, Peter Kaul, “Sensor-monitored impact sensitivity investigations on HMTD of different aging stages with accompanying PTR-TOF measurements of the substances”
DOI: 10.1080/07370652.2023.2295280
as published in
Journal of Energetic Materials 2024, 42, 1-15.
3. Emre Ünal, Matthias Muhr, Jennifer Braun, Thomas M. Klapötke, Peter Kaul, ”Investigation of Laser-Initiation of Graphite Spray-Coated TATP Accompanied by Sensor-Safe Surveillance and Analytical Monitoring Using Microphone and PTR-ToF-MS”
Accepted for publication in
Journal of Energetic Materials, Taylor & Francis, Open Select.
4. Emre Ünal, Matthias Muhr, Thomas M. Klapötke, Peter Kaul, ”Investigation of Laser Initiation of Graphite-Coated TATP and HMTD With Regard to the Influence of Coating Thickness Accompanied by Sensor-Safe Surveillance Using a Microphone”
Accepted for publication in
Propellants, Explosives, Pyrotechnics.

8.7 Conference Presentations

1. Matthias Muhr, Emre Ünal, Dominik Wild, Cathrin Theiss, Gerhard Holl, Peter Kaul, Development and testing of a laser cutting system with control-relevant sensor technology for mobile use on objects with explosives, Proceedings of the SICCC Series - CBRNe Conference, Third Edition, 25-29 September 2023, Rome, Italy.

8.8 Conference Poster Presentations

1. Matthias Muhr, Thomas Klapötke, Peter Kaul, Investigating the Impact Sensitivity and Aging Effects of Hexamethylene Triperoxide Diamine (HMTD) Using Advanced Sensor Systems, Proceedings of the SICCC Series - CBRNe Conference, Third Edition, 25-29 September 2023, Rome, Italy.
2. Matthias Muhr, Emre Ünal, Peter Kaul, Device Development for Rapid Identification of Energetic Materials, Proceedings of the International Conference CBRNE Research & Innovation 2024, 19 - 21 March 2024, Strasbourg, France.
3. Emre Ünal, Matthias Muhr, Evaluation of Dog Training Agents With the Real Substances TATP and HMTD, Poster presentation at the 53rd Annual International Conference of the Fraunhofer ICT, 27 June 2024, Karlsruhe, Germany.

Acknowledgement

Mein größter Dank gilt zunächst meinem Doktorvater, Herrn Prof. Dr. Thomas M. Klapötke, für die herausragende Betreuung meiner Arbeiten während meiner Promotion. Sie haben mir nicht nur die Möglichkeit gegeben, die Geräte und Materialien Ihres Arbeitskreises zu nutzen, sondern auch stets durch anregende Diskussionen wertvollen wissenschaftlichen Input geliefert. Besonders hervorzuheben sind Ihre schnellen Antworten und die zeitnahe Terminfindung für Telefonate, durch die viele Aufgaben und Probleme oft sehr schnell gelöst werden konnten.

Weiterhin möchte ich mich bei Herrn Prof. Dr. Gerhard Holl bedanken. Ohne dich wäre diese Arbeit überhaupt nicht zustande gekommen. Ich danke dir für die Initiierung des Promotionsprojekts, die Vermittlung und natürlich für deine umfassende Betreuung. Diskussionen mit dir haben stets neue Ideen hervorgebracht und der Arbeit eine klare Richtung gegeben. Oft haben Gespräche in unmotivierten Zeiten neuen Antrieb und wertvolle Denkanstöße geliefert. Außerdem danke ich dir dafür, dass ich mit viel Freiraum arbeiten und experimentieren konnte, wobei stets Material und Geräte zur Verfügung standen. Auch im nicht-wissenschaftlichen Kontext konnte ich viel von dir lernen.

Mein Dank gilt auch Prof. Dr. Peter Kaul für die Betreuung meiner Promotion. Danke, dass du stets mit wissenschaftlicher und organisatorischer Expertise zur Seite gestanden hast. Außerdem danke ich dir dafür, dass du mir ermöglicht hast, Konferenzen und andere wissenschaftliche Institutionen zu besuchen, sowie dafür, dass du stets für eine Anstellung an der Hochschule gesorgt hast.

Ein besonderer Dank geht an Emre Ünal. Ohne dich wäre ich nicht hier hin gekommen. Du hast mir stets Motivation gegeben, Herausforderungen anzunehmen und Probleme zu lösen.

Großer Dank gilt auch meinen Eltern, die mir überhaupt erst die Möglichkeit zur Promotion gegeben haben. Danke, dass ihr mein Studium ermöglicht und mich stets motiviert habt.

